Julius Silver Institute of Biomedical Engineering

Technion, Israel Institute of Technology, Haifa, Israel 32000

GRANT AFOSR-89-0054

CEREBRAL-BODY PERFUSION MODEL

S. Sorek[1], J. Bear[2], and M. Feinsod[3]

in Collaboration with

K. Allen[4], L. Bunt[5] and S. Ben-Haim[6]

July 1990

SCIENTIFIC REPORT NO. 4

Approved for public release, distribution unlimited.

Prepared for

The United States Air Force, Air Force Office of Scientific Research

and

The European Office of Aerospace Research and Development, London, England

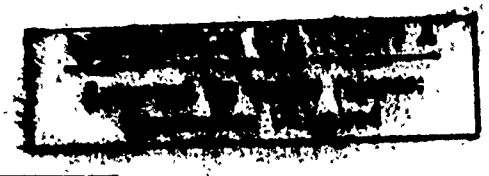

[1] J. Blaustein Inst. for Desert Research, Ben-Gurion University of the Negev, Sede Boker Campus 84990, Israel.
[2] Department of Civil Engineering, Technion-IIT, Haifa 32000, Israel.
[3] Department of Neurosurgery, Technion-IIT, Haifa 32000, Israel.
[4] Neurosurgeon, Medical Center, POB 133, Sedgefield 6573, South Africa.
[5] School of Mechanical Engineering, Witwatersrand, South Africa.
[6] School of Medicine, Technion-IIT, Haifa 32000, Israel.

REPORT DOCUMENTATION PAGE

Form Approved
OMB No. 0704-0188

1a. REPORT SECURITY CLASSIFICATION Unclassified	1b. RESTRICTIVE MARKINGS
2a. SECURITY CLASSIFICATION AUTHORITY	3. DISTRIBUTION/AVAILABILITY OF REPORT Approved for public release;
2b. DECLASSIFICATION/DOWNGRADING SCHEDULE	Distribution unlimited.
4. PERFORMING ORGANIZATION REPORT NUMBER(S)	5. MONITORING ORGANIZATION REPORT NUMBER(S) EOARD TR 90-09
6a. NAME OF PERFORMING ORGANIZATION Technion - Research and Development Foundation 6b. OFFICE SYMBOL (If applicable)	7a. NAME OF MONITORING ORGANIZATION European Office of Aerospace Research and Development
6c. ADDRESS (City, State, and ZIP Code) Technion-Israel Institute of Technology Technion City - Haifa 32000, Israel	7b. ADDRESS (City, State, and ZIP Code) Box 14 FPO New York 09510-0200
8a. NAME OF FUNDING/SPONSORING ORGANIZATION AFWAL and EOARP 8b. OFFICE SYMBOL (If applicable) MLSA/LRP	9. PROCUREMENT INSTRUMENT IDENTIFICATION NUMBER AFOSR-89-0054
8c. ADDRESS (City, State, and ZIP Code) AFWL/MLSA Wright-Patterson AFB OH 45433-6533 EOARD/LRP Box 14 FPO New York 09510	10. SOURCE OF FUNDING NUMBERS PROGRAM ELEMENT NO. 61102F PROJECT NO. 2308 TASK NO. A3 WORK UNIT ACCESSION NO.
11. TITLE (Include Security Classification) Cerebral - Body Perfusion Model	
12. PERSONAL AUTHOR(S) S. Sorek, J. Bear, M. Feinsod	
13a. TYPE OF REPORT Annual 13b. TIME COVERED FROM Nov.88 TO Apr. 90 14. DATE OF REPORT (Year, Month, Day) July 1990 15. PAGE COUNT	
16. SUPPLEMENTARY NOTATION	
17. COSATI CODES FIELD / GROUP / SUB-GROUP	18. SUBJECT TERMS (Continue on reverse if necessary and identify by block number) Compartmental modeling. Perfusion flux and pressure; Interaction between cerebral, respiratory and heart systems; sensitivity analysis.

19. ABSTRACT (Continue on reverse if necessary and identify by block number)

A lumped parameter model is developed to focus on the dynamic flow and pressure interactions between the cerebral, cardiovascular and the respiration systems. The interrelated pressures and fluxes are excited by left cardiac pressure, by expiration/inspiration fluxes and by pressure exerted on the abdomen. Sensitivity analysis examines changes in pressure and flux at the cerebral carotid arteries and capillaries resulting from a sudden rise to an upright position, changes in inhale/exhale patterns, presurizing the abdomen, changes in gravity acceleration, changes in blood viscosity and heart frequency. Animal experiments are performed to validate model predictions and to enable parameter estimations.

20. DISTRIBUTION/AVAILABILITY OF ABSTRACT ☐ UNCLASSIFIED/UNLIMITED ☐ SAME AS RPT. ☒ DTIC USERS	21. ABSTRACT SECURITY CLASSIFICATION Unclassified
22a NAME OF RESPONSIBLE INDIVIDUAL Dr. Jeff Wigle, Capt.	22b. TELEPHONE (Include Area Code) 22c. OFFICE SYMBOL EOARD/LRP

DD Form 1473, JUN 86 *Previous editions are obsolete.*

Julius Silver Institute of Biomedical Engineering

Technion, Israel Institute of Technology, Haifa, Israel 32000

GRANT AFOSR-89-0054

CEREBRAL-BODY PERFUSION MODEL

S. Sorek[1], J. Bear[2], and M. Feinsod[3]

in Collaboration with

K. Allen[4], L. Bunt[5] and S. Ben-Haim[6]

July 1990

SCIENTIFIC REPORT NO. 4

Approved for public release, distribution unlimited.

Prepared for

The United States Air Force, Air Force Office of Scientific Research

and

The European Office of Aerospace Research and Development, London, England

[1] J. Blaustein Inst. for Desert Research, Ben-Gurion University of the Negev, Sede Boker Campus 84990, Israel.
[2] Department of Civil Engineering, Technion-IIT, Haifa 32000, Israel.
[3] Department of Neurosurgery, Technion-IIT, Haifa 32000, Israel.
[4] Neurosurgeon, Medical Center, POB 133, Sedgefield 6573, South Africa.
[5] School of Mechanical Engineering, Witwatersrand, South Africa.
[6] School of Medicine, Technion-IIT, Haifa 32000, Israel.

Table of Contents

Page

Abstract

Non-Steady Compartmental Model of Interactive Perfusion between Cerebral and Body Systems: I.Theory

Abstract 1

Introduction 2

Model Topology 3

Flow Equations 7

Parameter Estimation 17

Pressure Waves 25

Conclusion 26

References 39

Non-Steady Compartmental Model of Interactive Perfusion between Cerebral and Body Systems: II. Sensitivity Analysis

Abstract 40

Introduction 41

Governing equations 42

Sensitivity analysis 45

Conclusion 49

References 67

The Effect of Positive Pressure Ventilation on Cordio-Pulmonary and Brain Dynamics

Methods 69

General preparation 69

Data acquisition 70

Results 70

ABSTRACT

A lumped parameter model is developed to focus on the dynamic flow and pressure interactions between the cerebral, cardiovascular and the respiration systems. The interrelated pressures and fluxes are excited by left cardiac pressure, by expiration/inspiration fluxes and by pressure exerted on the abdomen. Sensitivity analysis examines changes in pressure and flux at the cerebral carotid arteries and capillaries resulting from a sudden rise to an upright position, changes in inhale/exhale patterns, pressurizing the abdomen, changes in gravity acceleration, changes in blood viscosity and heart frequency. Animal experiments are performed to validate model predictions and to enable parameter estimations.

NONSTEADY COMPARTMENTAL MODEL OF INTERACTIVE PERFUSION BETWEEN CEREBRAL AND BODY SYSTEMS: I. THEORY

S. Sorek,[1] K. Allen,[2] M. Feinsod,[3] S. Ben Haim[4]
J. Bear[5] and L. Bunt[6]

ABSTRACT

A lumped parameter model is developed to simulate flow and pressure interaction between the cerebral and the body systems. Its objective is to study the dynamic interaction between the cranio-spinal, body respiratory and the heart systems that influence the brain, as well as the influence of conditions in the environment on the body. By providing forecasts of departures from a normal behavior, the model will serve the following medical purposes: (a) facilitate the understanding of the physiology and the mechanisms that preserve the delicate brain in the face of living stress, and (b) provide information for management in deviant cases.

The compartmental model consists of six compartments that describe the cerebral system, and eight compartments that are assigned to the body system. The model also accounts for the surrounding environment affecting the abdominal, and respiratory fluxes. Altitudes assigned to the compartments introduce the effect of hydrostatic pressure.

Key Words: Compartmental modelling, interaction between cerebral respiratory and heart systems; perfusion flux and pressure; conductances; compliances; environmental pressure; hydrostatic pressure; inhale/exhale fluxes.

Abbreviated Title: Cerebral and body perfusion model

[1] Ben Gurion University of the Negev, J. Blaustein Instit. for Desert Research, Sede Boqer 84990, Israel.
[2] Neurosurgeon, Medical Center, POB 133, Sedgefield 6573, South Africa
[3] Department of Neurosurgery, The Technion, Haifa, Israel
[4] School of Medicine, The Technion, Haifa, Israel
[5] Department of Civil Engineering, The Technion, Haifa, Israel
[6] School of Mechanical Engineering, Witwatersrand, South Africa

1. INTRODUCTION

In earlier papers (Karni et al. 1987; Sorek et al. 1988, 1989), a compartmental model was built to simulate the perfusion in the cerebrovascular system. The model provided information on pressures and fluxes in response to excitation in the form of temporal flux and pressure changes at the internal carotid artery. The influx to and efflux from the cerebrovascular system were introduced, respectively, as external conditions imposed on the internal carotid artery, and the jugular bulb.

In the present work, this model is extended to include both the cerebrovascular and the body system in a single model. The objective is to enable the study of the dynamic interaction between these two systems. In this model, relevant parts of the brain and of the human body are represented as compartments that interact with each other, e.g., in the form of pressure transmission and exchange of fluid. Each such compartment is represented by lumped, or averaged, properties and state variables of that organ. Examples of such lumped parameters are pressure in a compartment, influx/efflux through its boundaries and fluid source/sink terms.

The compartmental model is comprised of six compartments that represent the cerebral system and eight compartments assigned to the body system. The body portion of the compartmental design involves only those parts of the body that are relevant to the cerebral system, i.e., interact grossly with the latter. Accordingly, these parts include mainly the heart and the respiratory systems.

The model also accounts for the influence of the environment surrounding the body, e.g., atmospheric pressure, pressure at high and low altitudes, high underwater pressure, vacuum and excessive gravity acceleration, such as encountered in flight maneuvers. It also takes into consideration differences in elevation between compartments. This means that it takes into account hydrostatic pressure.

Excitations of the model are introduced through changes in inhale/exhale rates, activation pressure of the left cardiac ventricle and outside (environmental) pressure exerted on the abdominal. Extreme intervention, such as resuscitation and/or clogging in the heart system, can be introduced via changes in the appropriate compartmental conductances and compliances.

The diagrammatic layout of the compartments is such as to assist a medical clinician in the interpretation of the model image of the human body, as when examining an X-ray plate. The model will guide clinicians by predicting the brain-body perfusion responses to various excitation, thus enhancing the physiological understanding, fault finding and consequent management in deviant cases of this complex system.

2. MODEL TOPOLOGY

The cerebral section of the model is based on the works of Karni et al. (1987) and Sorek et al. (1988, 1989), and is comprised of the following compartments (Fig. 1):

Arterial Cranium (A_C) - Consists of four supply vessels through the right and left internal carotid and vertebral arteries, with arteriolar branches.

Capillaries (C) - Represents the suit of brain capillaries, choroid plexus and arteriolar/venous capillaries.

Venous Cranium (V_C) - This is a 'lake' of blood confined by thin walls immersed in the brain mass. It contains a controlled mechanism (not expressed in the mathematics of the model) to influence quick and slow fluid movement in the brain during stress. It comprises deep and superficial systems, normally freely anastomising.

Venous Sinuses (S) - These are encased in semi-rigid walls to prevent collapse in all but extreme conditions of compression.

The Cerebro-Spinal Fluid is contained in two compartments:

Ventricles (F_{IV}) - The four ventricles are treated as a true compartment with its own inflow and outflow. Although, normally, the resistance to the latter is low (as the aqueduct of Silvius depends on a pulsative drive to maintain its patency), in disease, high resistance and even occlusion may occur and isolate part of the ventricular system. In such cases, we introduce in the model the extra ventricular and the spinal fluid as an additional compartment.

Extra Ventricular CSF + Spinal Fluid (F_{EV}) - The cisterns sulci and spinal fluid compartment maintains a free communication with the CSF extra ventricular and, to a lesser extent, with

the four main ventricles.

Compartments representing the extra-cranial venous (systemic) circulation are:

Extra-thecal venous plexus (V_{ET}) - A by-pass of the systemic flow included in the bony spinal portion of the cranial-spinal compartment. Normally, this compartment is much less involved in the circulation to the cerebral system. However, in special cases it communicates directly with the ventricles through the spinal and extra ventricular fluid. Therefore, we include it to accommodate abnormal situations.

Brain Tissue (B) - This compartment is placed diagrammatically as a central one, emphasizing its vulnerability, especially due to its location between the venous compartments. All pressures acting on B must be in such balance as to preserve the tissue physically, yet allow and promote optimal macro and micro circulation of fluid transporting metabolites.

The body section of the model is comprised of the following compartments:

Respiratory System (R) - This compartment is activated by the inhale/exhale flux. Its volume deforms through interaction with the heart system, abdominal, superior vena cava and body's arteries.

Abdominal (B_D) - This compartment is subject to volume changes initiated by the environment pressure, inferior vena cava and the respiratory system.

The heart system circulation receives an input perfusion from the superior vena cava and a feedback input from the inferior vena cava. It serves as a circulatory pump to ensure forward flow of blood. Measured mean fluxes are imposed on this system so that without respiration there still is a mechanism forcing blood to flow in a specified circulation. The input flux is injected to the Right Ventricle (R_V) which mutually interacts, by volume deformation, with the respiratory system, and by flow with the Left Ventricle (L_V). The left ventricle exchanges volume deformations with the respiratory systems and discharges flow to the body arteries.

Body Arteries (A_B) - This compartment receives its inflow from the left heart ventricle and introduces the major inflow to the cerebral arteries. It interacts, via volume deformation, with the respiratory system, and discharges flow into the superior and inferior vena cava compartments.

Superior Vena Cava (V_{SC}) - This compartment receives the outflow from the cerebral system. It also receives inflow from the inferior vena cava and from body arteries and discharges it to the right ventricle. Volume deformation interaction exists with the respiratory system.

Inferior Vena Cava (V_{IC}) - This compartment enables flow between body arteries and superior vena cava. It interacts by volume deformations with the abdominal, thus implicitly obtaining information from the environment which is then transmitted as back flow to the right ventricle.

Next we describe the resistances $R_{ij}(\equiv R_{ji})$ and compliances $C_{ij}(\equiv C_{ji})$, ascribed to the various compartments. Here, subscript ij in $(\ )_{ij}$ denotes the mutual boundary of compartments i and j.

$R_{A_C A_B}$ Carotid Body resistance that regulates and controls the inflow from the body to the cerebral arteries. The control is governed by the flux, Q_A, to the cerebral system.

$C_{A_C B}$ Compliance between the brain tissue and cranial arteries compartments.

$C_{A_C F_{EV}}$ Compliance that attenuates the arterial pulse transmitted by large vessels traversing the basal, cisternal, sulcal spaces.

$R_{A_C C}$ The sum of the cranial arteries, capillary and choroid plexus resistances. The resistance associated with the capillary is under autoregulatory control. This control between the arteriolar and capillary vessels, attenuates the systole artery pulse. The autoregulatory effect will not be reflected in the mathematics of the model.

R_{CV_C} Resistance of the Arteriolar/Venous capillary, accounting for the pressure drop observed between them.

R_{CB} Resistance of the Blood-Brain barrier (between the capillary and the brain tissue).

$R_{CF_{IV}}$ Endothelial resistance of the Blood-CSF barrier. It describes the choroid plexus and ependymal secretion.

$C_{CF_{IV}}$ Compliance manifesting the arterial pulse transmitted to the ventricle CSF by the choroid plexus and the extra-cellular fluid.

R_{V_CB} Resistance representing the Blood-Brain barrier (involved in cerebral oedema).

R_{V_CS} A resistance comprised of two gates. First, the outlet from the deep venous circulation into the straight sinus via the great cerebral vein of Galen. According to Le Gros Clark, an auto-regulatory control may be associated with this outflow.
The second component is the superior cortical veinous outflow into the sagittal sinus. An observable pressure drop exists across this resistance under normal conditions.

$R_{F_{IV}B}$ Ependymal resistance of the CSF-Brain barrier.

$C_{BF_{IV}}$ Multifrequency pulsed compliance, transmitted rhythmically by the brain to the ventricle for axial drive of CSF.

$R_{F_{IV}F_{EV}}$ Resistance that exists only in the case of strong stenosis, between the ventricles and the extra ventricular compartments.

$R_{F_{EV}S}$ Resistance manifesting villous tufts secretion into the venous sinus.

$C_{SF_{EV}}$ A low Compliance across the semi-rigid sinus walls.

$R_{F_{EV}V_{SC}}$ Resistance that manifests the slow secretion area around the spinal root sleeves.

$C_{F_{EV}V_{ET}}$ Compliance between the Intradural spinal fluid and the systemic venous flux, across the dura and the extra-thecal venous plexus. This mediates postural, respiratory, abdominal and other body fluctuations, while setting up the intracranial pressure level.

$R_{V_{ET}V_{SC}}$ Resistance to secondary flow communication between the extra-thecal venous plexus and the superior vena cava.

$R_{V_{SC}A_B}$ Resistance to inflow from body arteries.

$C_{V_{SC}R}$ Compliance created by the respiratory venous flux. This compliance is controlled by the involuntary/voluntary variations in the respiratory rhythms.

$R_{V_{SC}R_V}$ Resistance between the superior vena cava and the heart system via the right ventricle

$R_{V_{SC}V_{IC}}$ Back flow resistance into the superior vena cava from the inferior one.

C_{RR_V}, C_{RL_V}

These are the compliances between the respiratory and the heart system, comprised of the right ventricle, and the left ventricle, respectively.

C_{RA_B} Compliance of the respiratory and body arteries.

C_{RB_D} Compliance between the respiratory and the abdominal. It transmits the environmental effects to the abdominal.

$R_{L_VA_B}$ Resistance to flow discharged from the left ventricle (leaving the heart system) into the body arteries.

$R_{A_BV_{IC}}$ Back flow resistance, from the body arteries into the inferior vena cava, to become a flow feedback to the heart system.

$C_{B_DV_{IC}}$ Compliance between the abdominal and the inferior vena cava, transmitting the environmental effect to the abdominal.

C_{B_DA} Compliance due to direct communication between the surrounding environment and the abdominal.

Next, we write the perfusion equations for the entire cerebral-body compartmental setup.

3. FLOW EQUATIONS

Let us consider a single incompressible fluid phase that approximately represents all the relevant fluids in the brain-body system.

In writing the fluid flow, or balance equations, we consider mass and momentum balances for each compartment of the cerebral-body compartment system.

Essentially, each balance equation states that the temporal rate of increase of either the fluid mass, or its momentum in a compartment, is equal to the amount of net influx of that quantity through the compartment's boundaries plus the external sources (e.g. injection or ejection of fluid) within the compartment. For a constant density fluid, the mass balance reduces to a volume

balance.

The fluid's volume balance equation in compartment n takes the form

$$\frac{dV_n}{dt} + \sum_i q_{ni} = Q_n \tag{1}$$

where $V_n(t)$ denotes the volume of fluid in compartment n at time t (equal to the compartment's volume), Q_n is the source associated with compartment n, and q_{ni} denotes the flux flowing out of compartment n, through the boundary of the compartment, to its adjacent i compartment. The non rigidity of the compartment's boundaries (=walls) is expressed by a compliance factor, C_{nj}, defined by

$$C_{nj} = \frac{dV_n}{d(p_{nj})} \tag{2}$$

where $p_{nj}(\equiv p_n - p_j)$ denotes the pressure difference between compartments n and j, on both sides of their common wall.

For low Reynolds number flow, the momentum balance of a fluid moving through a capillary tube can be shown to reduce to an equation that expresses linear proportionality between flux and driving force (Sorek et al. 1988). The latter is composed of a pressure gradient and a gravity term. Here we assume that a similar expression governs the flux between adjacent compartments. Hence

$$q_{ni} = Z_{ni}(p_{ni} + \gamma H_{ni}) = (zh)|_{ni} \tag{3}$$

where $(zh)|_{ni}$ $(\equiv z_{ni}(h_n - h_i))$, Z_{ni} is the conductance associated with the flow wall between compartments n and i, $H_{ni}(\equiv H_n - H_i)$ is the altitude difference between compartments n and i, γ is the fluid's specific weight, $h_{ni}\left(=\frac{p_{ni}}{\gamma} + H_{ni}\right)$ denotes the piezometric head difference between compartments n and i and $z_{ni}(=\gamma Z_{ni})$ is called the hydraulic conductivity factor between compartments n and i.

Upon substituting (2) and (3) into (1), we obtain

$$\sum_i (zh)|_{ni} + \sum_j (C\dot{p})|_{nj} = Q_n \tag{4}$$

where $\dot{p}_{nj} (\equiv \frac{d}{dt}(p_n - p_j) = \dot{p}_n - \dot{p}_j)$ denotes the temporal rate of increase in the difference in pressure between compartments n and its adjacent one, j.

Under certain abnormal conditions, a number of compartments become active. These are the extra ventricular and spinal fluid (F_{EV}) and extra-thecal venous plexus (V_{ET}). In the mathematical model, this fact is expressed by introducing a parameter λ_{mn} which can be set either to $\lambda_{nm} = 0$ for normal conditions, or to $\lambda_{nm} = 1$ for abnormal ones.

During the pressure cycle, a situation may occur in which the flow can change its direction through two adjacent compartments as a result of change in their pressure difference. To prevent this, we introduce a value term denoted by η_{nm} which, accordingly, may have the values $\eta_{nm} = 0$ for normal flow direction, or $\eta_{nm} = 1$ for abnormal one.

In previous reports (Sorek et al. 1988, 1989) the flow problem of the cerebral system was solved using arterial pulsatile flow as a boundary condition. The pulsatile nature of the flow (arterial and all other vessels for that matter) is now transmitted via the cyclic behavior of the piezometric head.

In view of (4), we write the following compartmental fluid balance equations:

$$A_C: \quad 0 = -(zh)|_{A_n A_c} + (zh)|_{A_c C} + (C\dot{p})|_{A_c B} + (\lambda C\dot{p})|_{A_c F_{EV}} \tag{5.1}$$

$$C: \quad 0 = -(zh)|_{A_c C} + (zh)|_{CB} + (zh)|_{CV_c} + (zh)|_{CF_{IV}} + (C\dot{p})|_{CF_{IV}} \tag{5.2}$$

$$V_C: \quad 0 = -(zh)|_{CV_c} - (zh)|_{BV_c} + (zh)|_{V_c S} + (C\dot{p})|_{V_c B} \tag{5.3}$$

$$B: \quad 0 = -(zh)|_{CB} - (zh)|_{F_{IV}B} + (zh)|_{BV_c} + (C\dot{p})|_{BV_c} + (C\dot{p})|_{BF_{IV}} + (C\dot{p})|_{BA_c} \tag{5.4}$$

$$S:\ 0=(zh)|_{SV_{SC}}-(zh)|_{V_CS}-(zh)|_{F_{EV}S}+(C\dot{p})|_{SF_{EV}} \tag{5.5}$$

$$F_{IV}:\ 0=-(zh)|_{CF_{IV}}+(zh)|_{F_{IV}B}+(\lambda zh)|_{F_{IV}F_{EV}}+(C\dot{p})|_{F_{IV}B}+(C\dot{p})|_{F_{IV}C} \tag{5.6}$$

$$F_{EV}:\ 0=(zh)|_{F_{EV}S}+(\lambda zh)|_{F_{EV}V_{SC}}-(\lambda zh)|_{F_{IV}F_{EV}}+(C\dot{p})|_{F_{EV}S}+$$
$$+(\lambda C\dot{p})|_{F_{EV}A_C}+(\lambda C\dot{p})|_{F_{EV}V_{ET}} \tag{5.7}$$

$$V_{ET}:\ 0=(\lambda zh)|_{V_{ET}V_{SC}}+(\lambda C\dot{p})|_{V_{ET}F_{EV}} \tag{5.8}$$

$$V_{SC}:\ 0=-(zh)|_{SV_{SC}}-(zh)|_{V_{IC}V_{SC}}-(zh)|_{A_BV_{SC}}+(zh)|_{V_{SC}R_V}-$$
$$+(\lambda zh)|_{V_{ET}V_{SC}}-(\lambda zh)|_{F_{EV}V_{SC}}+(C\dot{p})|_{V_{SC}R} \tag{5.9}$$

$$V_{IC}:\ 0=-(zh)|_{A_BV_{IC}}+(zh)|_{V_{IC}V_{SC}}+(C\dot{p})|_{V_{IC}B_D} \tag{5.10}$$

$$A_B:\ 0=(zh)|_{A_BA_C}-(zh)|_{L_VA_B}+(zh)|_{A_BV_{SC}}+(zh)|_{A_BV_{IC}}+(C\dot{p})|_{A_BR} \tag{5.11}$$

$$R_V:\ 0=-(zh)|_{V_{SC}R_V}+(zh)|_{R_VL_V}+(C\dot{p})|_{R_VR} \tag{5.12}$$

$$L_V:\ 0=-(\eta zh)|_{R_VL_V}+(\eta zh)|_{L_VA_B}+(C\dot{p})|_{L_VR} \tag{5.13}$$

$$R:\ Q_R=(C\dot{p})|_{RV_{SC}}+(C\dot{p})|_{RR_V}+(C\dot{p})|_{RP}+(C\dot{p})|_{RL_V}+(C\dot{p})|_{RB_D}+(C\dot{p})|_{RA_B} \tag{5.14}$$

$$B_D:\ 0=(C\dot{p})|_{B_DR}+(C\dot{p})|_{B_DV_{IC}}+(C\dot{p})|_{B_DA}\ . \tag{5.15}$$

For the compartment representing the environment, we can write the relation

$$(C\dot{p})\,|_{AB_D} + Q_R = 0 \tag{6.1}$$

If the environment is of infinite extent (i.e. atmosphere), we may write

$$\dot{p}_A = 0 \ . \tag{6.2}$$

We assume a Monro-Kellie postulate according to which the (almost) rigidity of the skull dictates that

$$\int_T Q_S\,dt = \int_T Q_A\,dt \tag{7}$$

where T is the time period.

A stenosis in the passage between the F_{IV} and F_{EV} compartments, initiates a build-up of the compliance between the F_{EV} and A_C compartments. This, in return, indicates that

$$\lambda_{F_{IV}F_{EV}} = \lambda_{F_{EV}A_C} \equiv \lambda \ . \tag{8.1}$$

Under normal conditions, with free communication between F_{IV} and F_{EV} compartments ($\lambda_{F_{IV}F_{EV}} \equiv \lambda = 0$), both the main ventricle and the extra ventricular will merge into one compartment (the F compartment), resulting in

$$h_{F_{IV}} = h_{F_{EV}} \equiv h_F \quad \text{with} \quad \lambda = 0 \ . \tag{8.2}$$

Note that in (9) we have assumed $H_{F_{IV}} = H_{F_{EV}} \equiv H_F$, because only minor differences exist between their values.

To prevent a build up of pressure in compartment L_V higher than that of R_V, we introduce a value term denoted by $\eta_{R_VL_V}$. Similarly $\eta_{L_VA_B}$ denotes the value between compartments A_B and L_V. The values are, therefore,

$$\eta_{R_V L_V} = \begin{cases} 0 \; ; \; h_{L_V} < h_{A_V} \\ 1 \; ; \; h_{L_V} \geq h_{R_V} \end{cases} \tag{9.1}$$

$$\eta_{L_V A_B} = \begin{cases} 0 \; ; \; h_{L_V} \geq h_{A_B} \\ 1 \; ; \; h_{L_V} < h_{A_B} \end{cases} \tag{9.2}$$

Let us now combine all compartmental balance equations into a global matrix form. The driving terms will involve respiration flux, left ventricle pressure and pressure rate exerted on the abdominal. For the normal behavior (i.e. $\lambda_{nm} = 0$), and in view of (5) and (9), we obtain

$$\underline{\underline{C}}\,\frac{d\underline{h}}{dt} + \underline{\underline{z}}\,\underline{h} = \underline{Q} \tag{10}$$

where

$$\gamma \frac{d\underline{h}}{dt} = \frac{d\underline{p}}{dt} \equiv \underline{\dot{p}} \qquad \left(\frac{d\underline{H}}{dt} = 0 \right) ,$$

$$\underline{h} = [h_{A_C}, h_C, h_B, h_{V_C}, h_F, h_S, h_{V_{SC}}, h_{V_{IC}}, h_{A_B}, h_{R_V},]^T \tag{11.1}$$

$$\underline{Q} = \begin{bmatrix} 0 \\ 0 \\ 0 \\ 0 \\ 0 \\ 0 \\ \frac{1}{C}\left[C_{V_{sc}R}C_{B_s}Q_R + C_{V_{sc}R}C_{B_s}C_{L_vR}\dot{h}_{L_v} + C_{V_{sc}R}C_{B_sR}C_{B_sA}\dot{h}_A\right] \\ \frac{1}{C}\left[C_{V_{sc}B_s}C_{B_sR}Q_R + C_{V_{sc}B_s}C_{B_sR}C_{L_vR}\dot{h}_{L_v} + C_{V_{sc}B_s}C_R C_{B_sA}\dot{h}_A\right] \\ \eta_{L_vA_s}Z_{A_sL_v}h_{L_v} + \frac{1}{C}\left[C_{A_sR}C_{B_s}Q_R + C_{A_sR}C_{B_s}C_{L_vR}\dot{h}_{L_v} + C_{A_sR}C_{B_sR}C_{B_sA}\dot{h}_A\right] \\ \eta_{R_vL_v}Z_{R_vL_v}h_{L_v} + \frac{1}{C}\left[C_{R_vR}C_{B_s}Q_R + C_{R_vR}C_{B_s}C_{L_vR}\dot{h}_{L_v} + C_{R_vR}C_{B_sR}C_{B_sA}\dot{h}_A\right] \end{bmatrix} \quad (11.2)$$

The non zero elements of the $\underline{\underline{z}}$ matrix are:

$$z_{1,1}=[z_{A_C C}+z_{A_B A_C}] \quad z_{1,2}=-z_{A_C C} \quad z_{1,9}=-z_{A_B A_C}$$

$$z_{2,1}=-z_{A_C C} \quad z_{2,2}=[z_{A_C C}+z_{CB}+z_{CV_C}+z_{CF}] \quad z_{2,3}=-z_{CB} \quad z_{2,4}=-z_{CV_C} \quad z_{2,5}=-z_{CF}$$

$$z_{3,2}=-z_{CB} \quad z_{3,3}=[z_{CB}+z_{FB}+z_{BV_C}] \quad z_{3,4}=-z_{BV_C} \quad z_{3,5}=-z_{FB}$$

$$z_{4,2}=-z_{CV_C} \quad z_{4,3}=-z_{BV_C} \quad z_{4,4}=[z_{CV_C}+z_{BV_C}+z_{V_C S}] \quad z_{4,6}=-z_{V_C S}$$

$$z_{5,2}=-z_{CF} \quad z_{5,3}=-z_{FB} \quad z_{5,5}=[z_{CF}+z_{FB}+z_{FS}] \quad z_{5,6}=-z_{FS}$$

$$z_{6,4}=-z_{V_C S} \quad z_{6,5}=-z_{FS} \quad z_{6,6}=[z_{SV_{SC}}+z_{V_C S}+z_{FS}] \quad z_{6,7}=-z_{SV_{SC}} \qquad (11.3)$$

$$z_{7,6}=-z_{SV_{SC}} \quad z_{7,7}=[z_{V_{IC}V_{SC}}+z_{A_B V_{SC}}+z_{SV_{SC}}] \quad z_{7,8}=-z_{V_{IC}V_{SC}} \quad z_{7,9}=-z_{A_B V_{SC}} \quad z_{7,10}=-z_{R_V V_{SC}}$$

$$z_{8,7}=-z_{V_{IC}V_{SC}} \quad z_{8,8}=[z_{A_B V_{IC}}+z_{V_{IC}V_{SC}}] \quad z_{8,9}=-z_{A_B V_{IC}}$$

$$z_{9,1}=-z_{A_B A_C} \quad z_{9,7}=-z_{A_B V_{SC}} \quad z_{9,8}=-z_{A_B V_{IC}} \quad z_{9,9}=[z_{A_B V_{SC}}+z_{A_B V_{IC}}+\eta_{L_V A_B}+z_{L_V A_B}+z_{A_B A_C}]$$

$$z_{10,7}=-z_{V_{SC}R_V} \quad z_{10,10}=[z_{V_{SC}R_V}+\eta_{R_V L_V} z_{R_V L_V}]$$

The non zero elements of the $\underline{\underline{C}}$ matrix are:

$$C_{1,1} = C_{A_cB} \qquad C_{1,3} = -C_{A_cB}$$

$$C_{2,1} = C_{CF} \qquad C_{2,5} = -C_{CF}$$

$$C_{3,1} = -C_{A_cB} \qquad C_{3,3} = [C_{BV_c} + C_{BF} + C_{A_cB}] \qquad C_{3,4} = -C_{BV_c} \qquad C_{3,5} = -C_{BF}$$

$$C_{4,3} = -C_{BV_c} \qquad C_{4,4} = C_{BV_c}$$

$$C_{5,2} = -C_{CF} \qquad C_{5,3} = -C_{BF} \qquad C_{5,5} = [C_{BF} + C_{FS} + C_{CF} + C_{FV_{sc}}] \qquad C_{5,6} = -C_{FS} \qquad C_{5,7} = -C_{FV_{sc}}$$

$$C_{6,5} = -C_{FS} \qquad C_{6,6} = C_{FS}$$

(11.4)

$$C_{7,6} = -C_{FV_{sc}} \qquad C_{7,7} = C_{V_{sc}R}\left[1 - \frac{C_{V_{sc}R}C_{B_D}}{\overline{\overline{C}}}\right] + C_{FV_{sc}} \qquad C_{7,8} = \frac{C_{V_{sc}R}C_{B_DR}C_{B_DV_{ic}}}{\overline{\overline{C}}} \qquad C_{7,9} = \frac{C_{V_{sc}R}C_{B_D}C_{RA_s}}{\overline{\overline{C}}} \qquad C_{7,10} = \frac{C_{V_{sc}R}C_{B_D}C_{RR_v}}{\overline{\overline{C}}}$$

$$C_{8,7} = -\frac{C_{V_{ic}B_D}C_{B_DR}C_{RV_{sc}}}{\overline{\overline{C}}} \qquad C_{8,8} = C_{V_{ic}B_D}\left[1 - \frac{C_{V_{ic}B_D}C_R}{\overline{\overline{C}}}\right] \qquad C_{8,9} = -\frac{C_{V_{ic}B_D}C_{B_DR}C_{RA_s}}{\overline{\overline{C}}} \qquad C_{8,10} = -\frac{C_{V_{ic}B_D}C_{B_DR}C_{RR_v}}{\overline{\overline{C}}}$$

$$C_{9,7} = -\frac{C_{V_{sc}R}C_{A_sR}}{\overline{\overline{C}}} \qquad C_{9,8} = -\frac{C_{V_{ic}B_D}C_{A_sR}C_{B_DR}}{\overline{\overline{C}}} \qquad C_{9,9} = C_{A_sR}\left(1 - \frac{C_{B_D}C_{A_sR}}{\overline{\overline{C}}}\right) \qquad C_{9,10} = -\frac{C_{RR_v}C_{A_sR}C_{B_D}}{\overline{\overline{C}}}$$

$$C_{10,7} = -\frac{C_{R_vR}C_{B_D}C_{RV_{sc}}}{\overline{\overline{C}}} \qquad C_{10,8} = -\frac{C_{R_vR}C_{B_DR}C_{B_DV_{ic}}}{\overline{\overline{C}}} \qquad C_{10,9} = -\frac{C_{R_vR}C_{B_D}C_{RA_s}}{\overline{\overline{C}}} \qquad C_{10,10} = C_{R_vR}\left[1 - \frac{C_{RR_v}C_{B_D}}{\overline{\overline{C}}}\right]$$

The sum of the abdominal compliances, C_{B_D}, and that of the respitory, C_R, are given by

$$C_{B_D} \equiv C_{B_D R} + C_{B_D V_{IC}} + C_{B_D A} \tag{11.5}$$

$$C_R \equiv C_{RV_{SC}} + C_{RR_V} + C_{RL_V} + C_{RB_D} + C_{RA_B} \tag{11.6}$$

Also,

$$\bar{C} \equiv C_{B_D} C_R - C_{B_D R}^2 \ . \tag{11.7}$$

Equation (10) is to be solved for the unknown $\underline{\dot{h}}$ vector, subject to an initial condition of the form

$$\underline{h}_{(t=0)} = \underline{h}_o \ . \tag{12}$$

Upon solving (10), together with (12), we obtain the solution for the temporal rates of change in piezometric head, $\dot{h}_{B_D}$ and $\dot{h}_R$, in the forms

$$\dot{h}_{B_D} = \frac{1}{\bar{C}} [C_{B_D R} Q_R + C_{B_D R} C_{RA_B} \dot{h}_{A_B} + C_R C_{B_D V_{IC}} \dot{h}_{V_{IC}} + C_R C_{B_D A} \dot{h}_A + \tag{13}$$

$$+ C_{B_D R} C_{RV_{SC}} \dot{h}_{V_{SC}} + C_{B_D R} C_{RR_V} \dot{h}_{R_V} + C_{B_D R} C_{RL_V} \dot{h}_{L_V}]$$

$$\dot{h}_R = \frac{1}{\bar{C}} [C_{B_D} Q_R + C_{B_D} C_{RA_B} \dot{h}_{A_B} + C_{B_D R} C_{B_D V_{IC}} \dot{h}_{V_{IC}} + \tag{14}$$

$$C_{B_D} C_{RV_{SC}} \dot{h}_{V_{SC}} + C_{B_D} C_{RR_V} \dot{h}_{R_V} + C_{B_D R} C_{B_D A} \dot{h}_A + C_{B_D} C_{RL_V} \dot{h}_{L_V}] \ .$$

The compartmental balance equation, written in the global compact form (10), involves conductivities and compliances expressed by the matrices $\underline{\underline{z}}$ and $\underline{\underline{C}}$, respectively. In order to solve for the piezometric head vector, $\underline{h}$, we need to know the $\underline{\underline{z}}$ and $\underline{\underline{C}}$ values. We shall, next, discuss an inverse method for estimating these parameters.

4. PARAMETER ESTIMATION

To predict the pressure and flux response of the model to external changes, the values of the parameters $\underline{\underline{C}}$ and $\underline{\underline{z}}$ must be known. In order to estimate them, we need measured values of pressure in the various compartments at a sufficient number of points in time. Typical phasic pressures are depicted in Figs. 2-11.

In the present work, we assume that all conductivities and compliances have the form of a time-step function i.e., they change from one constant value to another constant value, due to abnormal situations such as disease. Because $\underline{\underline{C}}$ and $\underline{\underline{z}}$ are constant during long time intervals, and $\underline{h}(t)$ is assumed cyclic, by taking a temporal average of (10), i.e., integration over a period of time divided by the period, we obtain

$$\underline{\underline{z}}\,\underline{h}^{*} = \underline{Q}^{*} \tag{15}$$

where h^* and Q^* denote mean values of the piezometric head and of the source term, respectively. Since $\underline{h}^{*}$ and $\underline{Q}^{*}$ are known averaged values, in order to solve for $\underline{\underline{z}}$ values, we rewrite (15) in the form

$$\overline{\underline{\underline{h}}}^{*}\,\underline{z}^{V} = \underline{Q}^{*} \tag{16}$$

where $\overline{(\ )}$ denotes the head difference between two communicating compartments.

In the cerebral portion of the model, we face ten conductivities against six balance equations. However, by virtue of the Monro-Kellie doctrine which assumes absolute rigidity of the cranial vault, actually only five equations of the six are independent. Thus for this redundancy, five additional conditions are needed. One of them is the mean influx to the CSF (F) compartment $Q_F^{*} = 0.3$ml/min. (Cutalar, 1968). Two more conditions are stipulated by physiological data. These conditions determine the scalar coefficients (Sorek et al. 1987) α and β defined as

$$\alpha = \frac{z_{V_c S}}{z_{FB}} \qquad (\alpha > 0) \tag{17}$$

and

$$\beta = \frac{z_{CB}}{z_{FB}} \qquad (0 \le \beta < \infty) \tag{18}$$

where α (= 10000) indicates the ratio of the vein-venous sinous to the cerebrospinal fluid-brain barrier, and $\beta(=10^{-3})$ is the ratio of the blood-brain barrier to the cerebrospinal fluid-brain barrier.

The mean arterial influx, Q_A, which according to (3) equals the mean venous sinous efflux, is given by

$$Q_A^* = Q_S^* \equiv Q^* = 750\text{ml./min.}$$

Because Q_F^*, Q_A^* and Q_S^* are a-priori known, and the mean head values $h_{A_C C}^*$, h_{CF}^*, $h_{A_B A_C}^*$ and $h_{SV_{SC}}^*$ are also known, the following conductivities are immediately obtained.

$$z_{A_C A_B} = \frac{Q^*}{h_{A_B A_C}^*} \qquad z_{A_C C} = \frac{Q^*}{h_{A_C C}^*} \tag{19.1}$$

$$z_{CF} = \frac{Q_F^*}{h_{CF}^*} \qquad z_{SV_{SC}} = \frac{Q^*}{h_{SV_{SC}}^*} \; . \tag{19.2}$$

Also, for the given configuration of the heart system (Fig. 1), we impose the direction and magnitude of the same mean flux through conductances of the cardiac system ensuring a circulatory pump effect. Hence, such a condition, e.g., $Q_L^* = 5900\text{ml./min}$ through the boundary between compartments L_V and A_B, will yield

$$z_{L_V A_B} = \frac{Q_L^*}{h_{L_V A_B}^*} \tag{20.1}$$

$$z_{V_{SC} R_V} = \frac{Q_L^*}{h_{V_{SC} R_V}^*} \; . \tag{20.2}$$

We assume that the mean influx to the inferior vena cava compartment is a fraction, δ $(0 < \delta \leq 1)$, of the efflux Q_L^* from the left heart ventricle. Therefore, we obtain

$$z_{V_{IC}V_{SC}} = \frac{\delta Q_L^*}{h^*_{V_{IC}V_{SC}}} \tag{20.3}$$

$$z_{A_B V_{IC}} = \frac{\delta Q_L^*}{h^*_{A_B V_{IC}}} \tag{20.4}$$

$$z_{A_B V_{SC}} = \frac{(1-\delta)Q_L^* - Q^*}{h^*_{A_B V_s C}} \,. \tag{20.5}$$

Hence, in view of (17) to (20), equation (16) is constructed of the following matrix and vectors

$$\underline{\underline{h}}^* = \begin{bmatrix} h^*_{B_r} - \beta h^*_{CB} & 0 & 0 & h^*_{BV_C} \\ \beta h^*_{CB} & h^*_{CV_C} & 0 & 0 \\ h^*_{FB} & 0 & h^*_{FS} & 0 \\ \alpha h^*_{V_C S} & -h^*_{CV_C} & 0 & -h^*_{BV} \end{bmatrix} \tag{21.1}$$

$$\underline{z}^V = [z_{FB}, z_{CV_C}, z_{FS}, z_{BV_C}]^T \tag{21.2}$$

$$\underline{Q}^* = [0, Q^* - Q_F^*, Q_F^*, 0]^T \tag{21.3}$$

Upon solving the inverse problem for the conductivities, we move to the estimation of the compliances.

Given information of the simultaneous pulse wave recordings, $p_{(t)}$, and $\dot{p}_{(t)}$, in the different compartments and at various times $t^k, k = 1,2,\ldots,K$, equation (10) (or (5) and (6)) now yields a set of k relations for the compliances, for times t^k

$$\dot{\underline{\underline{h}}}^k \underline{C}^V = \underline{R}^k \tag{22}$$

where $\dot{(\ )} \equiv \frac{d}{dt}(\ )$.

$$\dot{h}^k = \begin{bmatrix} \dot{h}_{A_C B} & & & & & & & & & & & \\ & \dot{h}_{CF} & & & & & & & & & & \\ & & \dot{h}_{V_C B} & & & & & & & & & \\ & & & \dot{h}_{SF} & & & & & & & & \\ & & & & \dot{h}_{BF} & & & & & & & \\ & & & & & \dot{h}_{FV_{SC}} & & & & & & \\ & & & & & & \dot{h}_{V_{SC}R} & & & & & \\ & & & & & & & \dot{h}_{V_{IC}B_D} & & & & \\ & & & & & & & & \dot{h}_{R_V R} & & & \\ & & & & & & & & & \dot{h}_{L_V R} & & \\ & & & & & & & & & & \dot{h}_{A_B R} & \\ & & & & & & & & & & & \dot{h}_{RB_D} \\ & & & & & & & & & & & & \dot{h}_{B_D A} \end{bmatrix} \tag{23.1}$$

$$\underline{C}^V = [\, C_{A_C B}, C_{CF}, C_{V_C B}, C_{SF}, C_{BF}, C_{FV_{SC}}, C_{V_{SC}R}, C_{V_{IC}B_D}, C_{R_V R}, C_{L_V R}, C_{A_B R}, C_{B_D R}, C_{B_D A} \,]^T \tag{23.2}$$

$$\underline{R}^k = \begin{bmatrix} (zh)^k|_{A_B A_C} - (zh^k)|_{A_C C} \\ (zh^k)|_{A_C C} - (zh^k)|_{CB} - (zh^k)|_{CV_C} - (zh^k)|_{CF} \\ (zh^k)|_{CV_C} + (zh^k)|_{BV_C} - zh^k\ |_{V_C S} \\ (zh^k)|_{V_C S} + (zh^k)|_{FS} - (zh^k)|_{SV_S} \\ -(zh^k)|_{V_C S} + (zh^k)|_{FB} + (zh^k)\ |_{A_B R_C} - (zh^k)|_{A_C C} + (zh^k)\ |_{CB} + (zh^k)|_{CV_C} \\ -(zh^k)|_{SV_{SC}} + (zh^k)|_{A_B A_C} \\ (zh^k)|_{A_B A_C} + (zh^k)|_{A_B V_{SC}} + (zh^k)|_{V_{IC} V_{SC}} - (zh^k)|_{V_{SC} R_V} \\ (zh^k)|_{V_B V_{IC}} - (zh^k)|_{V_{IC} V_{SC}} \\ (zh^k)|_{V_{SC} R_V} - (\eta zh^k)|_{R_V L_V} \\ (\eta zh^k)|_{R_V L_V} - (\eta zh^k)|_{L_V A_B} \\ -(zh^k)|_{A_B V_{IC}} - (zh^k)\ |_{A_B V_{SC}} - (zh^k)|_{A_B A_C} + (\eta zh^k)|_{L_V A_B} \\ Q_R^k + (zh^k)\ |_{V_{IC} V_{SC}} \\ Q_R^k + Z_{V_{IC} A_B} h_{A_B V_{IC}} \end{bmatrix} \tag{23.3}$$

Note that the z values in (23.3) are already known.

By the Gauss-Markov theorem, the $\underline{C}$ values are derived as an assortment of the set of informations through all K time observations (Sorek et al. 1987b), namely

$$\underline{C} = (\pi^T \pi)^{-1} \pi^T \underline{B} \tag{24}$$

where,

$$\pi = \begin{bmatrix} \underline{\underline{h}}^1 \\ \hline \underline{\underline{h}}^2 \\ \hline \vdots \\ \underline{\underline{h}}^k \end{bmatrix}_{K*13} \tag{25.1}$$

$$\underline{B} = [\underline{R}^1, \underline{R}^2, \ldots, \underline{R}^K]^{\tau}_{1*K} \tag{25.2}$$

Since the $\underline{\underline{h}}^k$ submatrices of π are main diagonalized, we can evaluate the $\underline{C}$ values directly.

$$C_{A_CB} = \frac{\sum_{k=1}^{K} \dot{h}^k_{A_CB}[(zh^k)|_{A_BA_C} - (zh^k)|_{A_CC}]}{\sum_{k=1}^{K} (\dot{h}^k_{A_CB})^2} \tag{26.1}$$

$$C_{CF} = \frac{\sum_{k=1}^{K} \dot{h}^k_{CF}[(zh^k)|_{A_CC} - (zh^k)|_{CB} - (zh^k)|_{CV_C} - (zh^k)|_{CF}]}{\sum_{k=1}^{K} (\dot{h}^k_{CF})^2} \tag{26.2}$$

$$C_{V_CB} = \frac{\sum_{k=1}^{K} \dot{h}^k_{V_CB}[(zh^k)|_{CV_C} + (zh^k)|_{BV_C} - (zh^k)|_{V_CS}]}{\sum_{k=1}^{K} (\dot{h}^k_{V_CB})^2} \tag{26.3}$$

$$C_{SF} = \frac{\sum_{k=1}^{K} \dot{h}^k_{SF}[(zh^k)|_{V_CS} + (zh^k)|_{FS} - (zh^k)|_{SV_S}]}{\sum_{k=1}^{K} (\dot{h}^k_{SF})^2} \tag{26.4}$$

$$C_{BF} = \frac{\sum_{k=1}^{K} -\dot{h}^k_{FB}[(zh^k)|_{V_CS} - (zh^k)|_{FB} - (zh^k)|_{A_BA_C} + (zh^k)|_{A_CC} - (zh^k)|_{CB} - (zh^k)|_{CV_C}]}{\sum_{k=1}^{K} (\dot{h}^k_{FB})^2} \tag{26.5}$$

$$C_{FV_{SC}} = \frac{\sum_{k=1}^{K} \dot{h}^{k}_{FV_{SC}} \left[(zh^{k})|_{A_B A_C} - (zh)|_{SV_{SC}}\right]}{\sum_{k=1}^{K} (\dot{h}^{k}_{FV_{SC}})^2} \tag{26.6}$$

$$C_{V_{SC}R} = \frac{\sum_{k=1}^{K} \dot{h}^{k}_{V_{SC}R}\left[(zh^{k})|_{A_B A_C} + (zh^{k})|_{V_{IC}V_{SC}} + (zh^{k})|_{A_B V_{SC}} - (zh^{k})|_{V_{SC}R_V}\right]}{\sum_{k=1}^{K} (\dot{h}^{k}_{V_{SC}R})^2} \tag{26.7}$$

$$C_{V_{IC}B_D} = \frac{\sum_{k=1}^{K} \dot{h}^{k}_{V_{IC}B_D} \left[(zh^{k})|_{A_B V_{IC}} - (zh^{k})|_{V_{IC}V_{SC}}\right]}{\sum_{k=1}^{K} (\dot{h}^{k}_{V_{IC}B_D})^2} \tag{26.8}$$

$$C_{R_V R} = \frac{\sum_{k=1}^{K} \dot{h}^{k}_{R_V R}\left[(zh^{k})|_{V_{SC}R_V} - (\eta zh^{k})|_{R_V L_V}\right]}{\sum_{k=1}^{K} (\dot{h}^{k}_{R_V R})^2} \tag{26.9}$$

$$C_{L_V R} = \frac{\sum_{k=1}^{K} \dot{h}^{k}_{L_V R}\left[(\eta zh^{k})|_{R_V L_V} - (\eta zh^{k})|_{L_V A_B}\right]}{\sum_{k=1}^{K} (\dot{h}^{k}_{L_V R})^2} \tag{26.10}$$

$$C_{A_B R} = \frac{\sum_{k=1}^{K} \dot{h}^{k}_{A_B R}\left[(\eta zh^{k})|_{L_V A_B} - (zh^{k})|_{A_B A_C} - (zh^{k})|_{A_B V_{SC}} - (zh^{k})|_{A_B V_{IC}}\right]}{\sum_{k=1}^{K} (\dot{h}^{k}_{A_B R})^2} \tag{26.11}$$

$$C_{B_D R} = \frac{\sum_{k=1}^{K} \dot{h}^k_{RB_D} \, [Q^k_R + Z_{V_{SC} V_{IC}} h_{V_{IC} V_{SC}}}{\sum_{k=1}^{K} (\dot{h}^k_{RB_D})^2} \tag{26.12}$$

$$C_{B_D A} = \frac{\sum_{k=1}^{K} \dot{h}^k_{B_D A} [Q^k_R + (z h^k)|_{A_B V_{IC}}}{\sum_{k=1}^{K} (\dot{h}^k_{B_D A})^2} \tag{26.13}$$

Thus, we have completed writing the numerical algorithms for estimating the $\underline{\underline{z}}$ and $\underline{C}$ values. The mean and temporal values of the fluxes, pressure and pressure rates are derived from phasic changes as depicted in Figs. 2-11.

Note that for the body system, the compartmental pressure and temporal rate of pressure change ride on the appropriate respiratory wave. However, for the cerebral system, this effect is attenuated.

We assume a respiratory pressure wave of the form

$$p_R = 10 \sin \omega_R t \tag{27}$$

where $\omega_R = \frac{2\pi}{T_R}$ is the inspiration/respiration frequency, and $T_R \, (= 3.4\text{sec.})$ is taken as the respiratory cycle time.

We use the following altitude values:

H_{B_D} = 110 cm.	$H_{V_{SC}}$ = 140 cm.	H_{V_C} = 163 cm.
H_R = 135 cm.	$H_{V_{IC}}$ = 126 cm.	H_B = 163 cm.
H_{R_V} = 130 cm.	H_{A_B} = 116 cm.	H_F = 163 cm.
H_P = 130 cm.	H_{A_C} = 160 cm.	H_S = 163 cm.
H_{L_V} = 130 cm.	H_C = 163 cm.	

corresponding to a standing position. Also, we choose the following values for pressure and rates of pressure changes:

$$p_C = 30mm.Hg. \;;\; \dot{p}_C = 0$$
$$p_S = 2mm.Hg. \;;\; \dot{p}_s = 0$$
$$p_{V_{IC}} = 5mm.Hg. \;;\; \dot{p}_{V_{IC}} = 0 \;.$$

This concludes the calibration scheme for the brain-body compartmental model, with conductivities and compliances that remain constant during long time intervals.

5. PRESSURE WAVES

Once the linear model described by (10) has been calibrated, it is possible to obtain solutions for the pressure waves in all brain-body compartments. In incremental form, the solution of the differential matrix equation (10) for $\underline{h}$ is

$$\underline{h}_{(t+\Delta t)} = \exp(-\tau)[\underline{h}_{(t)} - \underline{\underline{z}}^{-1}\underline{Q}_{(t)}] + \underline{\underline{z}}^{-1}\underline{Q}(t) \;. \tag{28}$$

Here, $\Delta t\,(= t^{m+1} - t^m)$ denotes a time difference between the frontier time level, t^{m+1}, and the backtime, t^m. The matrix τ reads

$$\tau = \Delta t\; \underline{\underline{C}}^{-1}\underline{\underline{z}} \tag{29}$$

The rational expansion of $\exp(-\tau)$, leads to the following formula

$$\exp(-\tau) \cong \frac{\underline{\underline{I}} - (1-\theta)\tau}{\underline{\underline{I}} + \theta\tau} \quad (0 \le \theta \le 1) \tag{30}$$

in which $\underline{\underline{I}}$ is the unit matrix. Substituting (29) and (30) into (28), yields

$$\underline{h}_{(t+\Delta t)} = (\underline{\underline{I}} + \theta\tau)^{-1}[\underline{\underline{I}} - (1-\theta)\tau][\underline{h}_{(t)} - \underline{\underline{z}}^{-1}\underline{Q}_{(t)}] + \underline{\underline{z}}^{-1}\underline{Q}^{(t)} \;. \tag{31}$$

The coefficient θ controls the type of numerical solution scheme evolving in time. When $\theta = 0$, we have an explicit scheme $\theta = 1$, an implicit scheme, and $0 < \theta < 1$ is the mixed

scheme case.

Thus, with the choice of θ, the head waves in the various compartments are calculated according to (10). In view of (3) and (31), we can also evaluate the compartmental pressures

$$\underline{p}_{(t+\Delta t)} = \{(\underline{\underline{I}}+\theta\tau)^{-1}[\underline{\underline{I}}-(1-\theta)\tau][\underline{h}_{(t)}-\underline{\underline{z}}^{-1}\underline{Q}_{(t)}] + \underline{\underline{z}}^{-1}\underline{Q}_{(t)}-\underline{H}\}\gamma \qquad (32)$$

This completes the modelling of the brain-body perfusion pressure, as excited by environmental pressure and due to inspiration/expiration flux.

6. CONCLUSION

A compartmental model for perfusion pressure interplay between the cerebral, respiratory and heart systems is presented. The perfusion pressure response is initiated by compartments altitude, environmental pressure and inspiration/expiration flux.

Flow between compartments is governed by compartmental step function related conductivities and compliances that take the forms of time step functions.

Once the calibrated model is available, it will be used for the prediction of phasic pressures associated with perfusion, and the influence of various situation such as:

I: Flight maneuvers, subjecting the body to acceleration forces of several times the gravity acceleration (g), in the direction of head to foot.

The idea here is to increase the gravity head (which is part of the hydrodynamic head) gradually, in order to check its effect on the resulting perfusion fluxes, especially the influx to the arterial cranium and those in the cerebral system. Parameters influencing the deterioration of cerebral flux curves, manifesting the so-called "blackout", can also be investigated. For example, the effect can be studied of different inhale/exhale and/or different relative positioning between head-body, in overcoming the characteristics of phasic pressure curves resulting from the excessive g values.

II: High/low altitudes and vacuum, generating extreme environmental cases.

Such situations affect the pattern of inhale/exhale (amplitude and periodicity). These affects on

the phasic pressure, can be studied, taking into account possible changes in fluid density. In addition, at high altitudes, the fluid's viscosity varies and this, in turn, affects the conductance (inversely).

III: Different inhale/exhale maneuvers.

We intend to examine the response of phasic pressures in the various model compartments, for example, to artificial inhale/exhale, as applied in resuscitation.

IV: Different relative positioning of the Brain-Body as in physical exercises. We intend to check the influx, for example, into the common carotid artery, due to tilting the body relative to the head. Another example is the case of standing upside down.

V: Different degrees of occluding the heart and body conductances.

This relates, for example, to resuscitation procedures in which the abdominal and the respiratory systems are brought under cyclic pressure variations. In our model, this may cause changes in the conductances and compliances of the body model.

The developed model can be used to guide the neurosurgeon in the interpretation of possible consequences of management methods applied to abnormal cases. Following are some examples of management maneuvers that can be interpreted by numerical experiments of the model.

(a) Correction of a fault if recognizable and accessible, e.g., tumours, blockage of flow channels. This is the ideal case.

(b) Offsetting of destructive tensions that, usually, would be of short duration, e.g., reducing excess pressure usually done by shunting the CSF volume.

(c) Correcting mechanisms that fail to confine or maintain the system in optimal yielding against repeated stress in the long term, e.g., introducing a gas bubble in a sac into the large hydrocephalic ventricle in order to hold down the pressure peaks and create better Pressure-Volume-Time relationship.

In practice, the management of (b) is on the CSF bulk, where as for (c) it also involves the blood volume as an indirect means of promoting optimum flux.

The model can provide information for fault-finding, target identification and monitoring the results of rational management.

ACKNOWLEDGEMENT

This paper is part of a research program on Modelling Brain Mechanics and Chemical Process, conducted in the Julius Silver Institute, Department of Biomedical Engineering, Technion-Israel Institute of Technology, Haifa, Israel. The research is sponsored in part by the U.S. Air Force (grant AFOSR-85-0233). The support of the Michael Kennedy Leigh Fund, London, and the British Technion Society is highly appreciated.

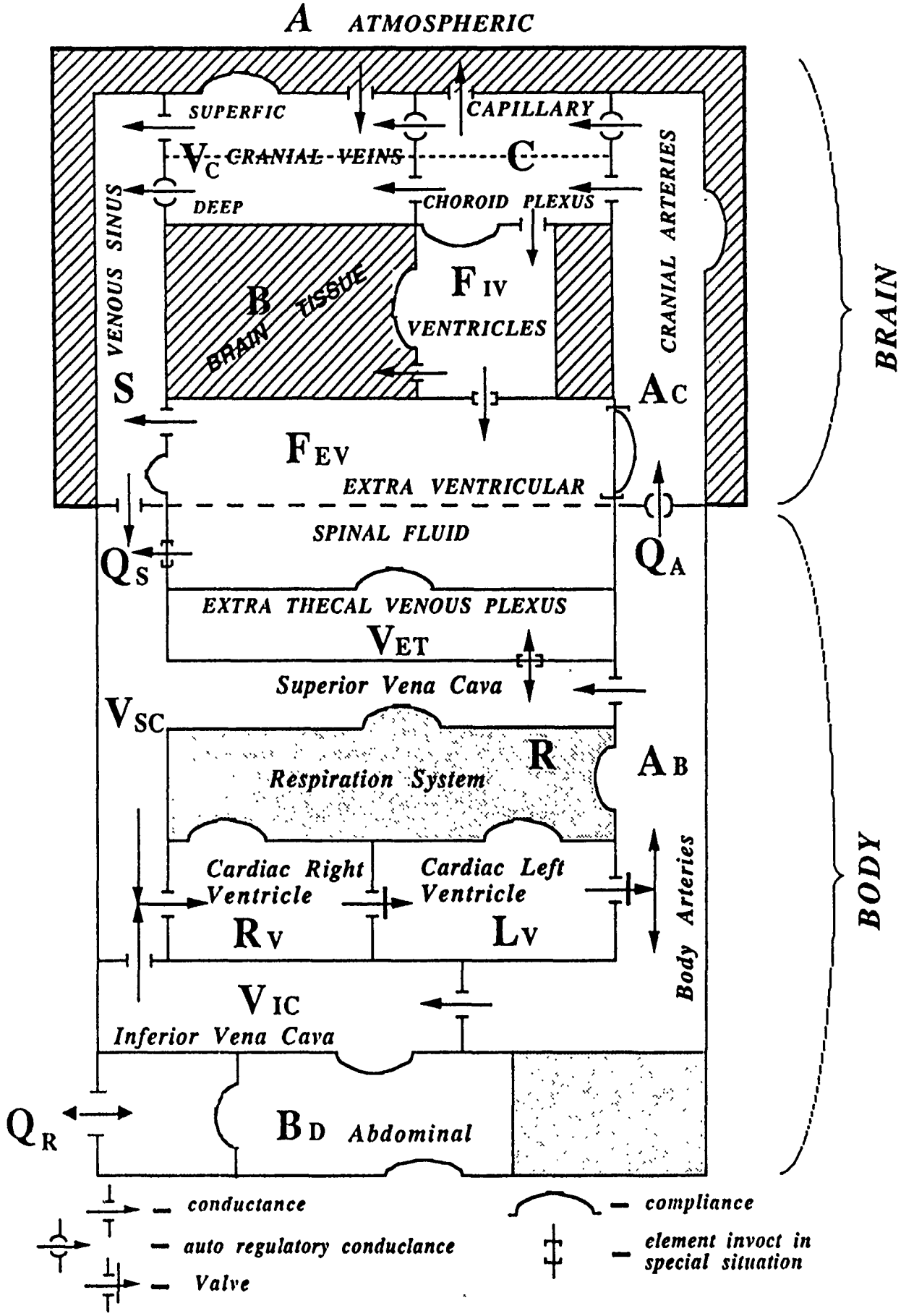

Figure 1: Cerebral - Body compartmental design.

TYPICAL PRESSURE IN Ac

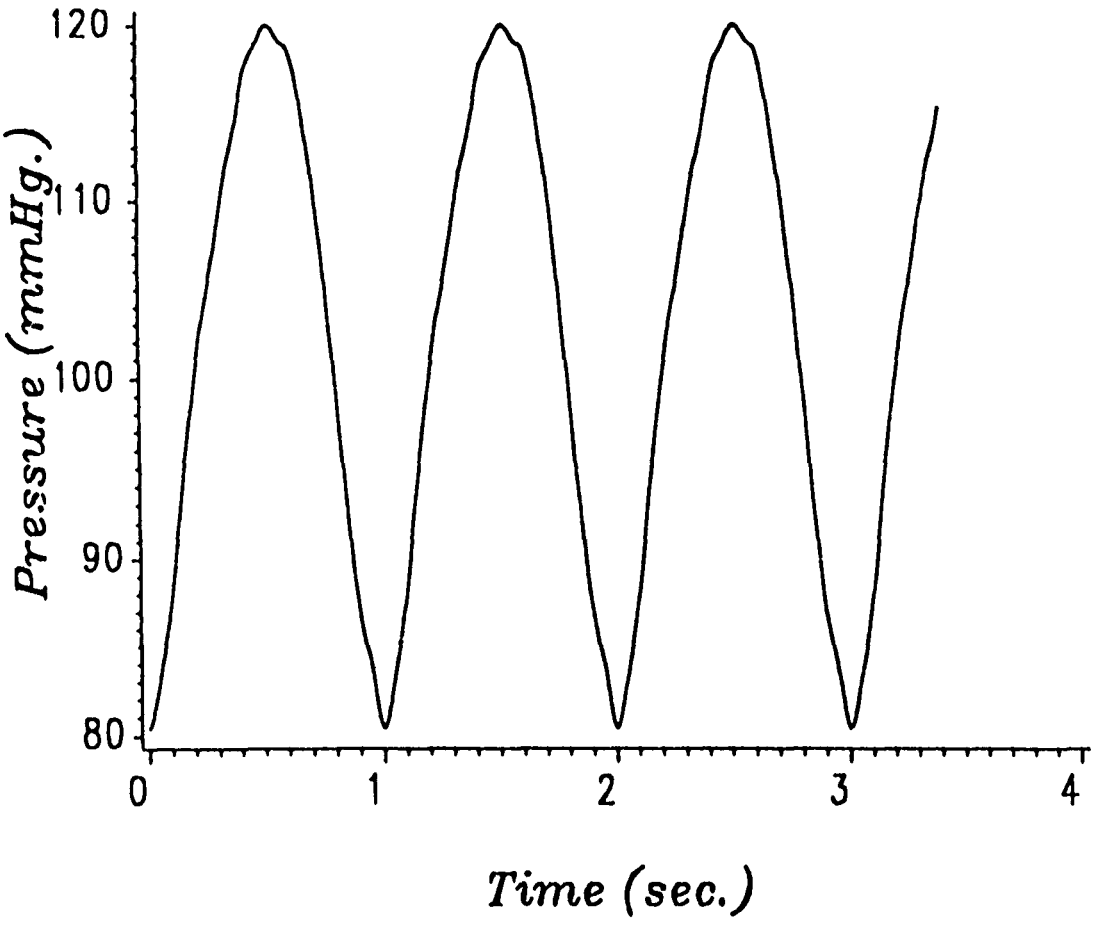

Figure 2: During one cycle of breathing (after Hamit et al.)

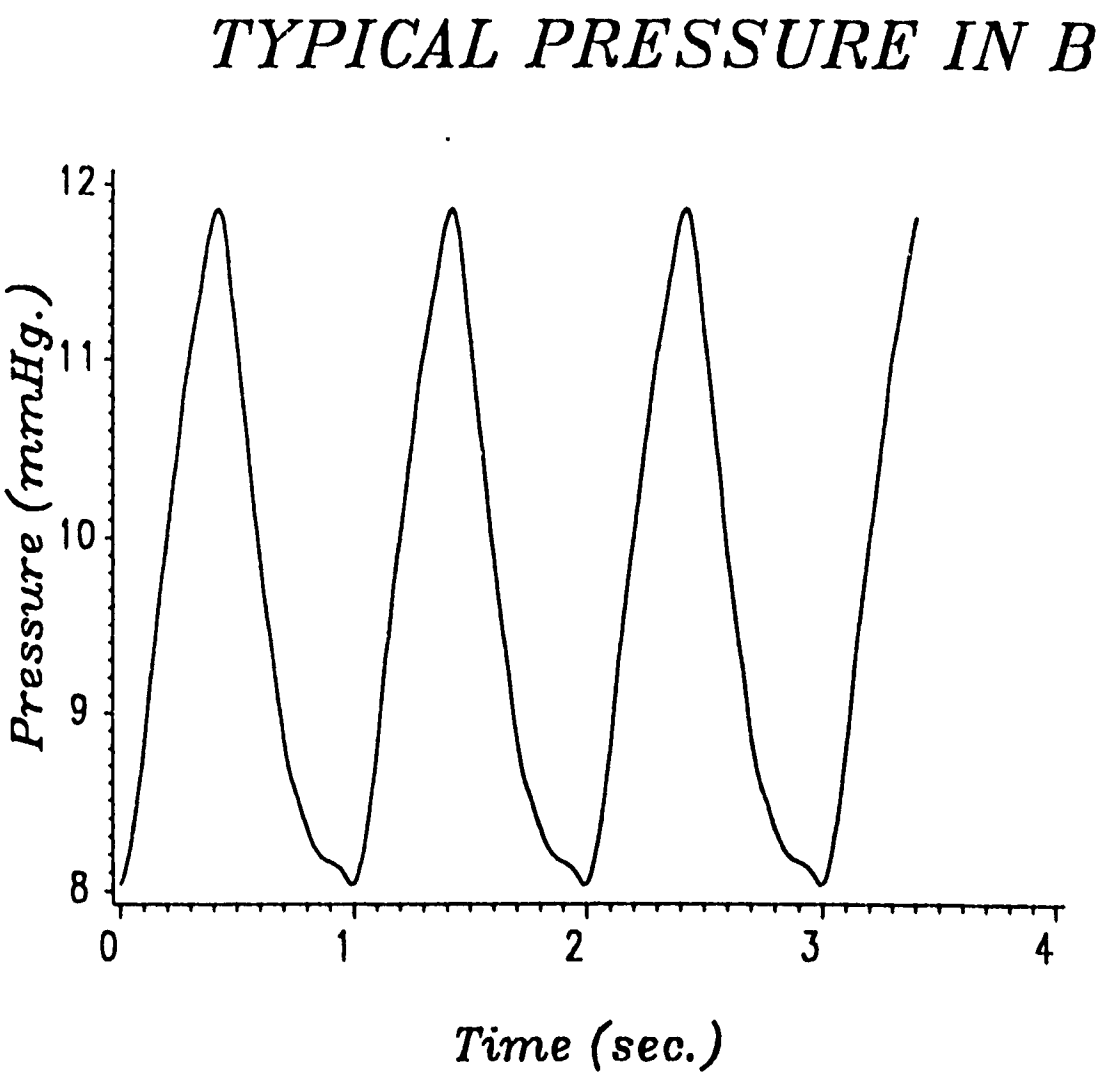

Figure 3: During one cycle of breathing (after Hamit et al.)

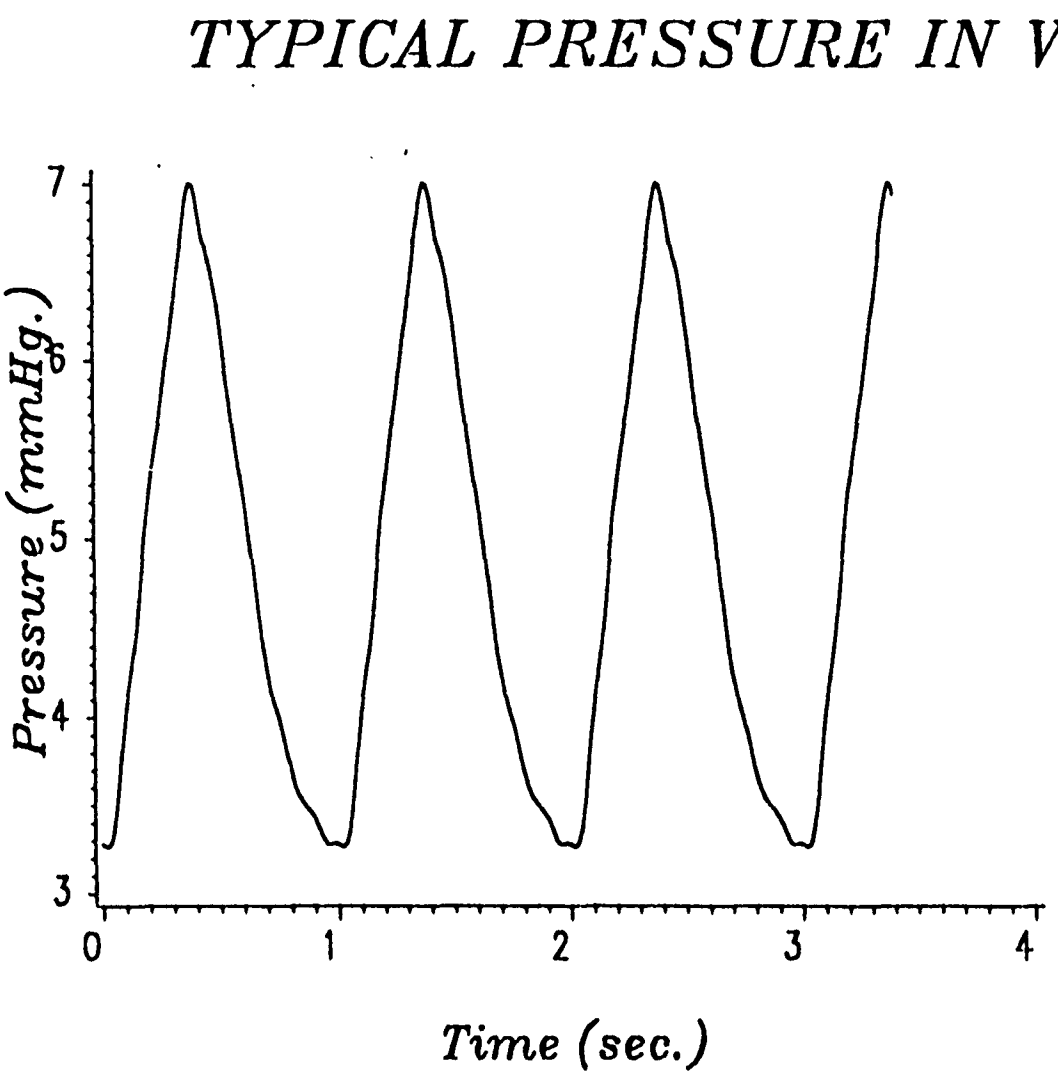

Figure 4: During one cycle of breathing (after Hamit et al.)

TYPICAL PRESSURE IN F

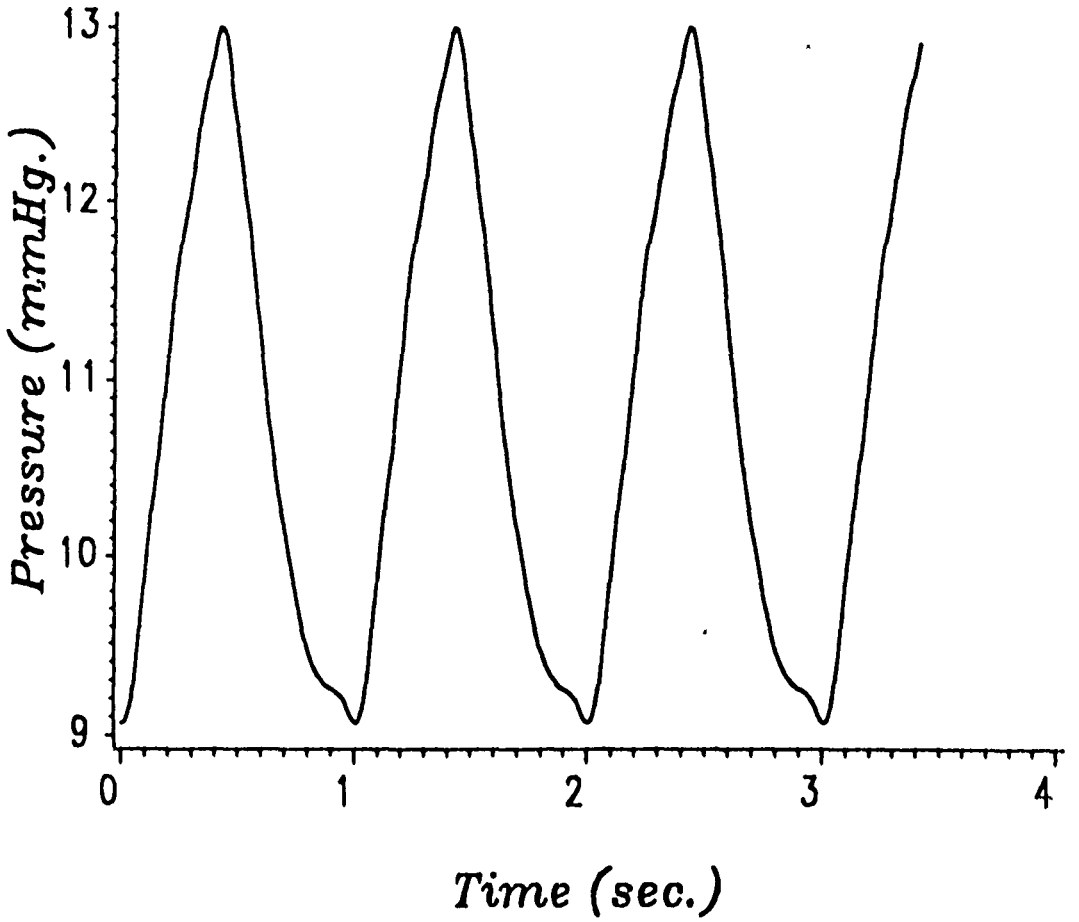

Figure 5: During one cycle of breathing (after Hamit et al.)

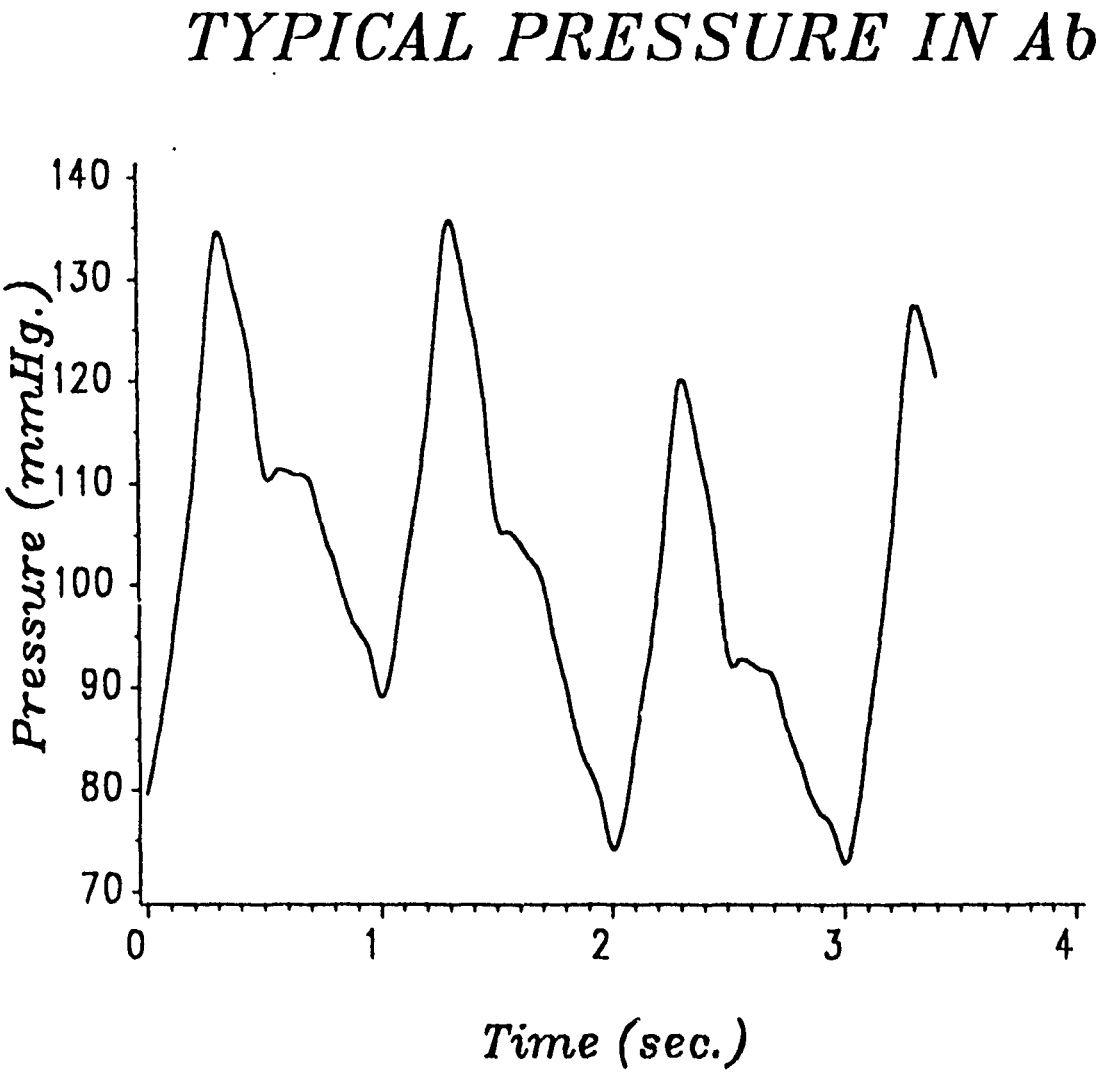

Figure 6: During one cycle of breathing (after Shepherd et al.)

TYPICAL PRESSURE IN Lv

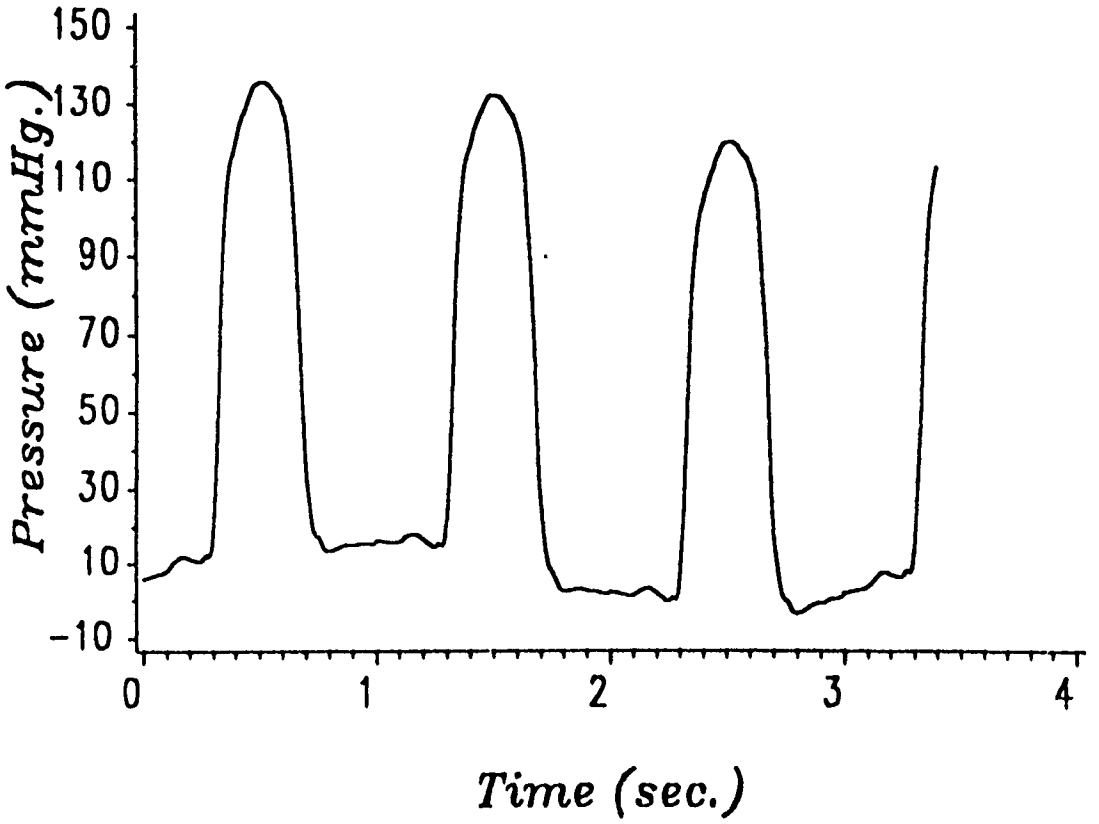

Figure 7: During one cycle of breathing (after Wiggers)

TYPICAL PRESSURE IN Rυ

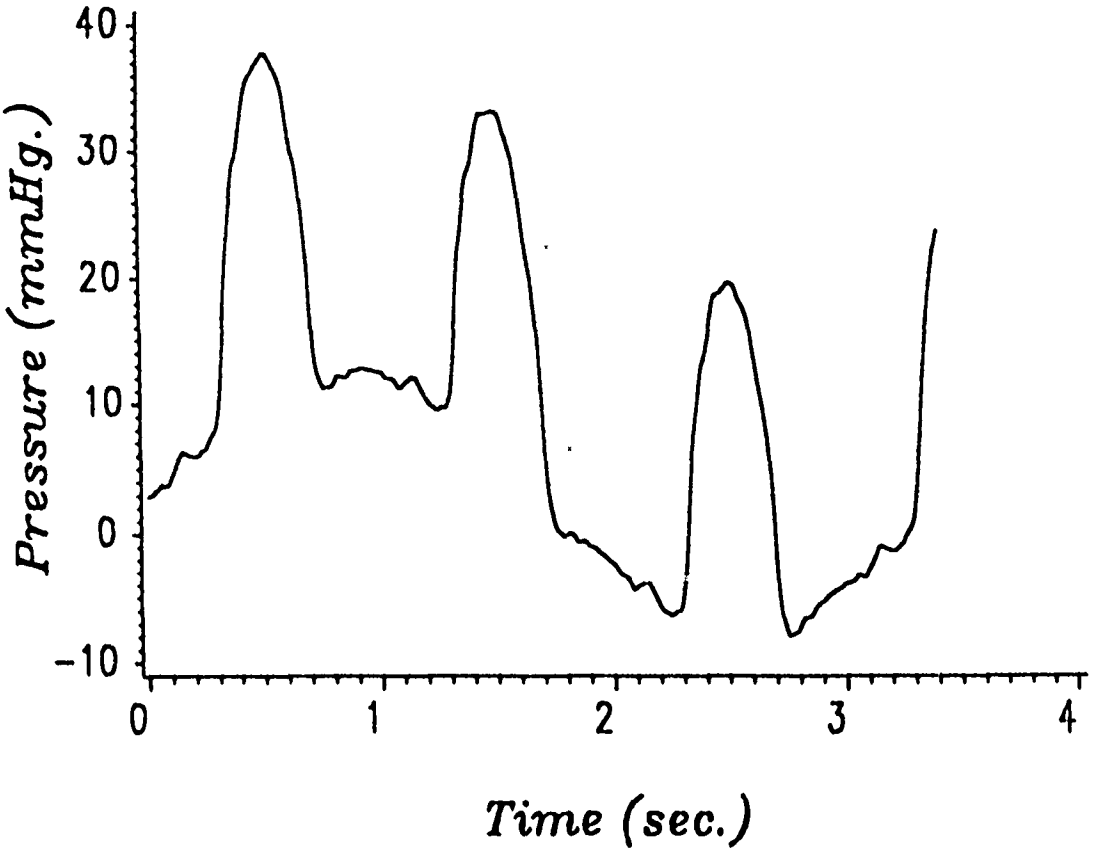

Figure 8: During one cycle of breathing (after Vernon et al.)

TYPICAL Inspiration/Expiration FLUX

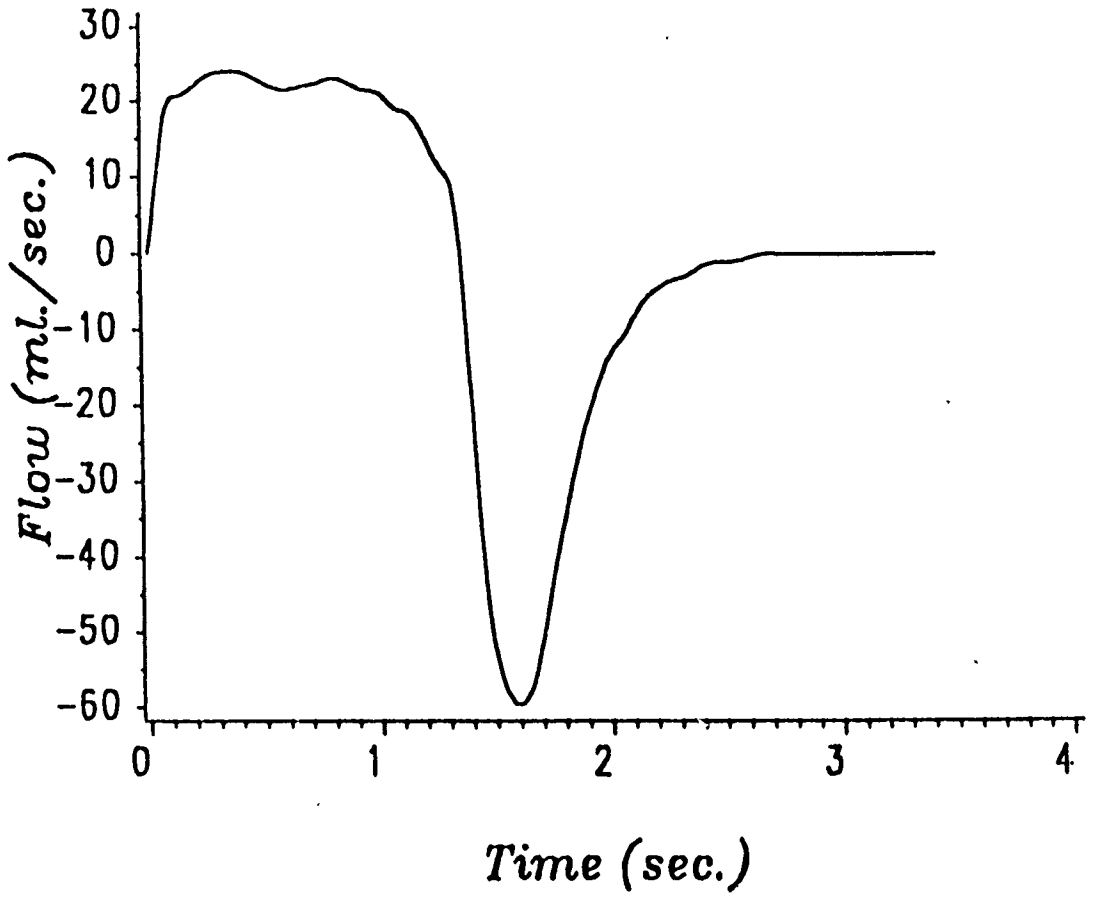

Figure 9: During one cycle of breathing (after Ben Haim et al.)

TYPICAL AORTIC FLOW

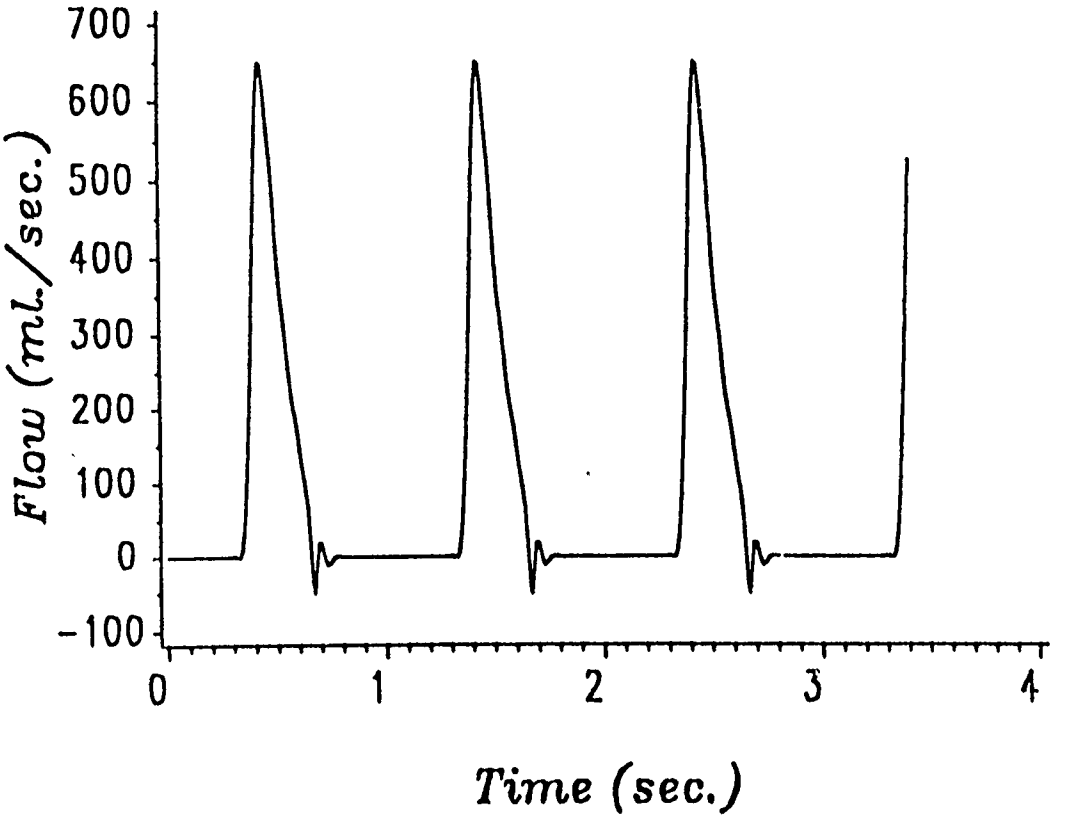

Figure 10: During one cycle of breathing (after Vernon et al.)

REFERENCES

A. A., Shoukas and K. Sagawa (1973).
Control of total systemic vascular capacity by the carotid sinus baroreceptors reflex, Circulation Research, 33,

S.A. Ben-Haim, U. Dinnar and G.M. Saidel (1988).
The effect of expiratory airflow obstruction on cardiac output during Cardio-Pulmonary Resuscitation (CPR): A mathematical simulation and experimental studies, J. of Critical Care, 3, 240-248.

R. W. P. Cutalar (1986).
Formation and observation of CSF in man, Brain, 9, 70.

J.M. Goldman, L.S. Rose, M.D.L. Morgan and D.M. Denison (1986).
Measurement of abdominal wall compliance in normal subjects and tetraplegic patients, Thorax, 41, 513-518.

A. C. Guytun (1969).
Function of the human body, 3rd ed. W.B. Saunders, Philadelphia.

H. F. Hamit, A.C. Beal, Jr. and M.E. DeBakely (1965).
Hemodynamic influences upon brain and cerebrospinal fluid pulsations and pressures, J. Trauma, 5, 174-184.

Z. Karni, J. Bear, S. Sorek and Z. Pinczewski (1987).
Quasi-steady-state compartmental model of intracranial fluid dynamics, Med. & Biol. Eng. & Comput., 25, 167-172.

G. Kellie (1824).
An account ..., with some reflections, on the pathology of the brain, Edin. Med. Chir. Soc. Trans., 1, 84-169.

J. Munro (1783).
Observations on the Structure and Functions of the Nervous System, W. Creech, Edinburgh.

J.T. Shepherd and P.M. Vanhoutte (1980).
The Human Cardiovascular System Facts and Concepts, Raven Press, New York.

S. Sorek, J. Bear and Z. Karni (1988).
A Non-Steady Compartmental Flow Model of the Cerebrovascular System, J. of Biomechanics 21, 9, 695–704.

S. Sorek, J. Bear and Z. Karni (1989).
Resistances and Compliances of a Compartmental Model of the Cerebrovascular System, Annals of Biomedical Eng., 17, 1-12.

B. Vernon, Mountcastle (Eds.) (1980).
Medical Physiology, 14th ed. St. Louis, Mosby.

C. J. Wiggers (1952).
Circulatory Dynamics, Grune and Stratton, New York.

NONSTEADY COMPARTMENTAL MODEL OF INTERACTIVE PERFUSION BETWEEN CEREBRAL AND BODY SYSTEMS II. SENSITIVITY ANALYSIS

S. Sorek[1], O. Lichtenstein[2], J. Bear[3], M. Feinsod[4] and S. Ben-Haim[5]

Abstract

A sensitivity analysis is performed in a lumped parameter model, focusing on the dynamic flow and pressure interactions between the cerebral, cardiovascular and the pulmonary systems.

The interrelated pressures and fluxes are excited by left cardiac pressure, by expiratory/inspiratory fluxes and by pressure exerted on the abdominal. The analysis examines changes in pressure and flux at the cerebral carotid arteries and capillaries resulting from a sudden rise of the body to an upright position, changes in inhale/exhale flux patterns, pressurizing the abdomen, changes in gravity acceleration, changes in blood viscosity and changes in heart frequency. Results are consistent with available clinical information and the outcome may be explained, qualitatively, on the basis of understanding the physiological mechanisms and on clinical observations.

Key Words: Compartmental modelling; perfusion flux and pressure; cerebral, cardiac and respiratory systems; conductances; compliances; gravity acceleration; cardiac and abdomen pressure amplitude and frequency; carotid and capillary to brain tissue influx.

[1] J. Blaustein Institute for Desert Research, Ben-Gurion University of the Negev, Sede Boker Campus 84990, Israel
[2] Bio-Medical Engineering, Technion, Haifa 32000, Israel
[3] Civil Engineering, Technion, Haifa 32000, Israel
[4] Department of Neurosurgery, Technion, Haifa 32000, Israel
[5] School of Medicine, Technion, Haifa 32000, Israel

A. Introduction

In the first paper (Sorek et al. 1990) a model was presented, in which the brain-body system was conceptualized as a compartmental configuration, representing lumped vessels and ventricles of similar physiological functions in transmitting perfusion flow. Physical laws, expressing fluid's mass and momentum balances, were then formulated and combined to form a set of equations that relate pressures to fluxes, using time step functions of conductances and compliances. The same concepts, when applied to modelling brain mechanics (Sorek et al., 1988a) suggested a possibility of excessive fluid accumulation in the ventricles, due to occluding perfusion between capillaries and brain tissue (i.e. blood-brain barrier). Actual brain surgery of an elderly patient suffering from Normal Pressure Hydrochephalus (NPH), verified this prediction (Sorek et al., 1988b). Conductances and compliances were then estimated by an inverse method (Sorek et al, 1989b). With these estimated values, temporal variations of pressure in the various compartments were derived by solving the model, subject to a given pressure cycle at the cerebral artery (Sorek et al., 1988c). The simulated temporal pressure variations of the Jugular Bulb and that of the Venous Sinus, demonstrated suction intervals during the pressure cycle. It was demonstrated that increasing drainage through a shunt implanted in the ventricles may cause intensified deterioration of the characteristic pressure curve of the ventricular CSF. These features are consistent with clinical observations and, together with previous results, justified the use of the compartmental brain mechanics model, CBMM (Sorek et al., 1988a).

Next, a multi compartmental brain-body (MCBBM) (Sorek et al., 1990) was constructed to account for various situations, such as:

A) Flight maneuvers subjecting the body to dynamic forces of several g (gravity acceleration) magnitudes in the direction of head to foot.

B) High/low altitudes and suction, generating extreme environmental cases.

C) Different respiratory maneuvers.

D) Different relative positioning between the brain and the body, as in physical exercises.

E) Different patterns of pressuring the abdomen.

F) Simultaneous application of a combination of the above maneuvers, as in the case of resuscitation.

Measurements of the actual changes in hemodynamics during these maneuvers is reported in the literature. Blood pressure changes during orthostatic testing (Wolthuis et al., 1979; Fulco et al., 1985); alteration in heart rate following linear accelerations (Lauritzen et al., 1987); perfusion pressures as well as intracranial pressure distribution at different head elevations (Rosner and Coley, 1980); changes in the venous pressures during orthostatic testing (Jonson and Rundcrantz, 1969) as well as alteration in cardiac output, total peripheral resistance following head-down tilt (London et al., 1983) were all reported and are a short listing of recent experimental literature. Most of these reports cannot delineate the direct effect of the maneuver studied on the cardio vascular system from the compensatory, reflex response brought about by the antonomic nervous system. Our approach may supply an analysis framework with which the direct effect of the studied perfurbation can be assessed.

The compartmental setup, as described in the first paper, is comprised of six cerebral compartments and eight compartments assigned to the body system (Fig. 1). Excitation of the model is imposed via respiratory fluxes, by activation pressure of the left cardiac ventricle and by external pressure exerted on the abdomen.

Let us first briefly discuss the theoretical base for constructing the flow equations for the brain-body compartmental assemblage. The sensitivity analysis will then follow, with the objective of assessing the influence of the aforementioned maneuvers, subject to the prescribed excitations driving the model.

B. Governing equations

Practically, within the range of regular brain-body functioning, we may regard its interconnecting fluid phases (i.e. blood and Cerbro Spinal Fluid, CSF) as being incompressible, not a function of constituents' concentrations and independent of temperature.

Therefore, for each compartment, we consider the mass and momentum balance expressions for a single fictitious fluid phase of constant density.

Each such balance equation states that the temporal increase of an extensive quantity of the fluid, here mass or momentum, within a compartment is equal to the net influx through the compartment's boundaries, plus the resultant sum of the external sources of the considered quantity.

For a constant density fluid, and for a compartment with a finite time dependent volume, the fluid mass balance reduces to a balance equation in the form

$$\frac{dV_n}{dt} + \sum_j q_{nj} - \sum_i q_{in} = Q_n - W_n \quad (1)$$

where $V_n(t)$ denotes fluid's volume within compartment n at time t, q_{nj} denotes the efflux from compartment n to the adjacent j one, through their common boundary, and q_{in} denotes influx to compartment n from compartment i, through their common boundary; Q_n denotes a source due to the injection fluid into compartment n and w_n denotes a sink ejection fluid out of compartment n. A storage argument is introduced as a result of the non-rigidity of the compartment boundaries. This is expressed by a time step compliance factor, C_{nl}, say at the mutual boundary between compartment n and l, defined by

$$C_{nl} = \frac{dV_n}{d(P_{nl})} , \quad (2)$$

where $P_{nl}(\equiv P_n - P_l)$ denotes the pressure difference between compartments n and l, on both sides of their common boundary.

For a viscous fluid moving slowly through a capillary tube, the compartmental momentum balance reduces to a linear proportionality between the flux crossing a compartmental boundary and the pressure and elevation difference on both sides of the boundary. Hence, for the flux leaving compartment n into compartment j through their common boundary nj, we write

$$q_{nj} = Z_{nj} (P_{ng} + \rho g H_{nj}), \quad (3.1)$$

where Z_{nj} denotes a conductance factor between compartment n and j; p denotes the fluid density; g denotes the gravity acceleration, and H_{nj} ($\equiv H_n - H_j$) denotes the elevation difference between compartments n and j. Similarly, for the flux entering compartment n from its adjacent one, i, through their common boundary, in, we write.

$$q_{in} = Z_{in} (P_{in} + \rho g H_{in}), \qquad (3.2)$$

The lumped conductance Z_{nj} (or Z_{in}) is assumed constant for long time periods.

Actually, expressions (3) relate to the differential form of the fluid's linear momentum balance equation known as Darcy's law, which is used in a continuum approach to flow through a porous medium. These equations may be interpreted as the integration of Darcy's law over a volume surrounding a common boundary of two compartments interacting by flow (Adar and Sorek, 1989a). Hence, like the permeability appearing in Darcy's law so is the conductance a function inversely proportional to fluid's viscosity (μ).

Upon substituting (2) and (3) into (1), we obtain a flow equation for each compartment n, in the form

$$\sum_l C_{nl} \frac{dP_n}{dt} + \left[\left(\sum_j Z_{nj} + \sum_i Z_{in} \right) P_n \right] - \left(\sum_l C_{nl} \frac{dP_l}{dt} + \sum_j Z_{nj} P_j + \sum_i Z_{in} P_i \right)$$

$$= Q_n - W_n + \rho g \left(\sum_i Z_{in} H_{in} - \sum_j Z_{nj} H_{nj} \right). \quad (4)$$

Note that a change in g levels introduces a modification of the driving force (i.e. the l.h.s. of (4)). A change in viscosity will produce an inverse change in all of the conductance terms on both sides of (4).

Given an initial setup of pressures in the various compartments we solve the set of equations (4) for the temporal pressure values, subject to prescribed time dependent values of

respiratory flux, external pressure exerted on the abdomen and activation pressure on the left ventricle.

C. Sensitivity analysis

The objective of this sensitivity analysis is to assess the clinical outcome when subjecting the brain-body system to changes in various control variables (e.g. changing the relative positioning between body and head), or changing the amplitude and frequency of the driving excitations (e.g. cardiac activation pressure, or external pressure applied on the abdomen). We focus on the resulting pressure at the carotid arteries and the cerebral capillaries, as well as on the influx into the arteries and from the capillaries into the brain tissue. In doing so, we may understand and predict clinical syndromes based on brain-body flow communications, such as the "black out" phenomenon experience by pilots in excessive g flights, or various resuscitation maneuvers.

Actually, in order to solve for the pressures in (4), from which we can then obtain the fluxes by employing (3), we need to know the true values of the conductances and the compliances. To evaluate these values, we should resort to some inverse process, such as the one described by Sorek et al. (1989b).

The estimation of these parameters will be reported in the future. Instead, we assume here, based on average fluxes and pressures, a set of values for the parameters. These values are so selected as to meet the prescribed flow direction between the compartments. Since the compliances and conductances are assumed to be constant within long time periods, we may check sensitivity expressed in terms of deviation from normal (average) variations of the selected state variable. Denoting α as the time dependent state variable (flux, or pressure), we express the normal value of α $\left(\alpha_n^*\right)$,by

$$\left(\alpha_n^*\right) = \frac{\alpha - \alpha_{ave}}{\alpha_{ave}} \qquad (5)$$

where α_{ave} denotes the average value of α over a time period, T_R, defined by

$$\alpha_{ave} = \frac{1}{T_R} \int_{T_R} \alpha dt \qquad (6)$$

We start our sensitivity analysis by asking whether we can verify the model against results known qualitatively.

Obviously the model does not include control mechanisms. For example, in a real physiological system we may sometimes observe an immediate influence due to neoronical, biochemical and mechanical regulation on, say, the pressure difference. The model, however, describes flow interrelations and, as such, its predictions are important in showing the result that may take place when control is malfunctioning.

The sensitivity to a sudden rise of the body to an upright position is shown in Figs. 2 and 3. Note the general trend of reduction in pressure in the body arteries, A_b (Fig. 2a), cerebral arteries A_c (Fig. 2b), cerebral capillaries, C (Fig. 3a) and in the cerebral ventricles, F (Fig. 3b), similar to results measured by Rosner et al. (1980). This serves as a reasonable validation of the reliability of the developed model.

The sensitivity to changes in respiratory flux is shown in Fig. 4. Note that a 50% change in amplitude yields only slight deviations at the end of the diastole in the influx from body to brain (Fig. 4a), as well as in the flux from capillaries to brain tissue (Fig. 4b). Hyperventilation results in the reduction of intracranial pressure, expressed in reducing the volume associated with changes of high inspiratory volume and frequency, but not in substantial flux changes. Therefore, Fig. 4 describes a valid situation within the accepted metabolism.

The sensitivity of flow in the carotid arteries and that between capillaries to brain tissue, to changes in cardiac driving pressure is shown in Figs. 5a and 5b, respectively. Note that a higher cardiac pressure may cause an amplification of brain tissue impedance, which, in return, will yield a lower capillary to brain flux (Fig. 5b).

The sensitivity to external pressure applied to the abdomen, is described in Fig. 6. The importance of synchronization with the driving heart cycle is demonstrated by comparing the

normal flow at the carotid arteries (Fig. 6a) and the one from capillaries to brain tissue (Fig. 6b). Note that although a higher external pressure is exerted, the sudden relief of the abdomen, creates a suction at some portions of the cycle and a flow buildup at others. This suggests an intensive pressure rise followed by a slow relief, accommodated by synchronization with heart cycle.

The sensitivity to changes in gravity acceleration and its impact on pressure and flow, is shown in Figs. 7, 8 and 9, respectively. Two extreme maneuvers are exemplified. The first simulates an uplift with a 4g acceleration. The second represents the simulation of going downward at an acceleration of 0.5g. In the first case, the body will experience a resultant acceleration of 5g directed from foot to head, while in the second one, the resultant acceleration of 0.5g will prevail. Note that in the 5g case (Figs. 7 and 8), a pressure buildup to and over the normal peak during the systole is indicated. However, a steep fall is exhibited during the diastole. This indicates a suction action which may reduce the oxygen level at that instant. The o.5g maneuver lowers the pressures accordingly, but causes a moderate fall from the systole peak to diastole. A similar behavior is demonstrated with regard to flow into the carotid arteries and to the one between capillaries and brain tissue (Fig. 9). Note the suction towards the end of the diastole period (Fig. 9a), associated with a steeper (compared to the 0.5g curve) fall in flow. Fig. 9b, showing the 5g case, strongly suggests a possible, so-called, "luxury perfusion", in which natural anatomic shunts (collaterals) are opened to by-pass sudden amplification of capillaries to brain tissue flow. In such a case, the tissue does not receive a sufficient supply of nutrients and the outcome may be the so-called "blackout" phenomenon.

The sensitivity to change in blood viscosity, affecting carotid and capillaries to brain tissue flow, is described in Figs. 10a and 10b, respectively. Lowering blood viscosity, which may take place at high altitudes, will reduce the flow into the carotid arteries (Fig. 10a), but will increase the capillaries to brain tissue flow (Fig. 10b). This, in return, may deplete the intake of oxygen by the tissue, which may result in a feeling of dizziness experienced at high altitudes.

Actually, Fig. 10a represents a prediction that may contradict clinical observations. We may explain this as an artifact of not using correct conductances. Lowering viscosity increases

the conductances and may thus result in lowering the influx into the carotid arteries at the expense of influx through other boundaries into surrounding compartments.

The sensitivity of the carotid influx to simultaneous changes in the frequency of cardiac activation pressure and magnitudes of the gravity acceleration, is shown in Fig. 11. Note that the relative flow surfaces depicted in Figs. 11 and 16 are the flow mean value (i.e., time integral over respiration cycle of temporal flow divided by respiration time interval) for each combination of g level and heart frequency and abdominal pulse frequence, respectively. Two cross-sections of the relative carotid flow surface of Fig. 11 are described in Figs. 12. It is demonstrated (Fig. 12a) that when experiencing an excess of 5.5g, lowering of heart frequency will result in gaining higher flow into the carotid arteries. On the other hand, when in values lower than the normal g ($g\% < 0$), this flow remains constant up to approximately 50% of the regular heart frequency. Two sections, at high and low heart frequencies (fig. 12b), predict a turning point (at about 1g value) of a higher flow for a higher g magnitudes and comparably lower flow rate for g values smaller than the normal one. This is more pronounced for lower frequency values.

The sensitivity of the carotid influx to simultaneous changes in the amplitude of the pulse pressure exerted on the abdomen and the g magnitudes, is described in Fig. 13. Figure 14a demonstrates that for excessive g values, the carotid flow will increase, while increasing the external pressure amplitude. This phenomenon is reversed when considering g values lower than normal. Fig. 14b exhibits the same phenomenon as that described in Fig. 12b. However, note the decrease in carotid flow beyond twice the regular g value. The carotid flow surface as a function of the frequency of the outside pressure applied to the abdomen and change of g levels, is depicted in Fig. 15. Figure 16a describes (in the case of excessive g values) a trend of increasing the carotid flow when the outside pressure frequency is lowered. Note also the support in raising the flow when this frequency meets the cardiac frequency. Figure 16b is similar to Fig. 14b.

D. Conclusion

A sensitivity analysis was carried out on a compartmental unsteady perfusion model that describes the brain-body flow system.

The sensitivity analysis was applied to various maneuvers in order to check the influence of changing control variables and excitations on pressure and flow levels at the carotid arteries and transmission between capillaries and brain tissue.

The results indicate that:

- A sudden rise causes the lowering of pressure at the cerebral arteries, capillaries and ventricles.
- Changes in inhale/exhale pattern is consistent with the Hyperventilation phenomenon that causes the reduction of inhale volume and does not change significantly vascular influxes.
- Changes in cardiac activation pressure produce a reduction of flow between capillaries and brain tissue.
- When subjecting the abdomen to outside pressure, it is important to synchronize the cycle with that of the heart.
- Excessive magnitudes of g cause an increase of influx from capillaries to brain tissue. This may be interpreted as the luxury perfusion situation which bypasses the flow with the nutrients it carries (through newly opened collaterals) and result in a "blackout" phenomenon.
- In low viscosity situation (e.g. when at very high altitude) the flow between capillaries to brain tissue increases. This (although not to the same degree as in excessive g magnitudes) may cause a sense of dizziness due to the depletion of some oxygen, following the above mentioned mechanism.
- Simultaneous changes of heart frequency and gravity acceleration predict that at excessive g levels the lowering of heart frequency will yield the rise of influx into the carotid arteries.
- Simultaneous change of amplitude of pressurizing the abdomen and changes of g magnitudes yield the rise of carotid influx when increasing pressure amplitude, at excessive g levels.

- Simultaneous change of the frequency of pressurizing the abdomen and changes of g magnitudes predicts the increase of the carotid flow upon lower pressure frequency.

Now that we have assessed the behavior of the brain-body model under various conditions, the next step will be to evaluate values for the various conductances and compliances. This will be reported, separately, in the future.

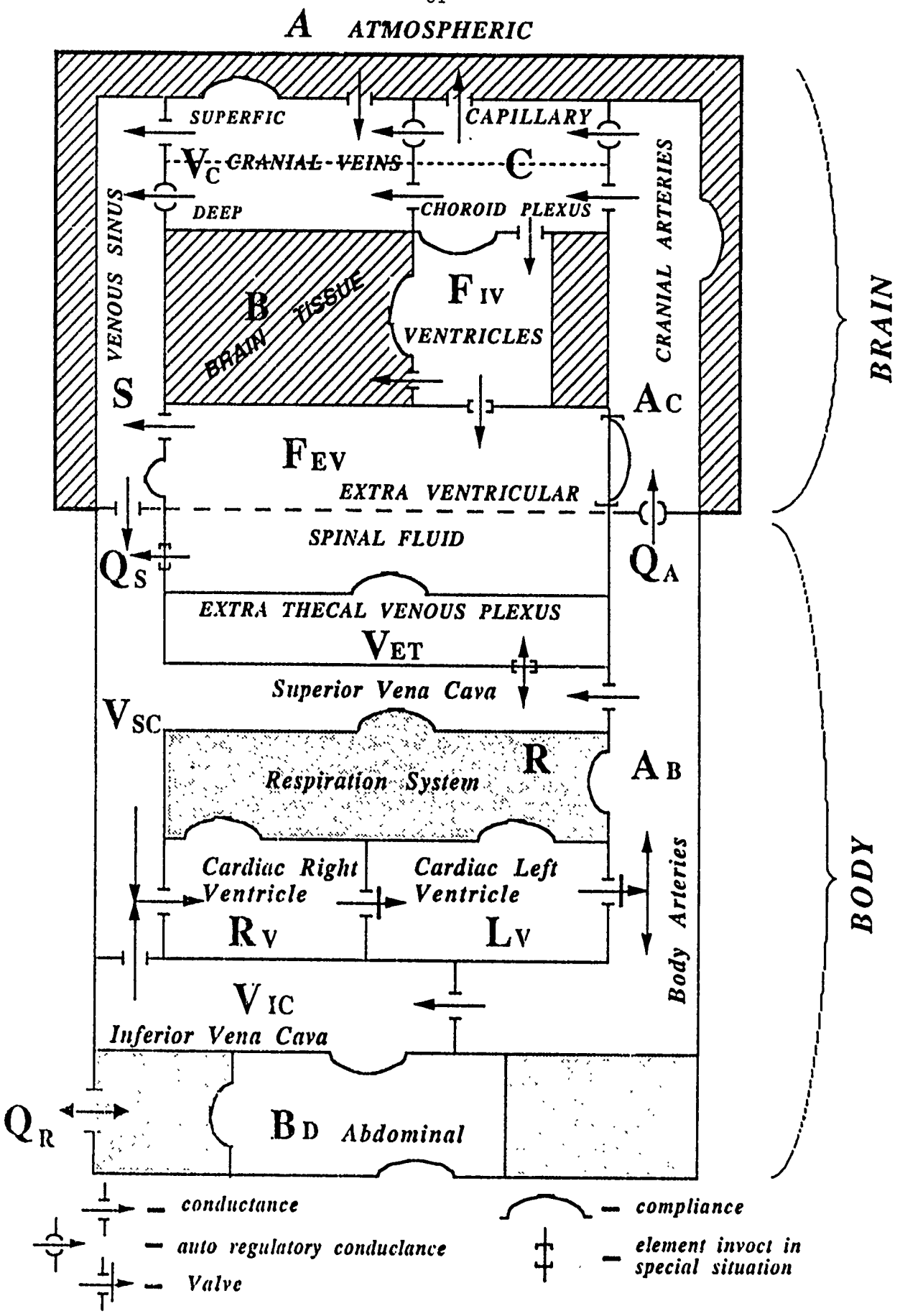

Figure 1: Cerebral - Body compartmental design.

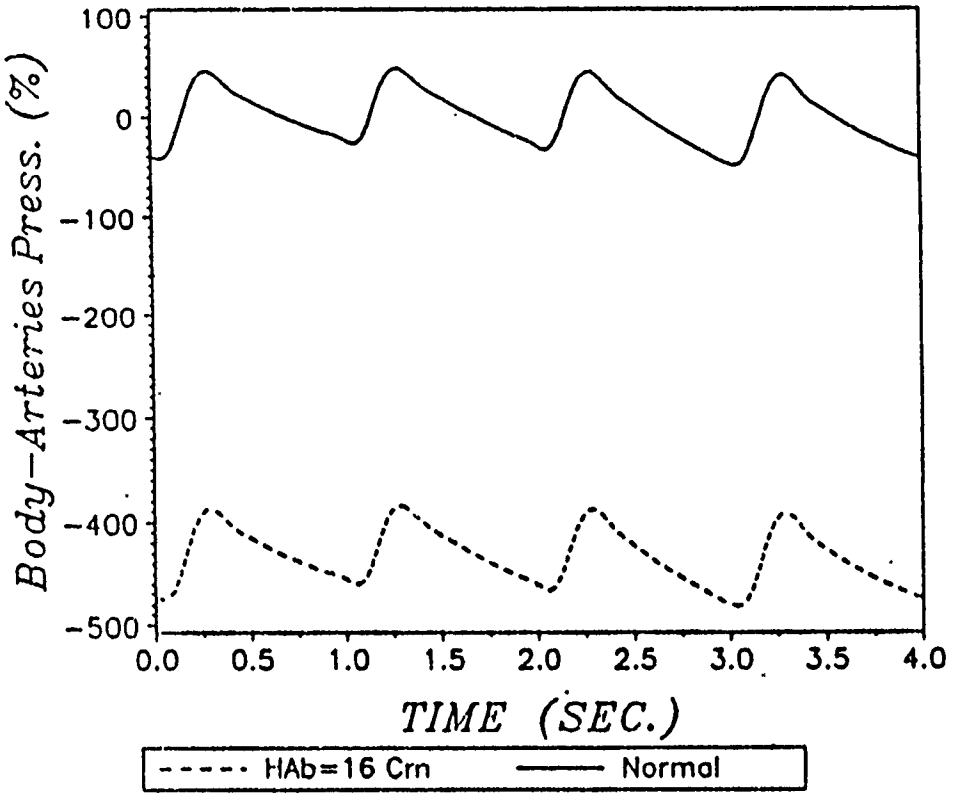

(A)

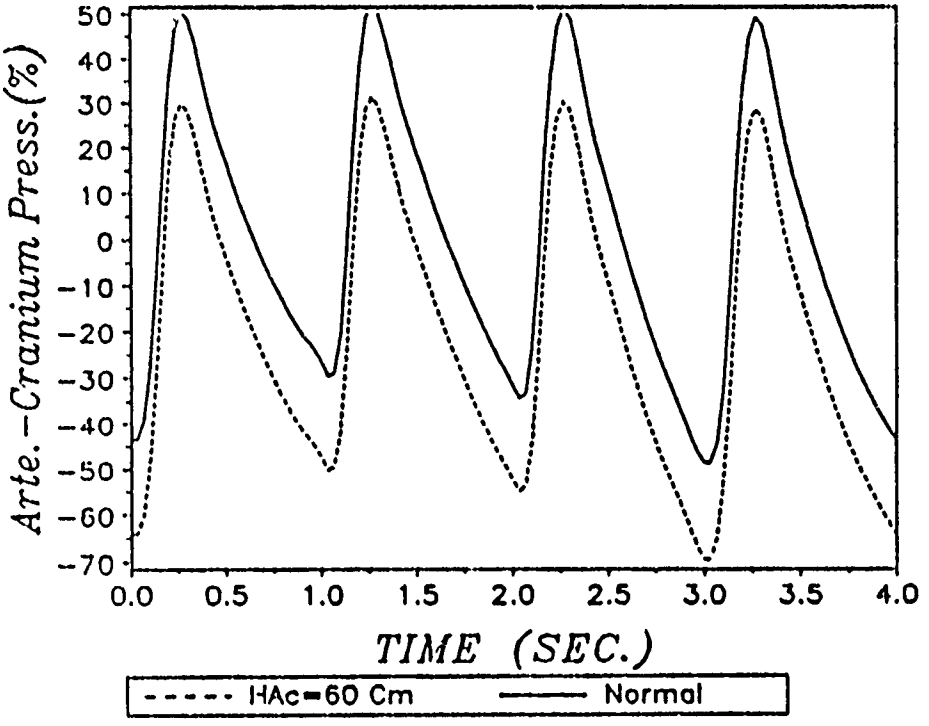

(B)

Figure 2: SENSITIVITY TO CHANGES IN RELATIVE POSITION

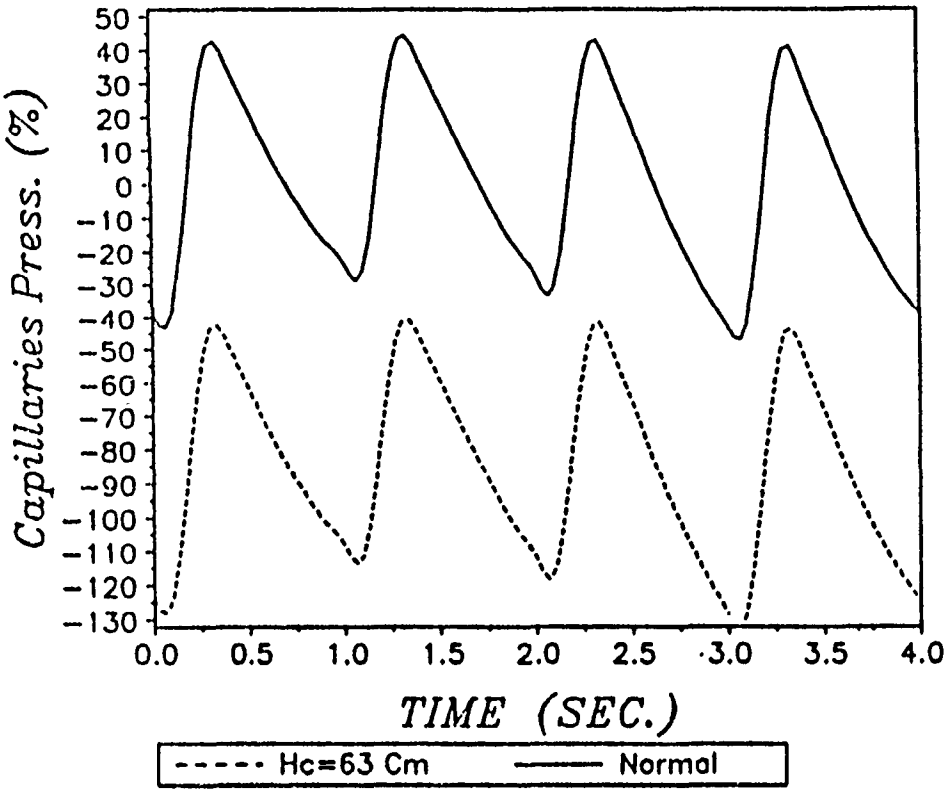

(A)

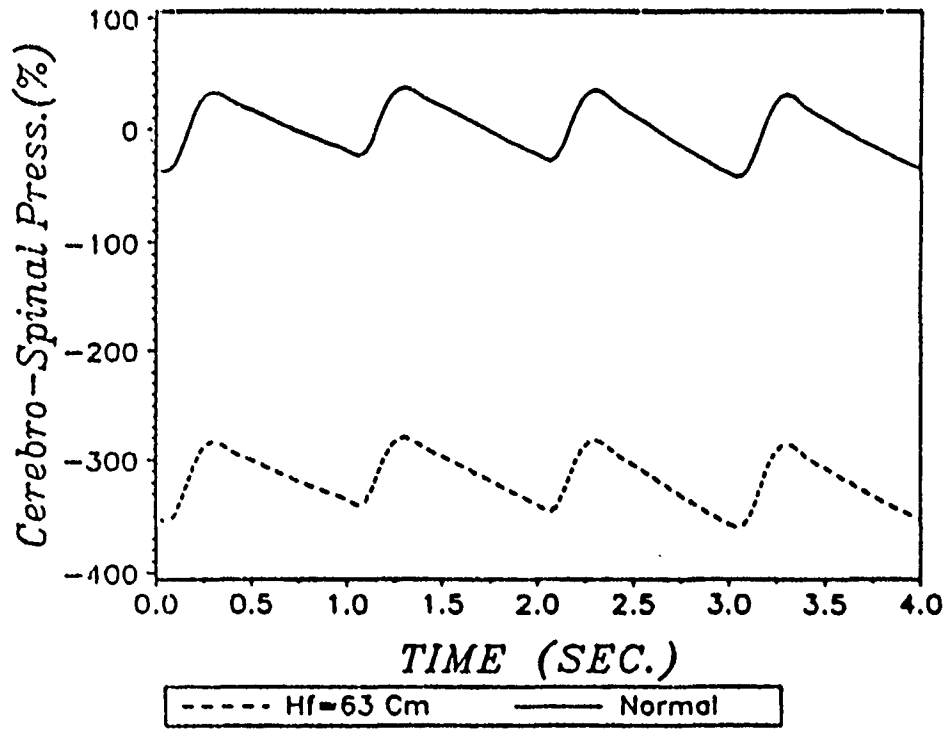

(B)

Figure 3: SENSITIVITY TO CHANGES IN RELATIVE POSITION

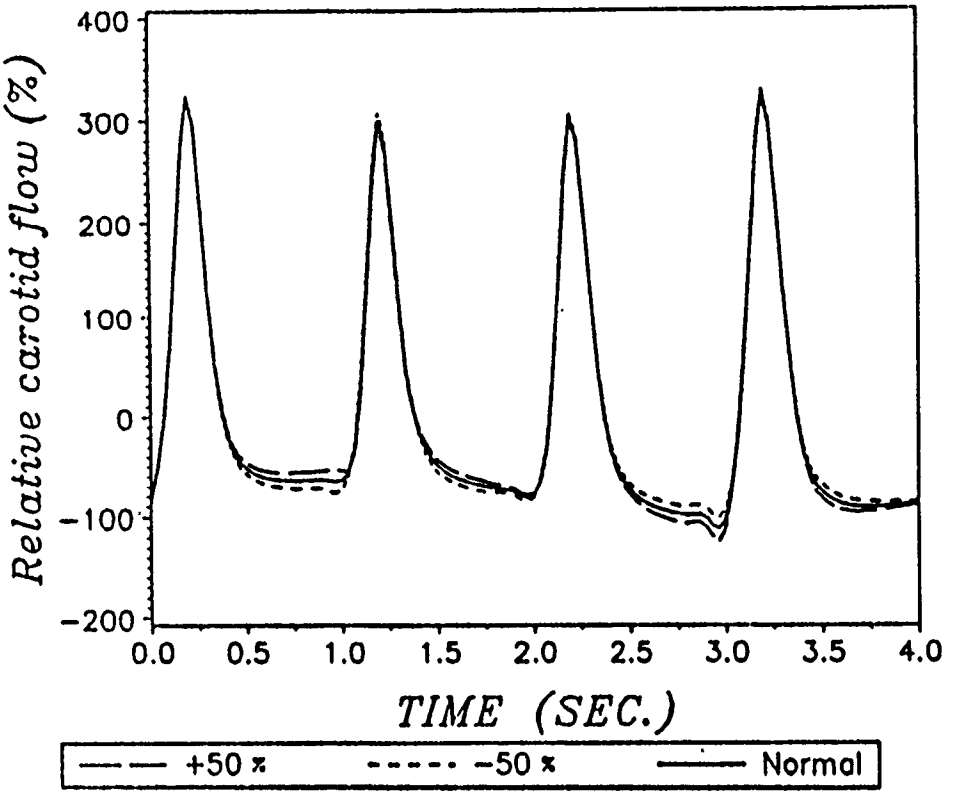

(A)

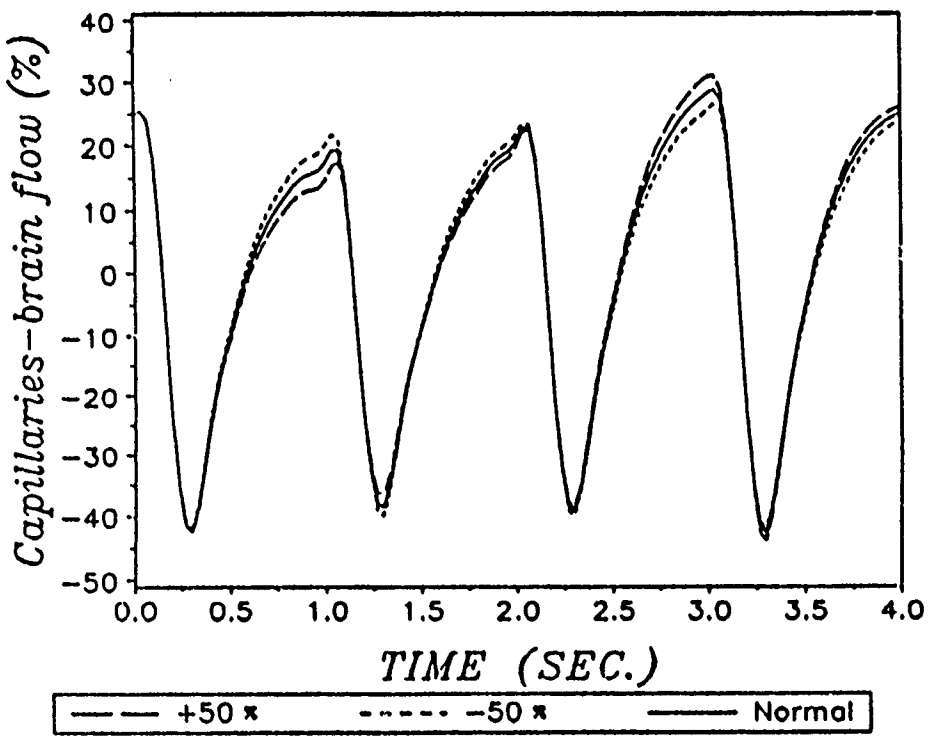

(B)

Figure 4: SENSITIVITY TO CHANGES IN INHALE-EXHALE FLOW

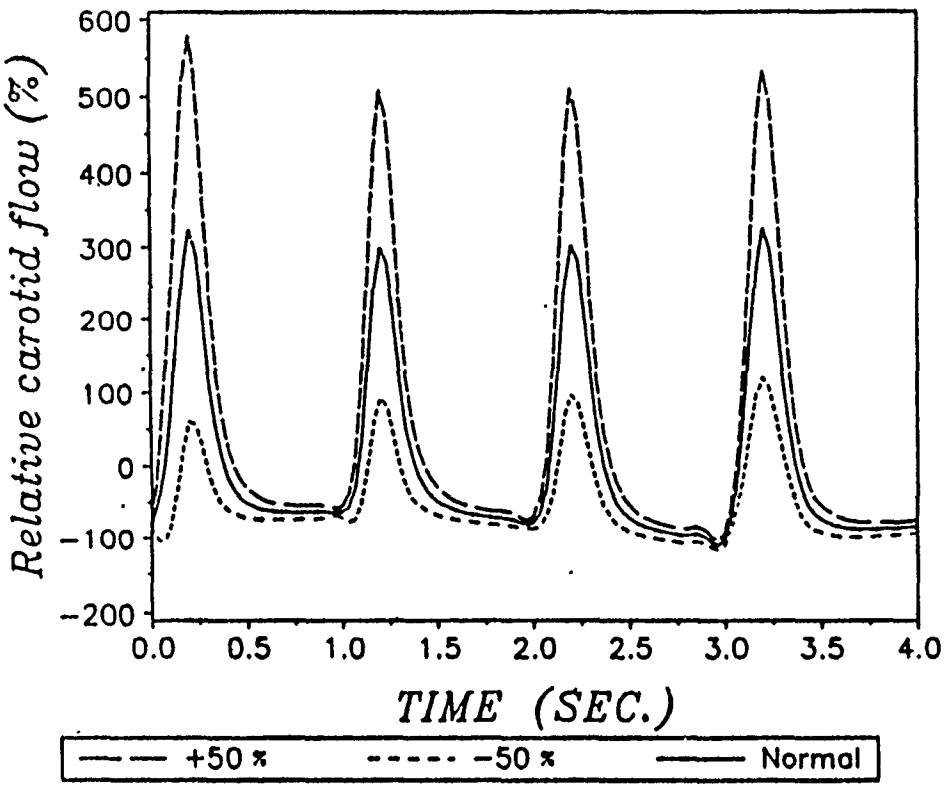

(A)

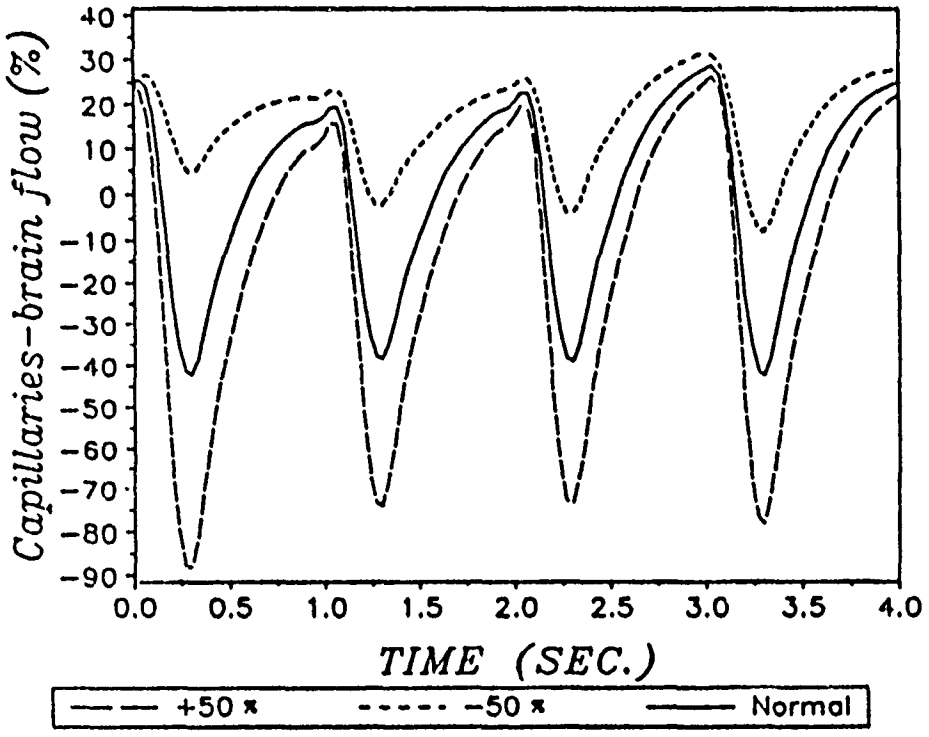

(B)

Figure 5:SENSITIVITY TO CHANGES IN CARDIAC LEFT VENTRICULAR PRESSURE

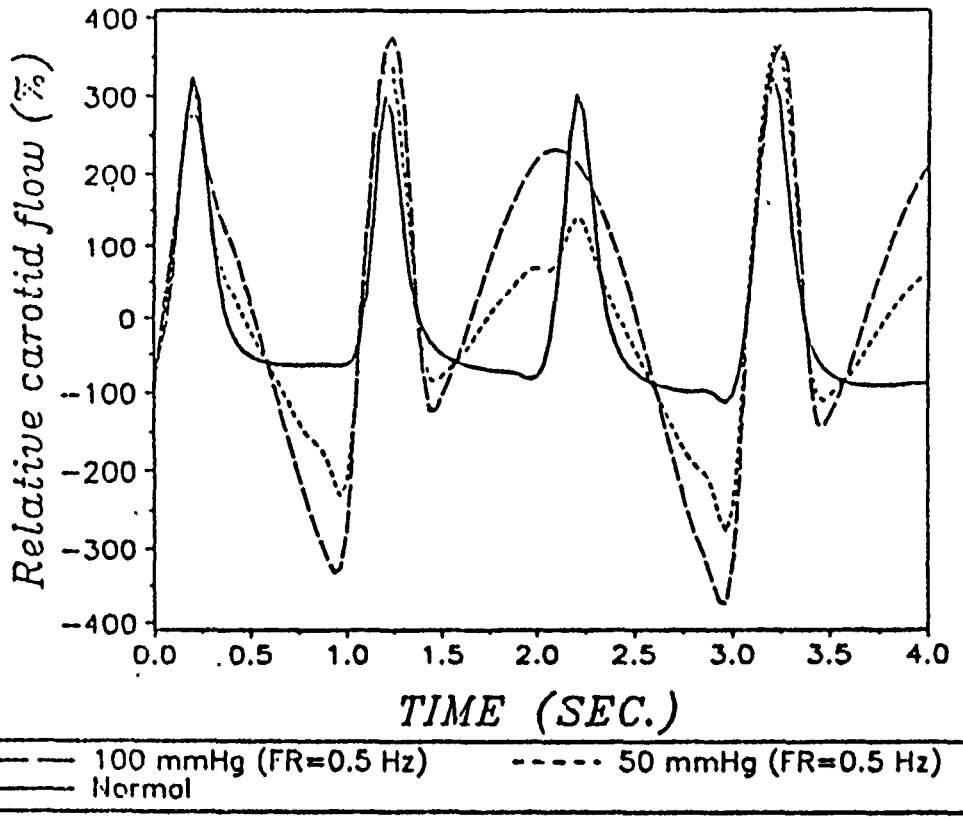

(A)

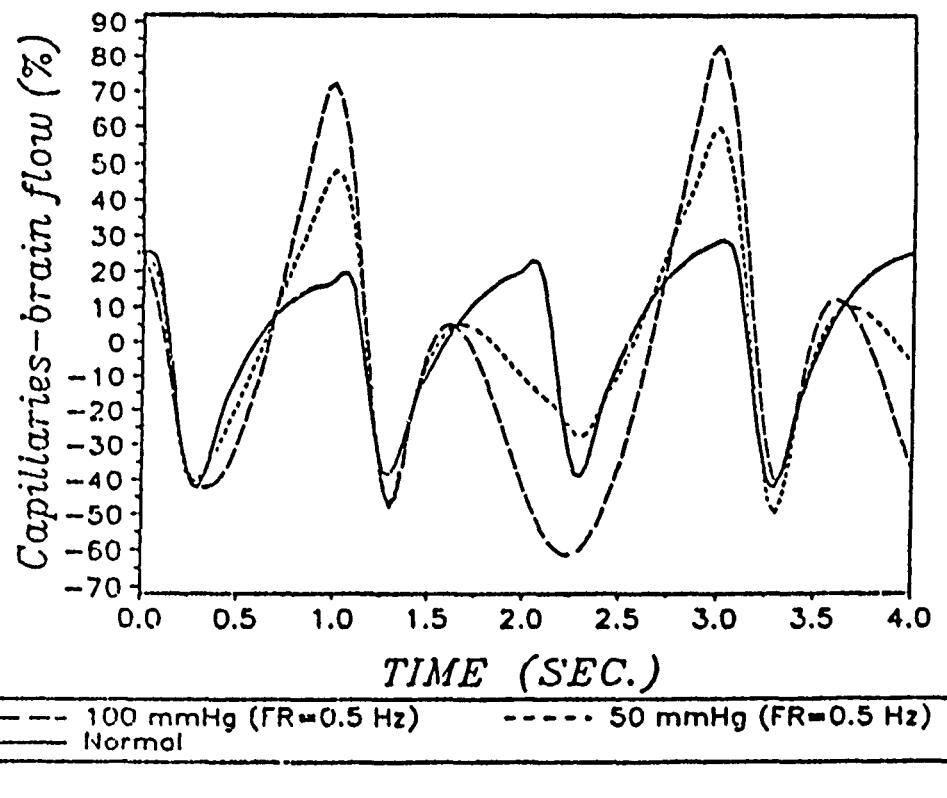

(B)

Figure 6: SENSITIVITY TO PRESSURE IMPOSED ON THE ABDOMEN

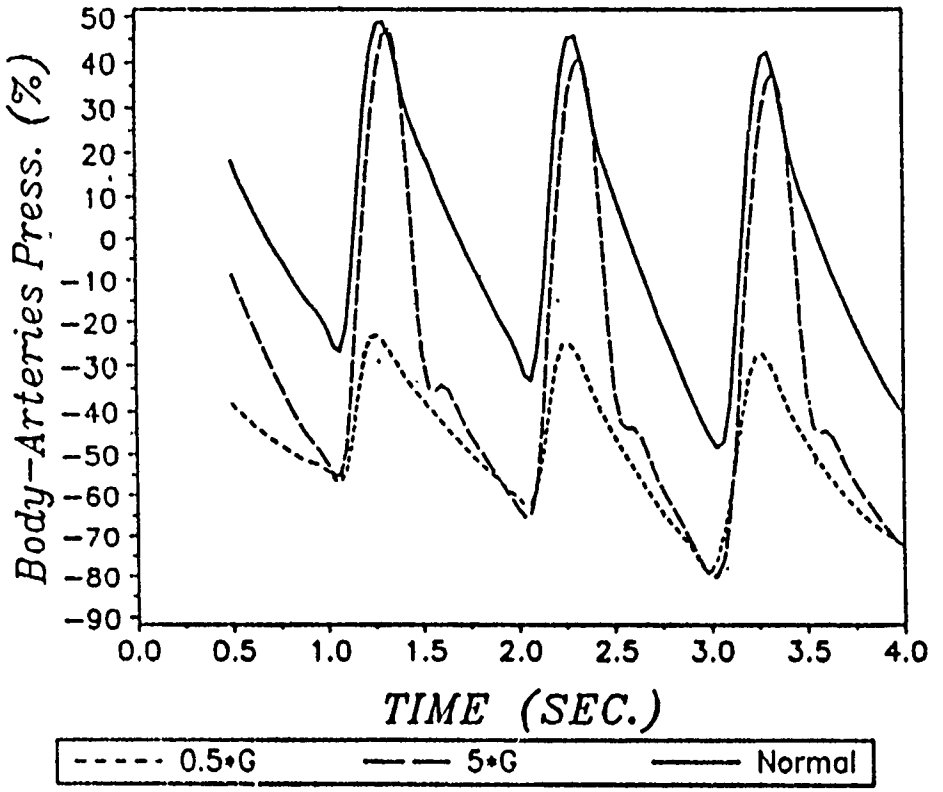

(A)

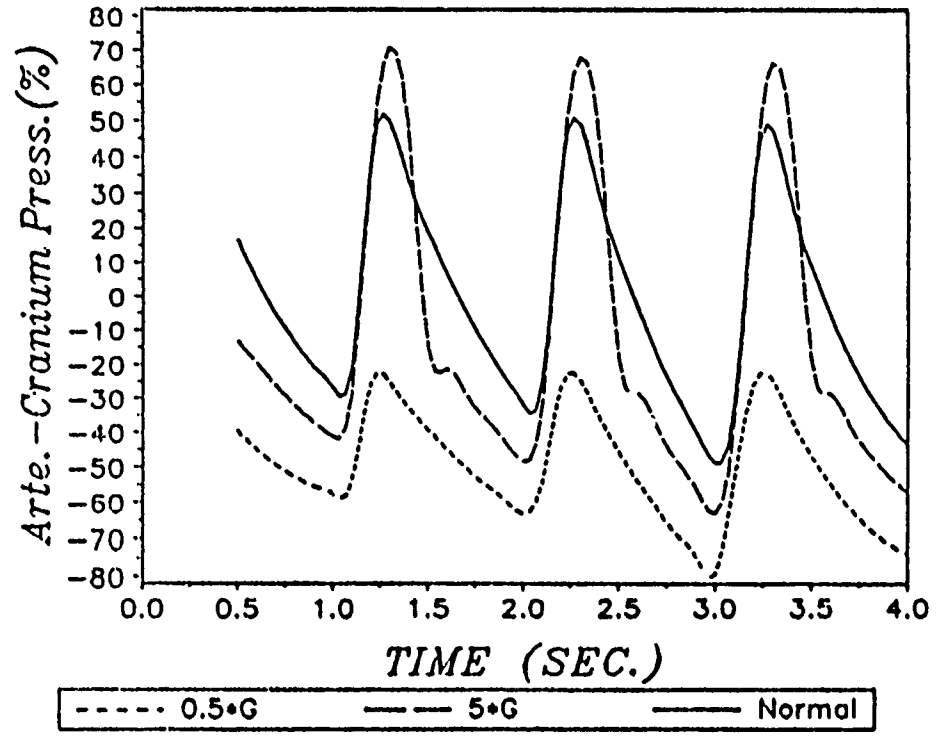

(B)

Figure 7:SENSITIVITY TO CHANGES IN GRAVITY ACCELERATION (g)

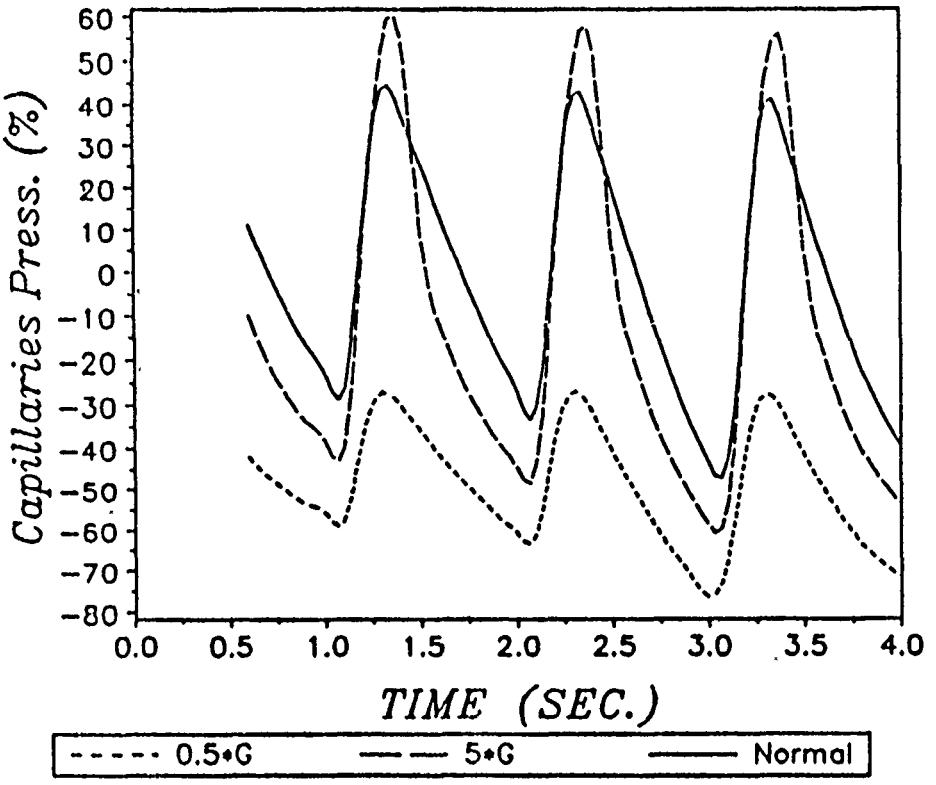

(A)

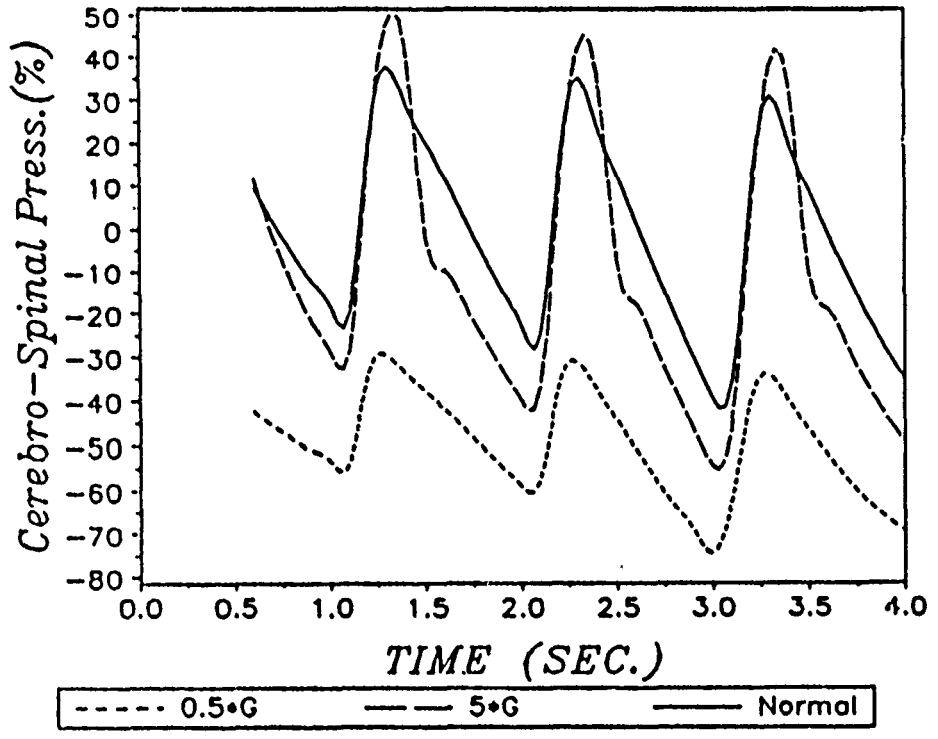

(B)

Figure 8:SENSITIVITY TO CHANGES IN GRAVITY ACCELERATION (g)

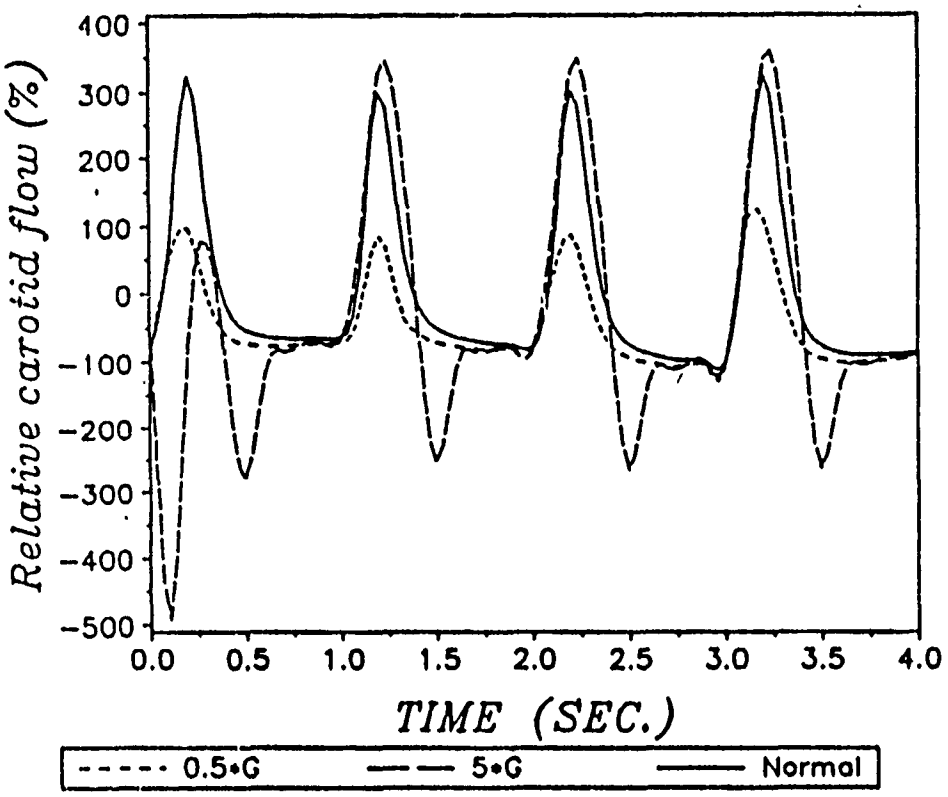

(A)

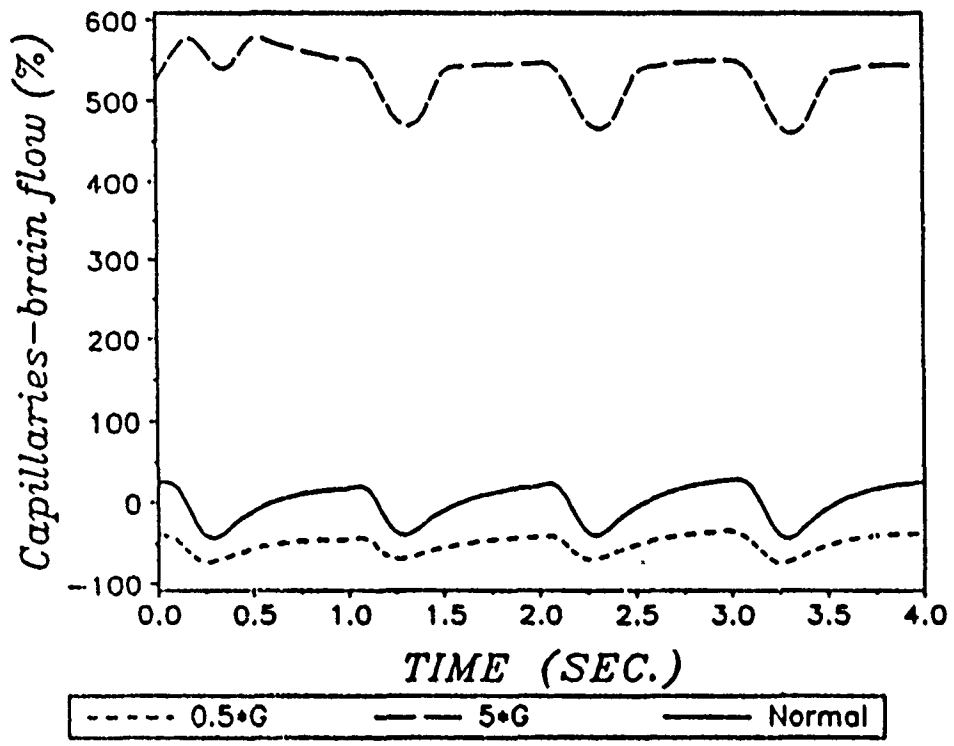

(B)

Figure 9: SENSITIVITY TO CHANGES IN GRAVITY ACCELERATION (g)

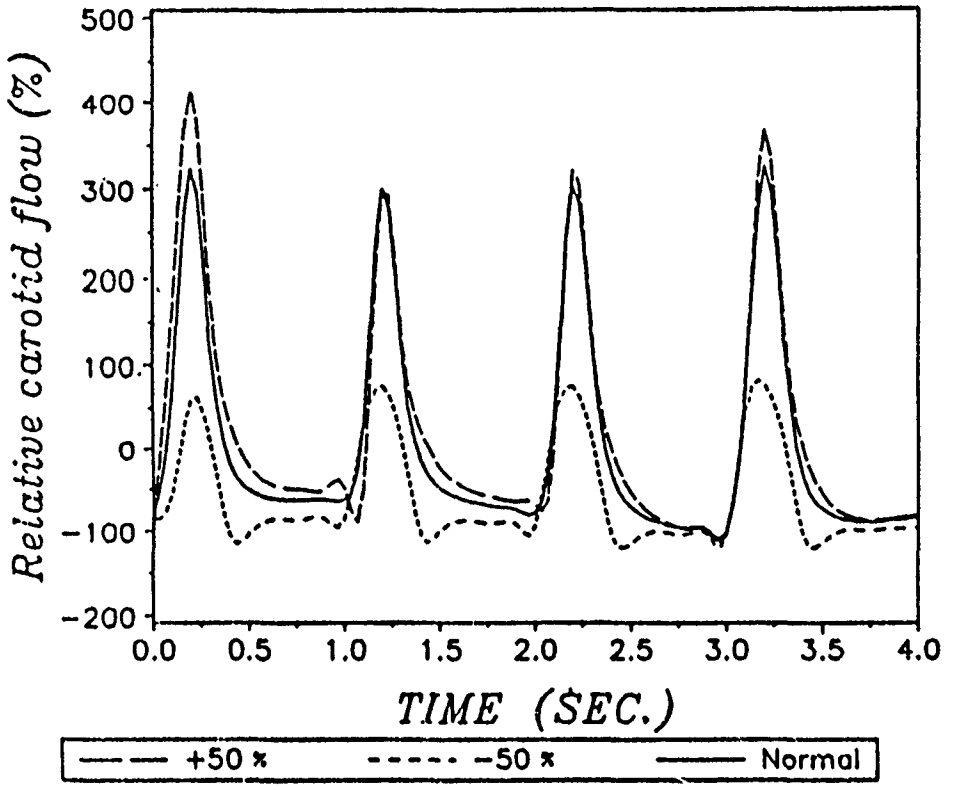

(A)

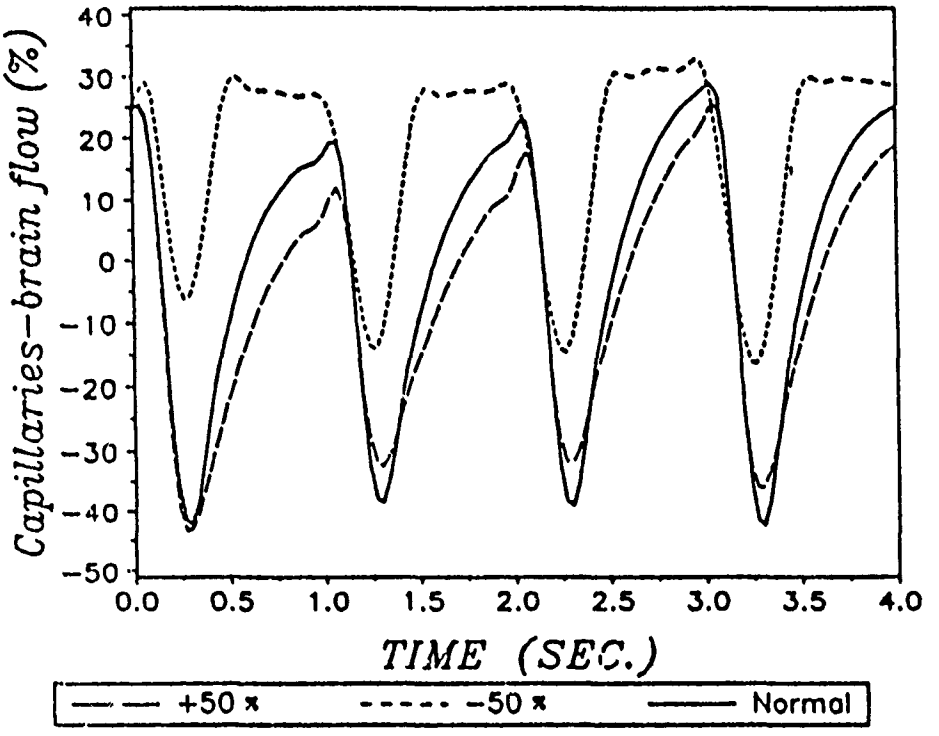

(B)

Figure 10: SENSITIVITY TO CHANGES IN BLOOD VISCOSITY

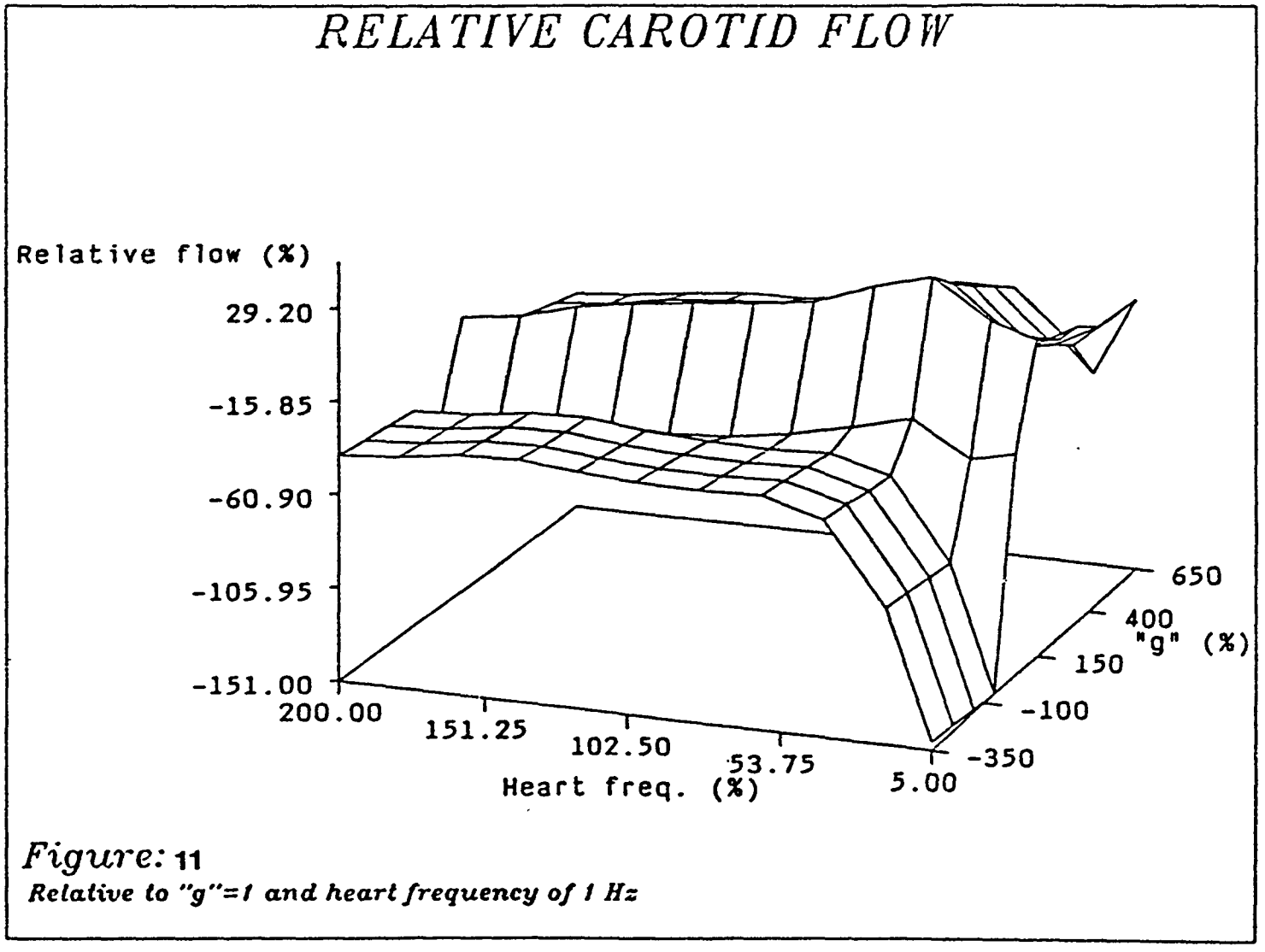

Figure: 11

Relative to "g"=1 and heart frequency of 1 Hz

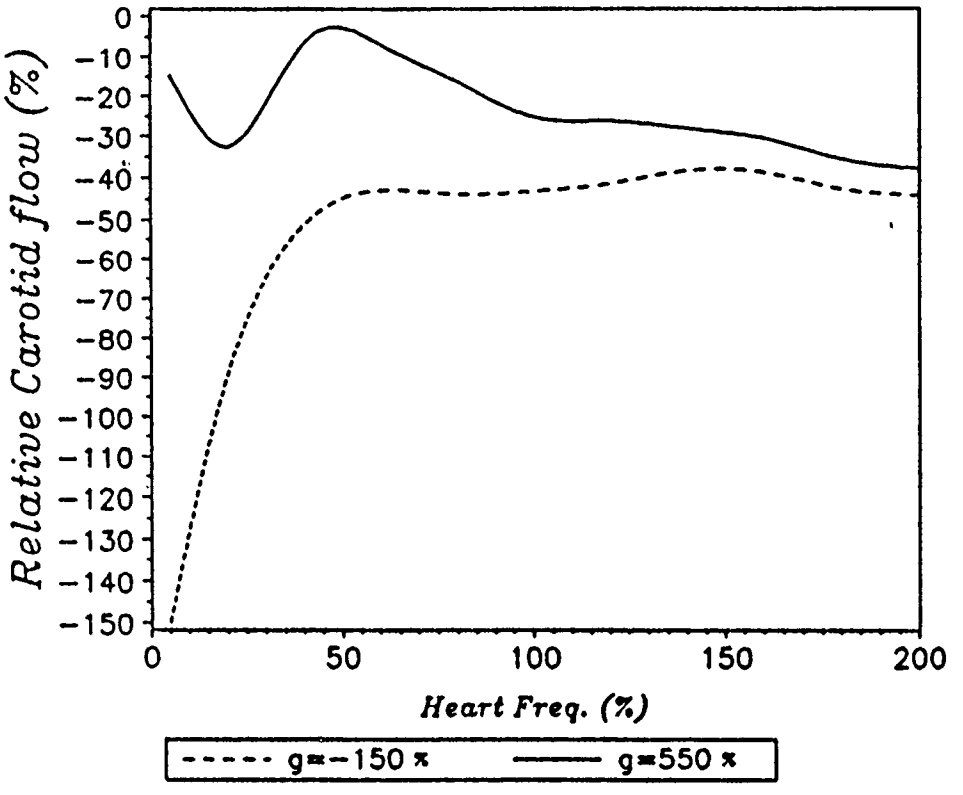

(A)

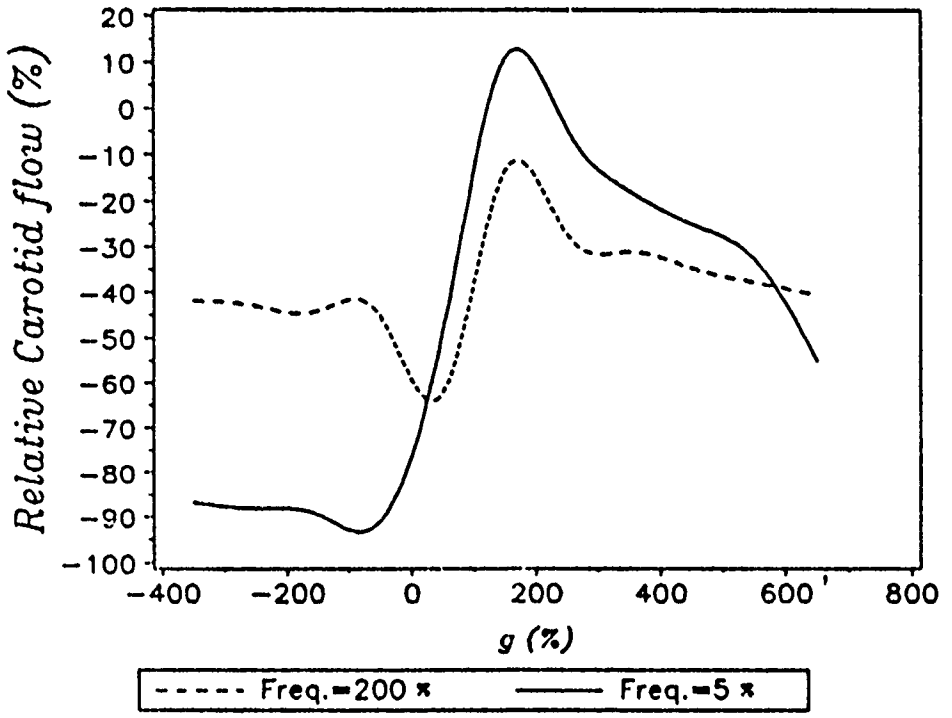

(B)

Figure 12: SENSITIVITY TO CHANGES IN RELATIVE CAROTID FLOW

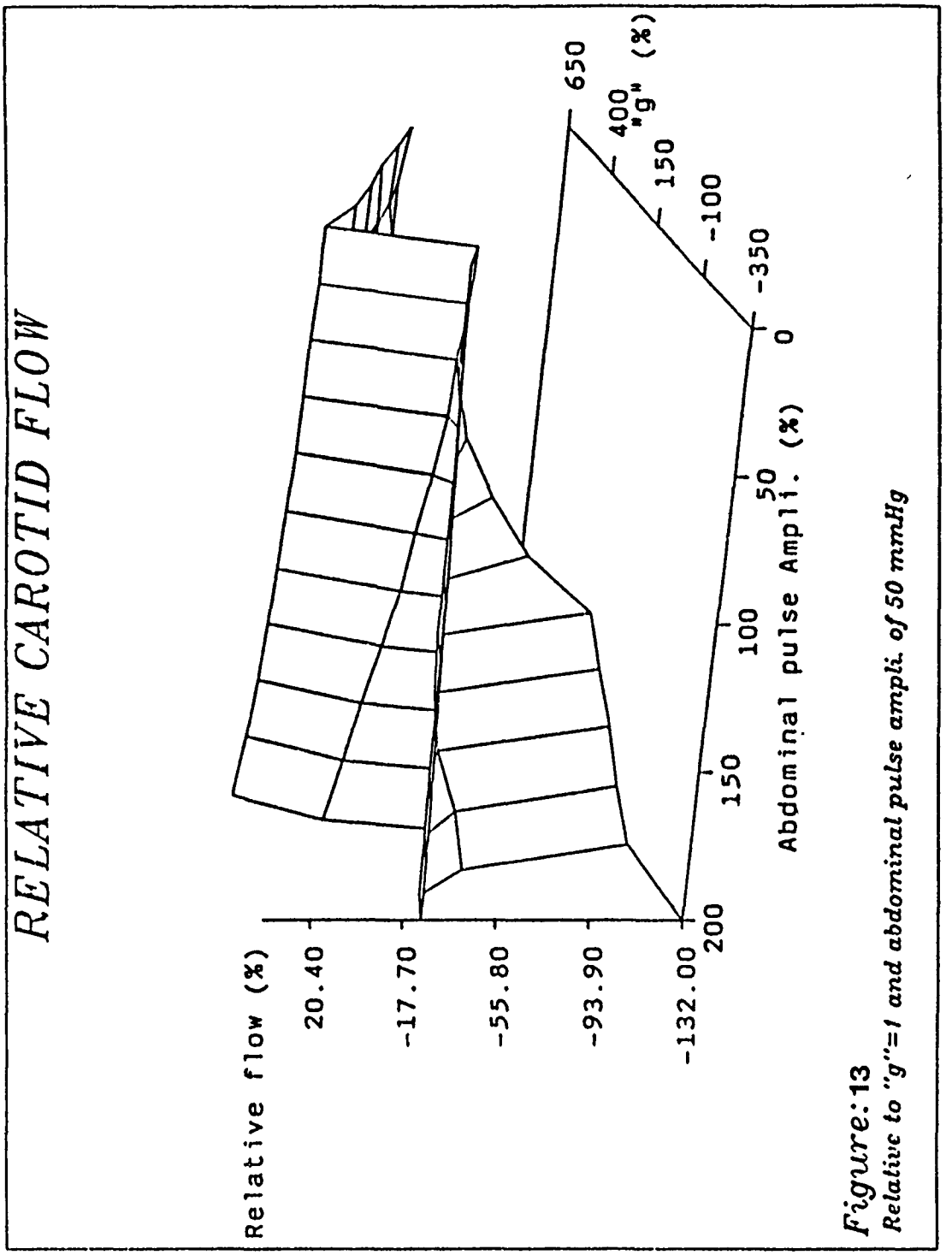

Figure:13
Relative to "g"=1 and abdominal pulse ampli. of 50 mmHg

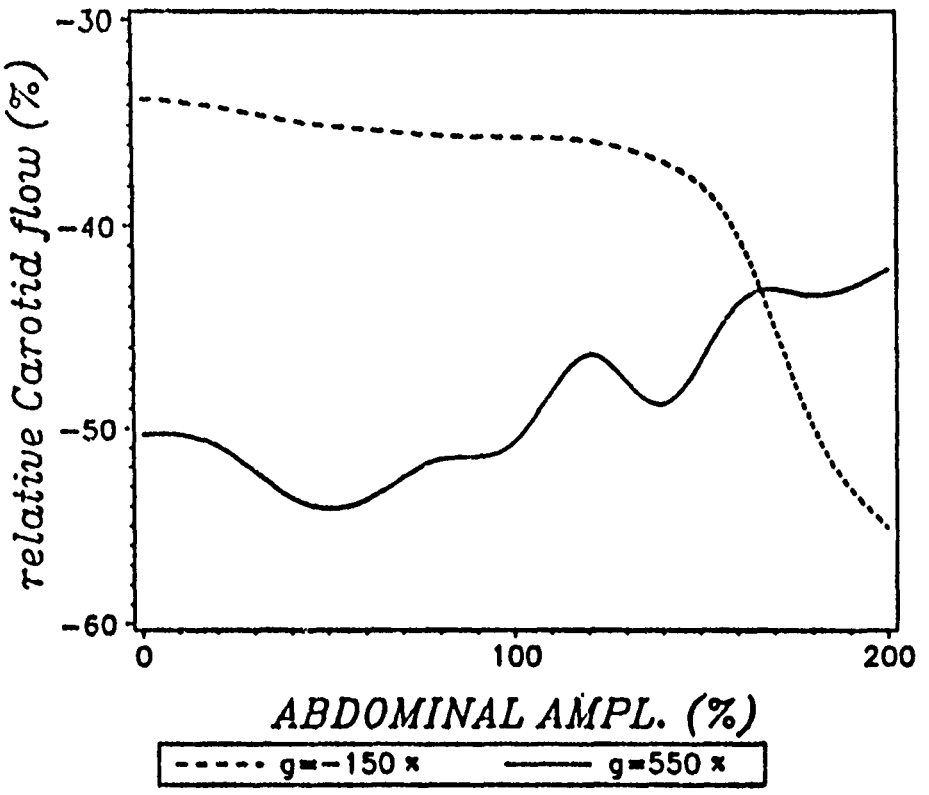

(A)

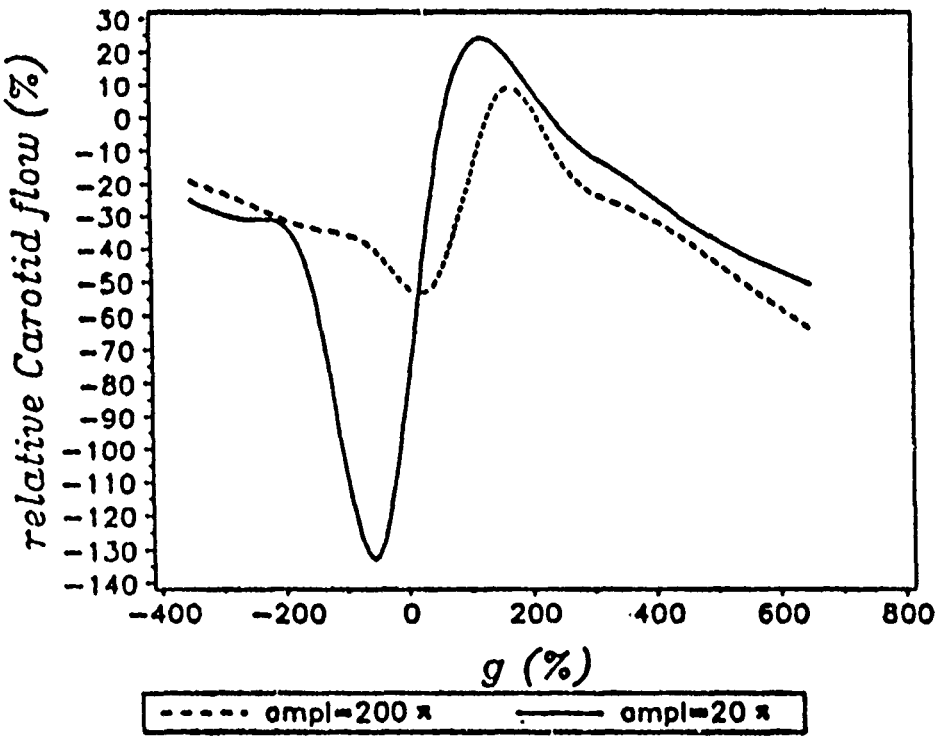

(B)

Figure 14: SENSITIVITY TO CHANGES IN RELATIVE CAROTID FLOW

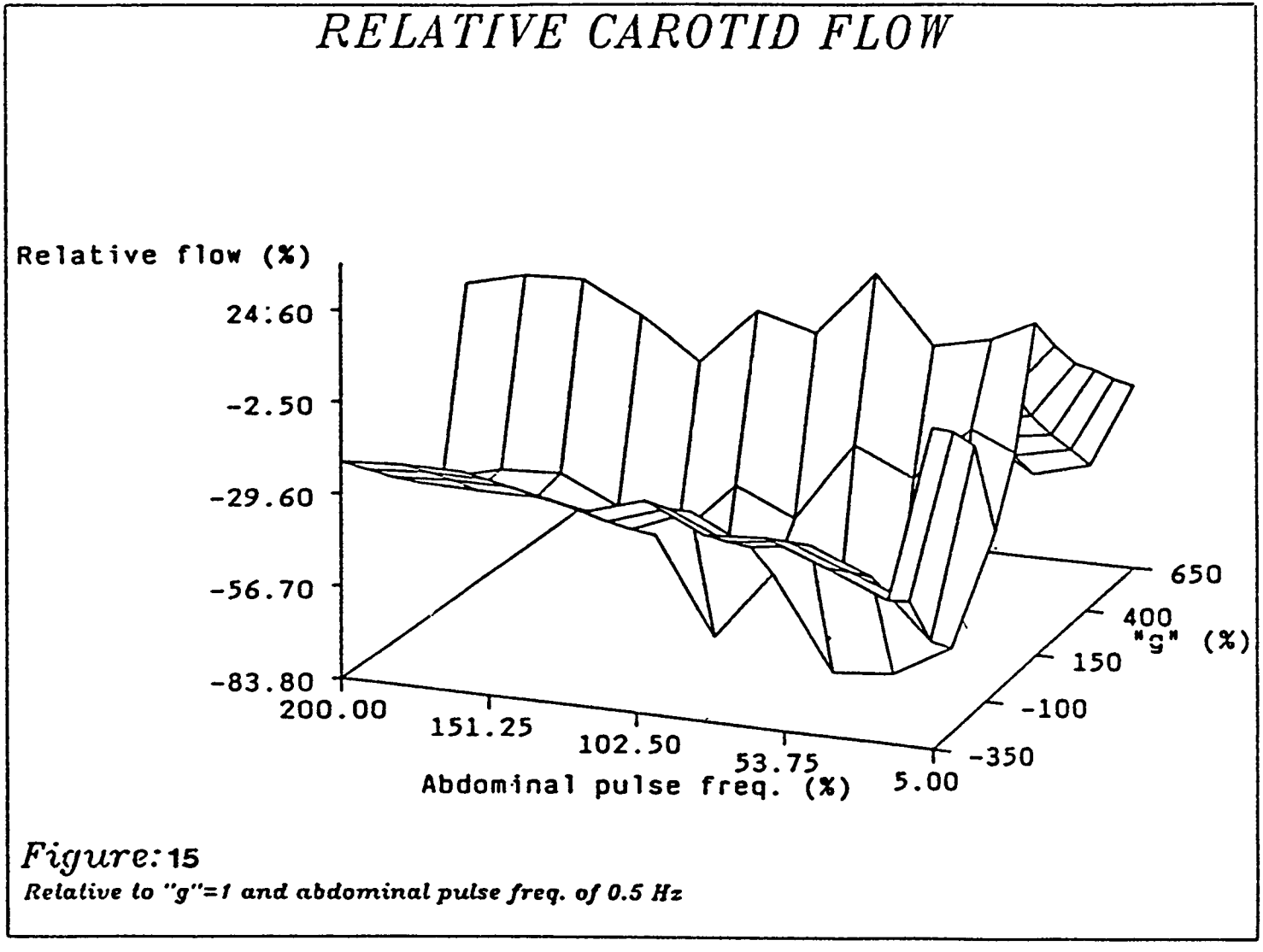

Figure: 15

Relative to "g"=1 and abdominal pulse freq. of 0.5 Hz

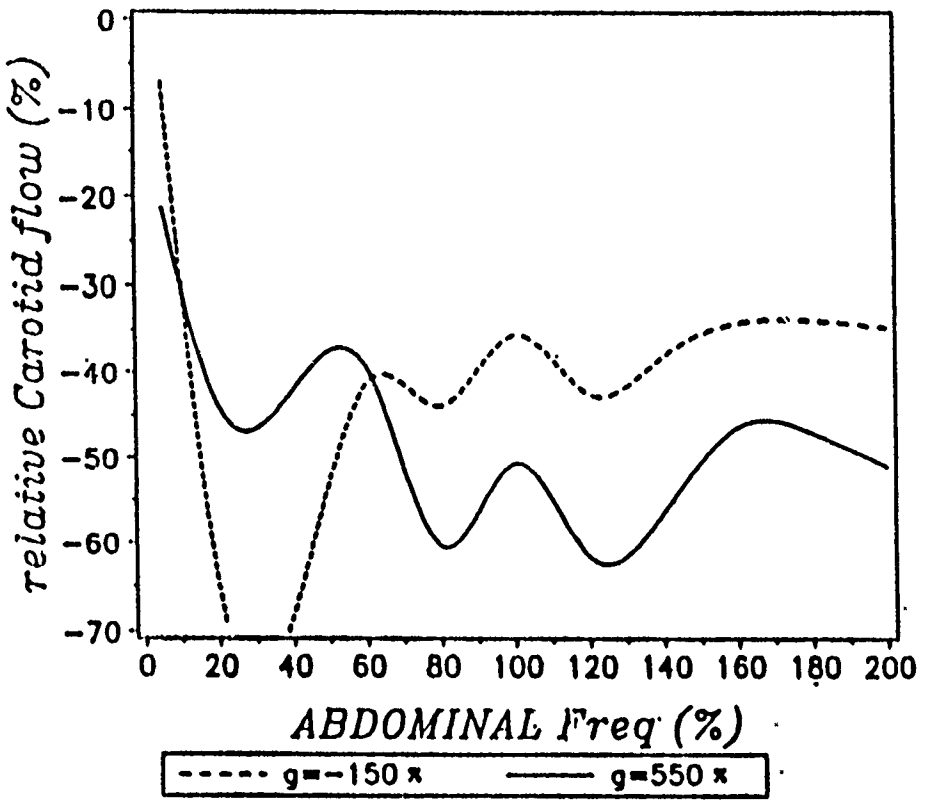

(A)

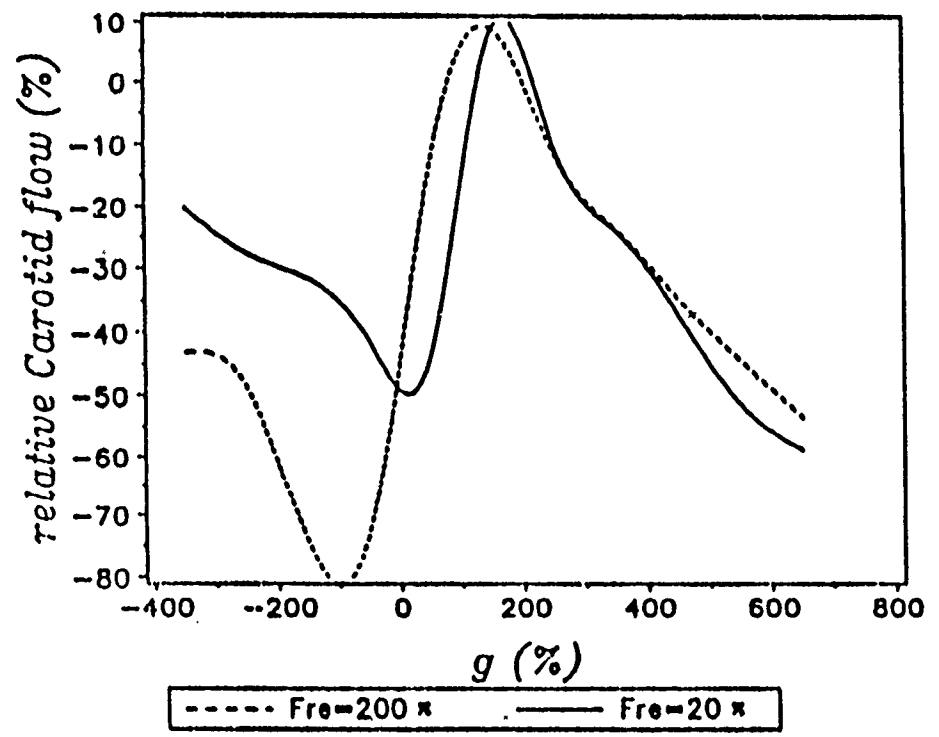

(B)

Figure 16: SENSITIVITY TO CHANCES IN RELATIVE CAROTID FLOW

References

E. Adar and S. Sorek (1989a) "Multi-Compartmental Modelling for Aquifer Parameter Estimation Using Natural Tracers in Non-Steady Flow," Adv. Water Resources. 12, 84-89.

Fulco, C.S., A. Cymerman, P.B. Rock and G. Farese (1985) "Hemodynamic Responses to Upright Tilt at Sea Level and High Altitude," Aviat. Space Environ. Med., 56:1172-6.

Jonson, B. and H. Rundcrantz (1969) "Posture and Pressure Within the Internal Jugular Vein," Aeta oto-laryngologica 68, 271-275.

Lauritzen, J.B., A. Lendorf, S. Vesterhauge and T.S. Johansen (1987) "Heart Rate Responses to Moderate Linear Body Accelerations: Clinical Implications in Aeromedical Evacuation," Aviat. Space Environ. Med., 58:248-51.

London, G.M., J.A. Levenson, M.E. Safar, A.C. Simon, A.P. Guerin and D. Payen (1983) "Hemodynamic Effects of Head-Down Tilt in Normal Subjects and Sustained Hypertensive Patients," Am. J. Physiol. 245 (Heart Circ. Physiol. 14): H194-H202.

Rosner, M.J. and I.B. Coley (1980) "Cerebral Perfusion Pressure, Intracranial Pressure and Head Elevation," J. Neurosurg., 65:636-641.

S. Sorek, J. Bear and Z. Karni (1988a) "A Non-Steady Compartmental Flow Model for the Cerebrovascular System," J. of Biomechanics, V. 29, 9, 695-704.

S. Sorek, M. Feinsod and J. Bear (1988b) "Can N.P.H. be Caused by Cerebral Small Vessel Disease? A New Look Based on Mathematical Model," Med. and Biol. Eng. and Comput. 26, 3, 310-313.

S. Sorek, J. Bear and Z. Karni (1988c) "Intracranial Compartmental Pulse Wave Simulation," Mathematical Biosciences, 89, 149-159.

S. Sorek, J. Bear and Z. Karni (1989b) "Resistances and Compliances of a Compartmental Model of the Cerebrovascular Fluid System," Annals of Biomedical Eng., 17, 1-12.

S. Sorek, K. Allen, M. Feinsod, S. Ben-Haim, J. Bear and L. Bunt (1990) "Non-Steady Compartmental Model of Interactive Perfusion Between Cerebral and Body Systems, I. Theory," (submitted).

Wolthuis, R.A., D.H. Hull, J.R. Fischer, D.A. McAfoose, and J.T. Curtis (1979) "Blood Pressure Variability of the Individual in Orthostatic Testing," Aviat. Space Environ. Med. 50(8); 774-777.

THE EFFECT OF POSITIVE PRESSURE VENTILATION ON CARDIO-PULMONARY AND BRAIN DYNAMICS

In order to obtain experimental validation to the model predictions and to enable parameter estimation we have performed animal experiments. The objective of the experimental setup was to enable us to record simultaneous pressure and flow signals from different sites in the cardiovascular, pulmonary and neural system. Recordings were performed under different pressure and volume perturbation introduced into the thorax. We studied 12 large dogs.

Methods

General Preparation

Mongrel dogs (18-25kg) were anesthetized with pentobarbital (60mg/kg IV), using supplemental doses (30mg) as dictated by presence of corneal reflex or pressor response to surgical incision. Animals were intubated and ventilated (Harvard large animal respirator) to maintain physiological PO_2 (80-110) and PCO_2 (35-45). Bolus injections of sodium bicarbonate (2mEq/ml) will be used to maintain arterial pH between 7.37 and 7.43. Rectal temperature was monitored and maintained between 37 and 40^o C, using a heating pad as needed.

Cannulae were placed in the right femoral artery and vein for measuring arterial pressure in the descending aorta and administration of fluids and pharmacological agents, respectively. Another set of cannulae were placed in the left femoral artery and vein for measuring arterial blood gases and inferior vena cava pressures, respectively (Fig. 1).

Via a ventral incision in the neck the common carotid artery and the internal jugular vein were isolated. Electromagnetic flow probes of appropriate size were placed on these vessels for measuring blood flow.

Through an incision above the parietal bone a burr hole (2 mm) was drilled, keeping the dura matter intact. After hemostassis was performed using bone wax, a Millar micro tip needle pressure transducer (3F) was introduced into the brain tissue for measuring tissue pressure (Fig. 2). Through a puncture of the cisterna magna another millar micro mannometer was introduced for measuring cisternal pressure.

Air way pressure was measured using Microswitch pressure transducer connected to a PE200 tube placed near the intratracheal tube opening. Airflow through the airways was measured using a Gould pneumotachograph connected at the intratracheal tube connection to the positive pressure ventilator (Fig. 3).

Pressure-Volume perturbation were introduced by a computer controlled positive pressure ventilator. This ventilator was built using a bellow connected to a stepper motor. The maximal displacement of the bellow as well as the acceleration and deceleration of its movements were externally controlled by a computer. An algorithm enabled on-line modification of two of these parameters (maximal displacement and acceleration). The deceleration of the bellow as well as the respiratory rate were calculated by the controlling computer to ensure constant minute ventilation. For evaluation the actual minute ventilation was measured continuously by integration of the pneumotachograph inspiratory signal.

Data acquisition

Analog signals were fed into a 12 bit A/D converter, and sampled at 1 Khz. Data were stored in a digital form for off line processing.

Results

12 dogs were studied. A typical tracing of the pressure and flow signals during normal positive pressure ventilation is depicted in Fig. 4.

It is evident that the pressure-volume perturbation introduced into the thorax had a significant and observable effect on each of the pressure and flow signals recorded.

In general the pressure responses were similar to a low pass filter operation to the applied airway pressure, with a varying degree of delay. Arterial blood flow into the brain was pulsatile but was superimposed on the lower frequency of the respiratory perturbation. The venous flow was continuous but varied periodically following the respiratory perturbation. Figure 5 depicts five typical recordings of the pressure flow time curves during ventilation with (a) trapezoid, (b) saw tooth, (c) triangle, (d) low inspiratory to expiratory ratio as well as (e) high inspiratory to expiratory ratio.

Figure Legends:

Fig. 1 Experimental setup (panel a) together with a schematic representation of sensors position in the corresponding theoretical model map (panel b). 1 - Aortic pressure, 2 - Carotid flow, 3 - Intraventricular pressure, 4 - Intracerebral tissue pressure, 5 - Jugular vein flow, 6 - Superior vena cava pressure, 7 - Intrathoracic pressure (pleural), 8 - Inferior vena cava pressure, 9 - Intrabdominal pressure.

Fig. 2 Parietal bone hole prepared for inserting intracranial pressure transducer.

Fig. 3 Pressure and flow transducers connected to the airway opening.

Fig. 4 A typical tracing of the pressure and flow signals during normal positive pressure ventilation.

Fig. 5 Typical recording of the pressure flow time curves during ventilation with (a) trapezoid, (b) saw tooth, (c) triangle, (d) low inspiratory to expiratory ratio as well as (e) high inspiratory to expiratory ratio.

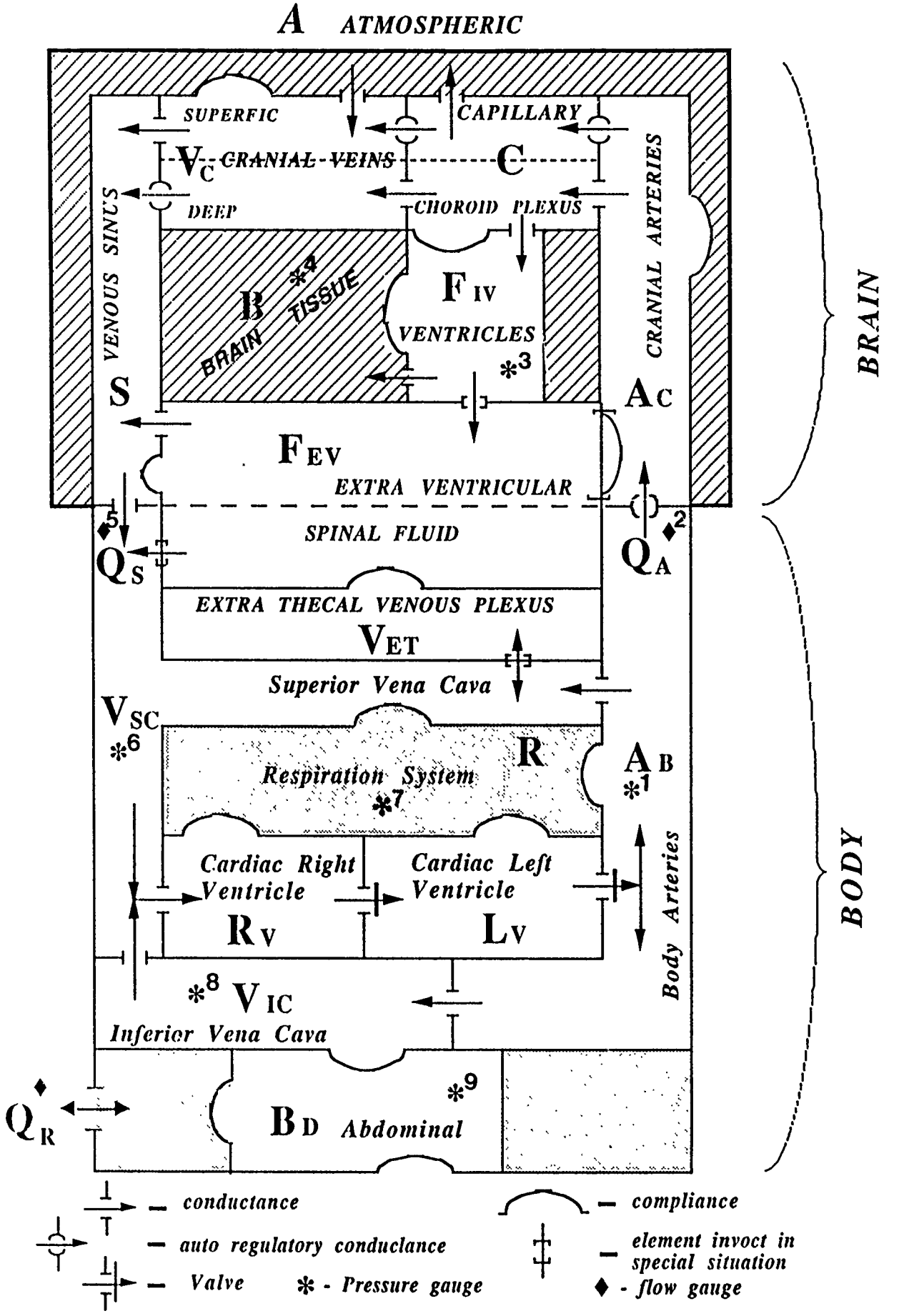

Figure 1: Cerebral - Body compartmental design.

FIGURE **1**

FIGURE **2**

FIGURE **3**

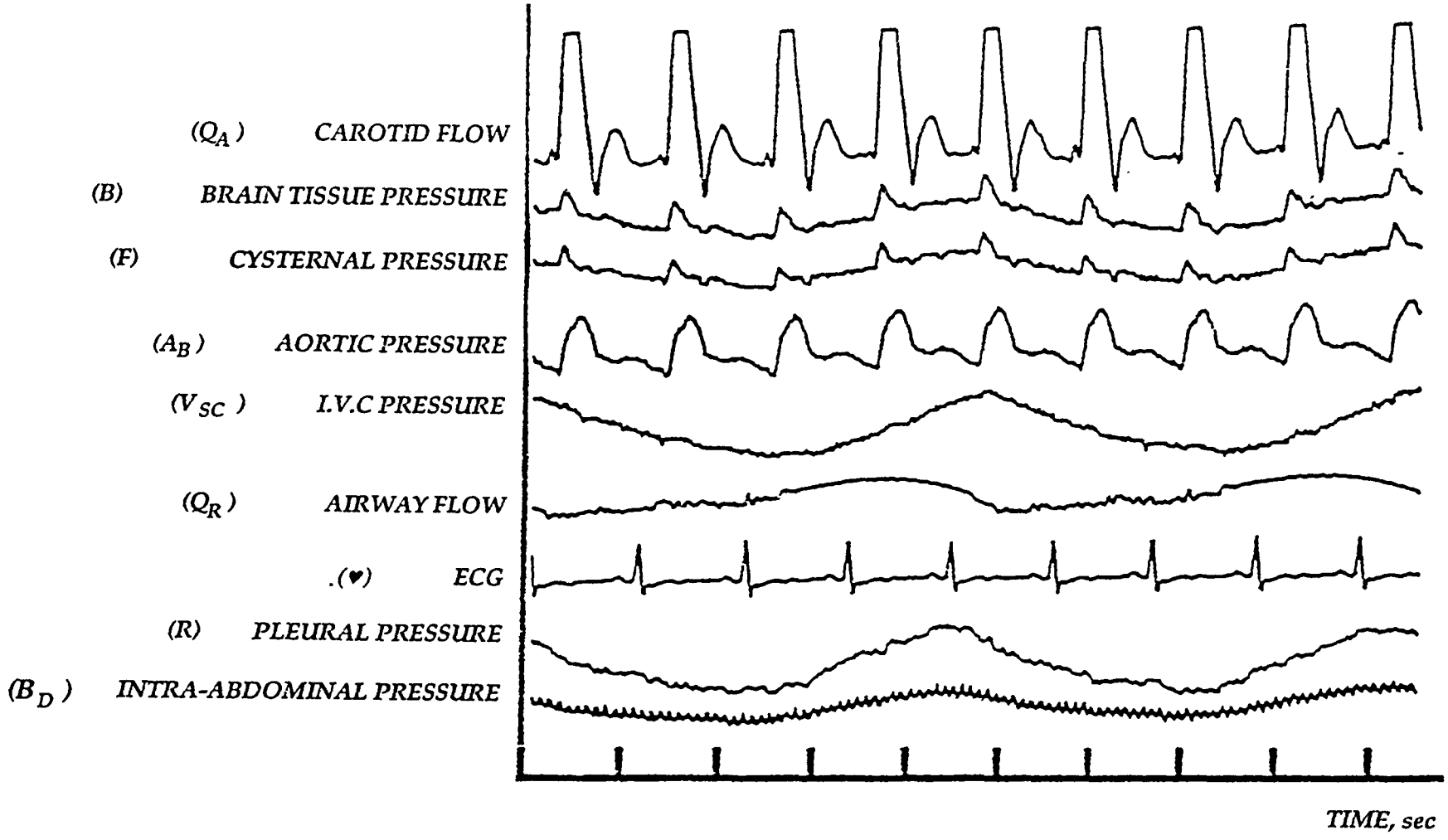

FIGURE 4 *NORMAL (FLOW) VENTILATION*

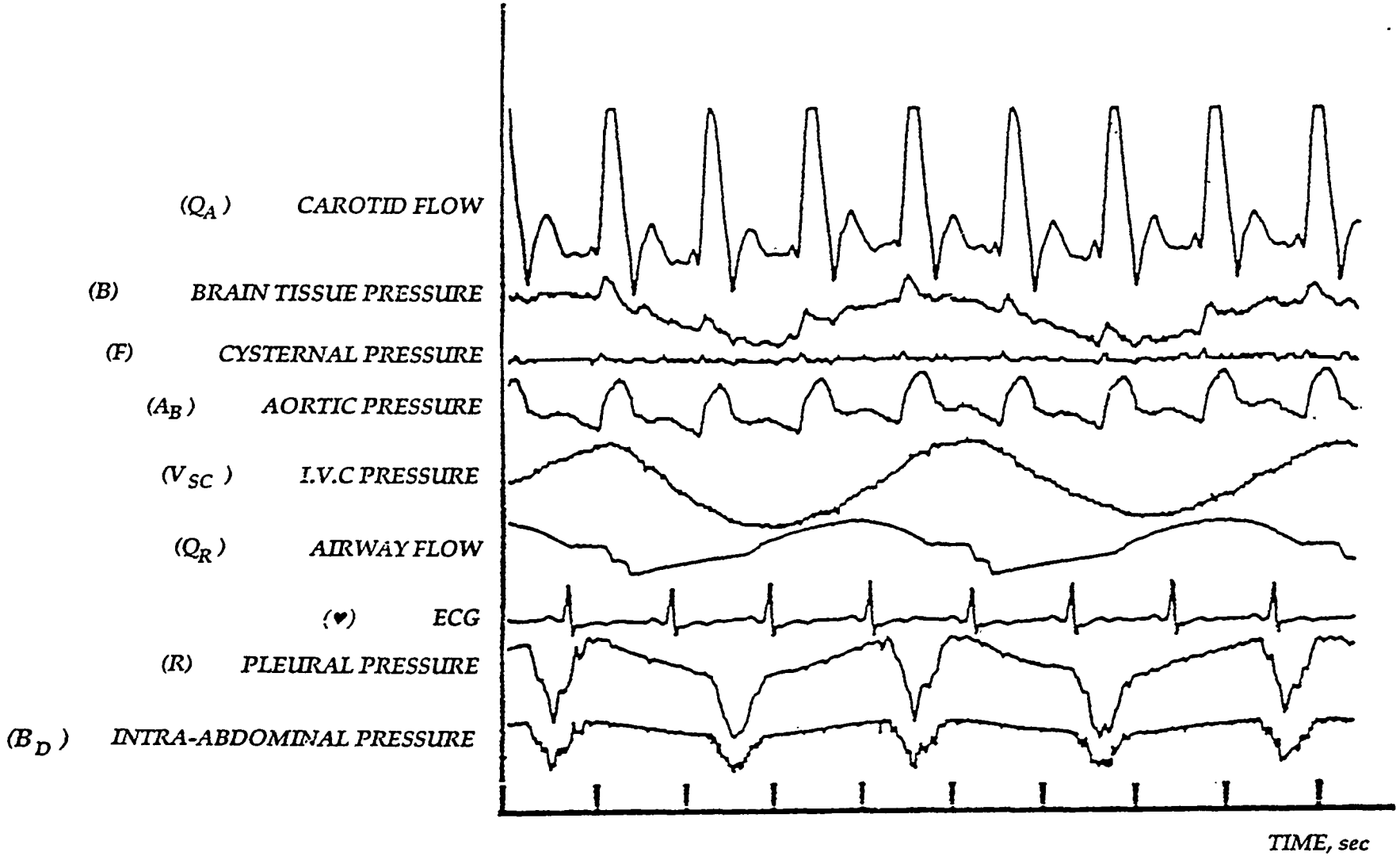

FIGURE 5a *TRAPEZOID (FLOW) VENTILATION*

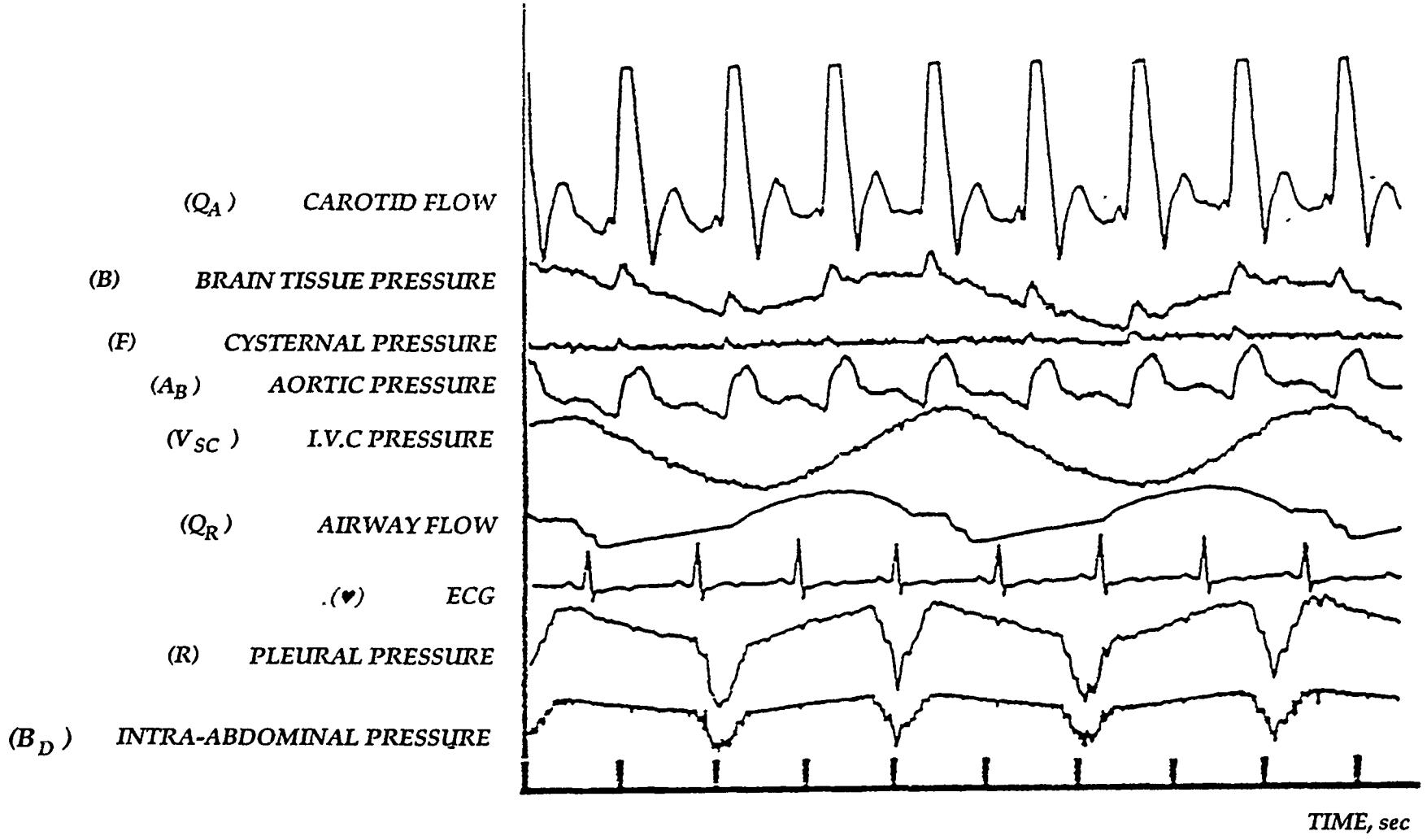

FIGURE **5b** *SAW TOOTH (FLOW) VENTILATION*

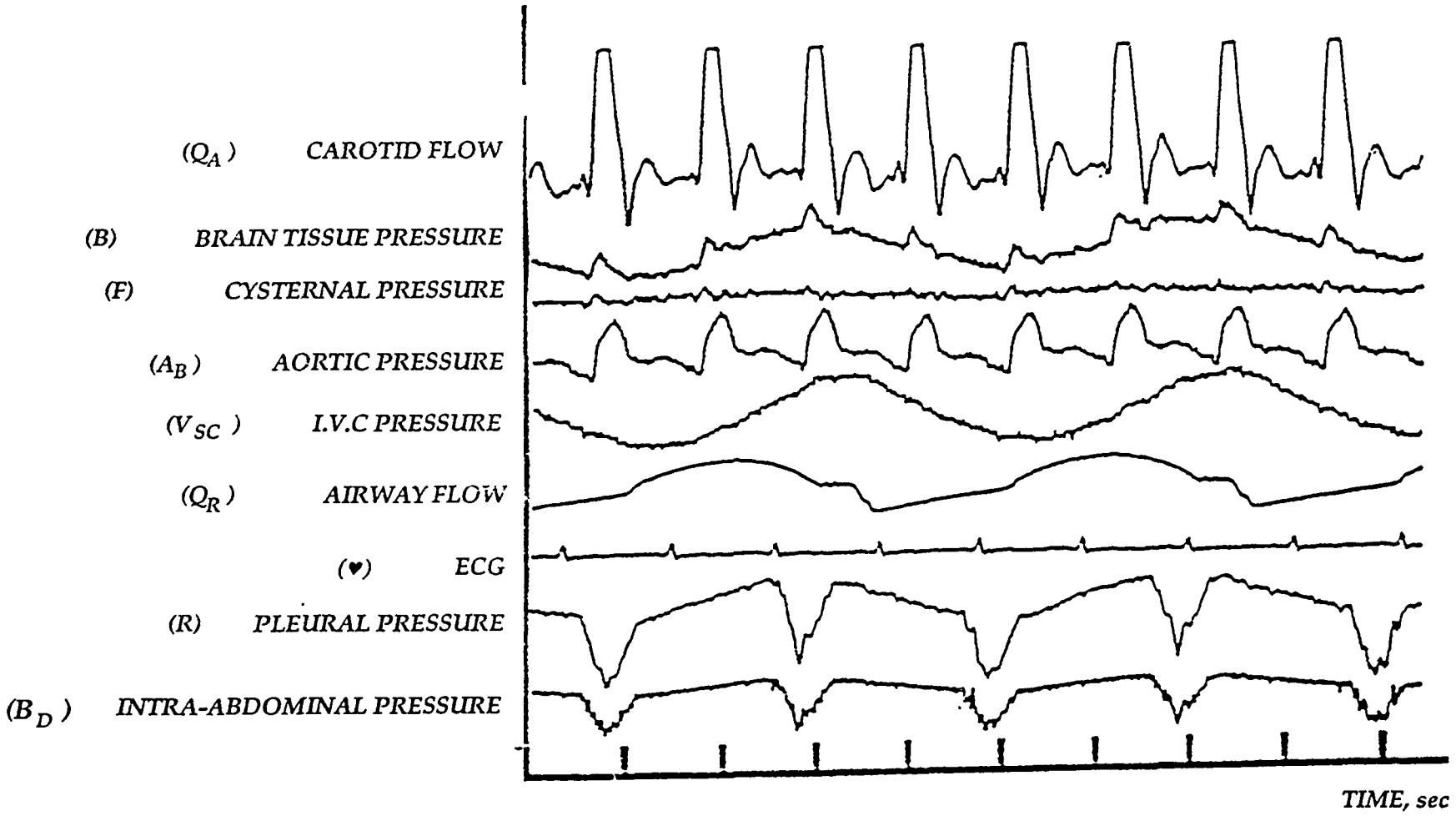

FIGURE 5c TRIANGLE (FLOW) VENTILATION

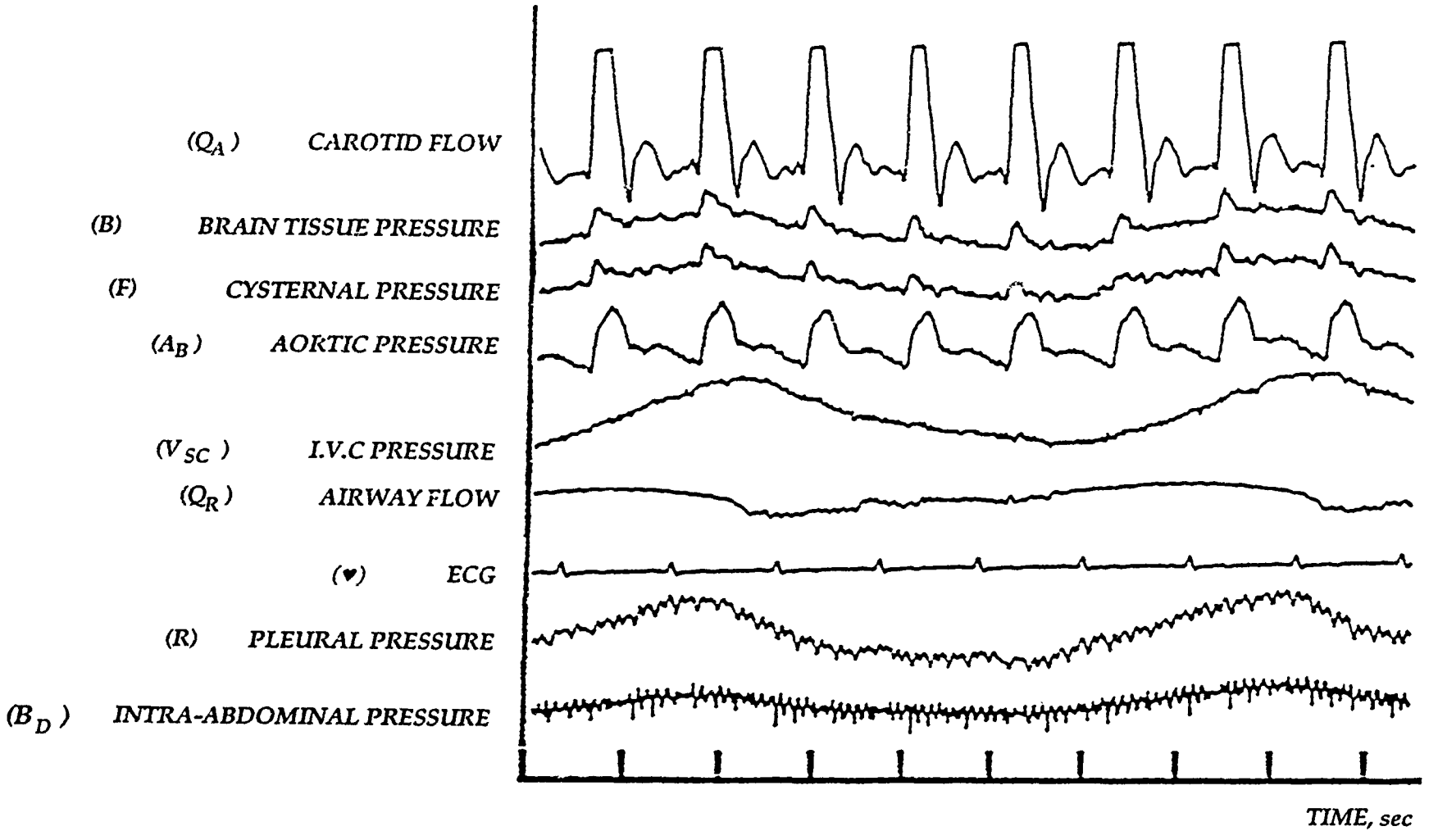

FIGURE 5d LOW I:E RATIO

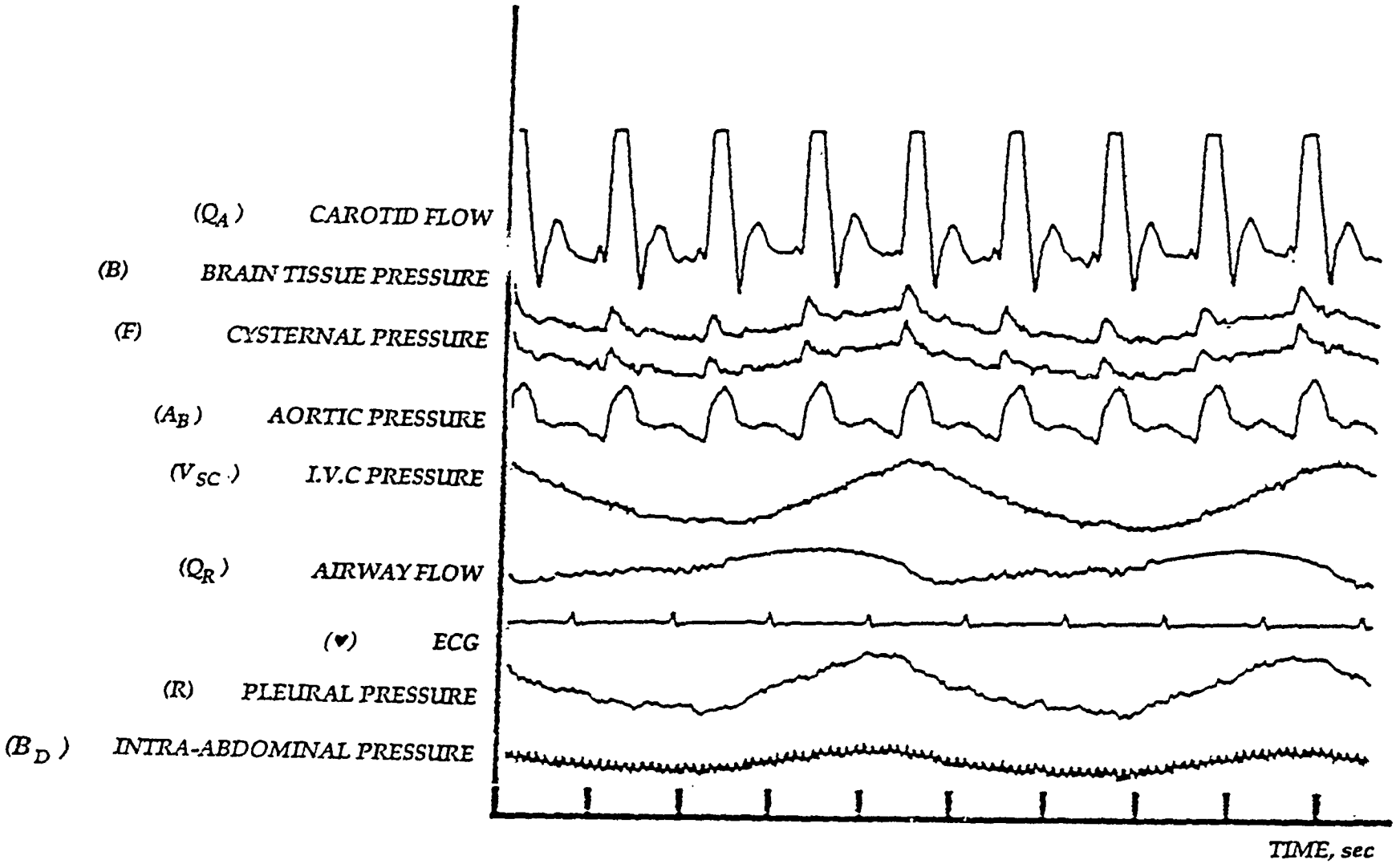

FIGURE 5e HIGH I:E RATIO